КОЛЛОИДНЫЙ
ЖУРНАЛ

COLLOID JOURNAL

(KOLLOIDNY ZHURNAL)

IN ENGLISH TRANSLATION

WITHDRAWN
POSTMASTER:
IF NOT DELIVERABLE NOTIFY
Chemical Abstracts
OHIO STATE UNIV., COLUMBUS 10, O.
AND POSTAGE WILL BE SENT
REC'D. SEP 29 1958 C. A. LIBRARY
ABSTRACTOR:
PLEASE RETURN PROMPTLY TO
CHEMICAL ABSTRACTS
OHIO STATE UNIV., COLUMBUS 10, O.

VOL. 19 1957 NO. 6

CONSULTANTS BUREAU, INC.
227 WEST 17TH STREET, NEW YORK 11, N. Y.
an agency for the interpretation of international knowledge

COLLOID JOURNAL

(KOLLOIDNY ZHURNAL)

Journal of Theoretical and Applied Physics and

Chemistry of Colloids

Volume XIX

(Number 6, November-December, 1957)

Editor

A. V. Dumansky

Editorial Board

P. N. Antipov-Karataev, B. V. Deryagin, B. A. Dogadkin (Deputy Editor), A. V. Dumansky,
V. A. Kargin, S. M. Lipatov, P. A. Rebinder, I. P. Serdobolsky (Secretary), M. P. Volarovich

Publication of the Academy of Sciences of the USSR

IN ENGLISH TRANSLATION

Copyright, 1958

CONSULTANTS BUREAU, INC.
227 West 17th Street
New York 11, N. Y.

Printed in the United States

Annual Subscription	$80.00
Single issue	20.00

Note: The sale of photostatic copies of any portion of this copyright translation is expressly prohibited by the copyright owners. A complete copy of any paper in this issue may be purchased from the publisher for $7.50.

SIGNIFICANCE OF ABBREVIATIONS MOST FREQUENTLY ENCOUNTERED IN SOVIET PERIODICALS

FIAN	Phys. Inst. Acad. Sci. USSR.
GDI	Water Power Inst.
GITI	State Sci.-Tech. Press
GITTL	State Tech. and Theor. Lit. Press
GONTI	State United Sci.-Tech. Press
Gosenergoizdat	State Power Press
Goskhimizdat	State Chem. Press
GOST	All-Union State Standard
GTTI	State Tech. and Theor. Lit. Press
IL	Foreign Lit. Press
ISN (Izd. Sov. Nauk)	Soviet Science Press
Izd. AN SSSR	Acad. Sci. USSR Press
Izd. MGU	Moscow State Univ. Press
LEIIZhT	Leningrad Power Inst. of Railroad Engineering
LET	Leningrad Elec. Engr. School
LETI	Leningrad Electrotechnical Inst.
LETIIZhT	Leningrad Electrical Engineering Research Inst. of Railroad Engr.
Mashgiz	State Sci.-Tech. Press for Machine Construction Lit.
MEP	Ministry of Electrical Industry
MES	Ministry of Electrical Power Plants
MESEP	Ministry of Electrical Power Plants and the Electrical Industry
MGU	Moscow State Univ.
MKhTI	Moscow Inst. Chem. Tech.
MOPI	Moscow Regional Pedagogical Inst.
MSP	Ministry of Industrial Construction
NII ZVUKSZAPIOI	Scientific Research Inst. of Sound Recording
NIKFI	Sci. Inst. of Modern Motion Picture Photography
ONTI	United Sci.-Tech. Press
OTI	Division of Technical Information
OTN	Div. Tech. Sci.
Stroiizdat	Construction Press
TOE	Association of Power Engineers
TsKTI	Central Research Inst. for Boilers and Turbines
TsNIEL	Central Scientific Research Elec. Engr. Lab.
TsNIEL-MES	Central Scientific Research Elec. Engr. Lab.—Ministry of Electric Power Plants
TsVTI	Central Office of Economic Information
UF	Ural Branch
VIESKh	All-Union Inst. of Rural Elec. Power Stations
VNIIM	All-Union Scientific Research Inst. of Meteorology
VNIIZhDT	All-Union Scientific Research Inst. of Railroad Engineering
VTI	All-Union Thermotech. Inst.
VZEI	All-Union Power Correspondence Inst.

Note: Abbreviations not on this list and not explained in the translation have been transliterated, no further information about their significance being available to us. — Publisher.

THE COAGULATION MECHANISM OF BUTADIENE–STYRENE LATEX

S. A. Glikman and E. P. Korchagina

Most authors attribute the stability of synthetic latexes mainly to the presence on the globule surfaces of an electric double layer, formed as the result of ionization of adsorbed soap molecules [1]. It has been reported that the structural film formed by colloidal soaps has a protective action [2]. However, calculations based on data on globule size [3-5] show that the amounts of adsorbed substances are not enough to coat the globules even with a monomolecular layer. Data on the coagulation thresholds of latexes by various cations [1, 6] are in general agreement with typical data for lyophobic sols. At the same time the role of univalent cations, the action of which can be compared with the salting-out effect [7, 2], gives rise to doubt.

Extension of our knowledge of the nature of synthetic rubber latex coagulation by electrolytes, and of means of influencing the course of this process, is of theoretical and practical interest. In particular, in the production of butadiene–styrene rubber (SKS-30A) it would be desirable in many respects to replace calcium chloride, generally used for coagulation of the latex, by sodium chloride; but 40 times as much of the latter as of $CaCl_2$ is needed to coagulate the latex, and the resultant blanket is difficult to dry, owing to its structural peculiarities.

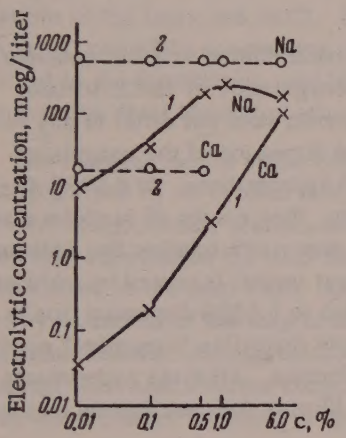

Fig. 1. Variation of coagulation thresholds (1) and complete coagulation concentration (2) with concentration of SKS-30A latex (logarithmic scale).

In order to investigate the nature of the action of mineral salts and certain other substances on the coagulation of SKS-30A latexes, we studied the effect of sodium and calcium chlorides and of certain nonelectrolytes on latexes at concentrations from 0.01 to 6%. The observations were carried out by means of a nephelometer 24 hours after preparation of the solutions. Aqueous solutions without added buffers were used, so that the influence of extraneous ions of buffer mixtures was excluded. The results are given in Fig. 1. Figure 1 shows that the coagulation thresholds of the diluted latexes are 200 times as high for NaCl as for $CaCl_2$. The coagulation thresholds increase with increasing latex concentration, and the difference between the effects of Na^+ and Ca^{2+} diminishes somewhat. At the same time, the complete coagulation concentrations remain unchanged at all latex concentrations, being 30 times greater for Na^+ than for Ca^{2+}. The absolute values of NaCl concentrations which cause complete coagulation even of concentrated latexes are several times less than the concentrations required for the salting-out effect. On the other hand, however, the fact that, for any latex concentration, equal amounts of Na^+ and Ca^{2+} are required for complete coagulation indicates that the role of electrolytes in latex coagulation is not confined to lowering the zeta potential. Our study [8] of the structural differences between the coagulation products obtained by the action of Na^+ and Ca^{2+}, and of the nature and porosity of the blankets formed from these products also indicates this, The nature of these differences is revealed by studies of the influence of certain nonelectrolytes on the course and character of the coagulation of SKS-30A latex.

Experiments showed that the coagulation threshold is not affected by addition of various amounts of hydroquinone to the latex. However, with an NaCl concentration which causes complete coagulation, the presence of 0.5% of hydroquinone in the latex gives a looser blanket, easier to dry. Addition of 2-5% hydroquinone to the latex makes blanket formation impossible, as with the amounts of NaCl used in the formulation a milky dispersion of very fine particles is formed, and visible coagulation does not occur at all. This dispersion, at a high degree of dilution with water, is as stable as the original latex; after it has been allowed to stand for many days not only does it show no signs of visible coagulation, but its turbidity remains quite unchanged.

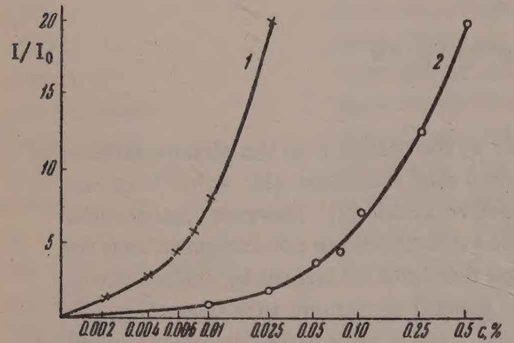

Fig. 2. Effect of rubber concentration on the relative light scattering of dispersion containing hydroquinone (1) and of latex (2).

Figure 2 shows the effect of concentration of rubber (in grams per 100 ml of liquid) on the relative light scattering (I/I_0, where I_0 is the light scattering of 0.01% latex) of dispersion with hydroquinone and of latex. These results show that at low concentrations of rubber in the latex light scattering is approximately proportional to the concentration, in accordance with Rayleigh's law; at higher concentrations the relationship is no longer linear. On the average, for equal concentrations of rubber in the latex and the dispersion, $I_{disp}/I_{lat} \sim 10$. This means that the volume of a particle of the dispersion is about 10 times the volume of a globule of the uncoagulated latex.

A latex dispersion diluted to a low concentration immediately after coagulation by NaCl, without additional hydroquinone, does not differ in any respect from a diluted dispersion of the coagulated latex containing 5% hydroquinone. In 0.005% dispersions of both types negligible amounts of NaCl and hydroquinone are present; they consist of particles about 10 times the size of the original latex particles. Visible coagulation of these dispersions requires the addition of 2.5% NaCl. Complete coagulation (with formation of flakes and a transparent serum) is caused by addition of 3.0% NaCl. However, if before addition of NaCl 5% of hydroquinone is added to 0.005% dispersion (made from latex coagulated by the usual formula), then after 24 hours of standing only reversible "creaming" occurs, whereas in control experiments (without hydroquinone) irreversible flakes are formed. All these experiments indicate that the size of the primary particles in latex coagulated by sodium chloride does not depend on the presence of hydroquinone in the latex.

It has been shown [8] that the difference between the blankets formed from latex coagulated by Na^+ and Ca^{2+} respectively lies in their macrostructure, in the volume and form of the intermediate pores, and the associated macrocavities. The specific surface, which is largely determined by the presence of micropores, is almost the same for both types of blanket. If this is considered in conjunction with the fact, noted above, that the dimensions of the primary aggregates of rubber globules remain constant, the idea of two stages in the coagulation process naturally arises. The first stage is the result of a fall of the zeta potential to the critical value, and consists of primary aggregate formation; the second stage consists of coalescence of these aggregates. This is evidently the stage which determines the difference between the structures of the blankets.

In the case of coagulation by calcium chloride, the fixation of molecules of insoluble Ca soaps on the globule surfaces should play an important role. Here not only the steric factor, which results in the formation of a looser structure, but also the energy factor, which consolidates this structure owing to interaction between the Ca soap molecules, may be of significance. In latexes coagulated by sodium salts the primary globule aggregates may be protected from coalescence by molecules of other constituents of the latex, including hydroquinone molecules, adsorbed on these particles.

After decrease of the zeta potential the surface soap film is not sufficient to protect the latex particles from coalescence resulting from autohesion, as this film does not completely cover the globule surface. On the contrary, the presence of such an incomplete film may sometimes intensify cohesion and coalescence of the particles, if, for example, this film is formed by soaps with bivalent cations, as is the case at a concentration of ~ 0.1% $CaCl_2$. Here, regardless of the latex concentration, the $CaCl_2$ concentration plays the dominant role, since exchange adsorption is the factor which determines the state of the system. Coagulation of the latex by calcium chloride is not only an autohesion effect, but is also ionic in character, and this leads to formation of loose coagulation products. The structure of the latter is determined by a combination of the steric and energy factors (ionic bonds).

The effect of sodium chloride on the coalescence of the primary aggregated latex particles is in fact analogous to (but not identical with) salting-out. The effect occurs at relatively high NaCl concentrations (of the order of 3 %), and does not depend on the concentration of the latex. The coalescence which takes place at a definite ratio of the interaction energies of the primary aggregates of latex globules with each other and with water, occurs at a certain limiting concentration of NaCl, in presence of which the adhesive power of water is diminished. Since the coalescence of the primary particles in the coagulation of latexes by NaCl is primarily due to autohesion, the secondary structures formed are dense, and this leads in its turn to the formation of a compact blanket, difficult to dry, typical of these conditions. The molecules of "diphilic" substances, which are adsorbed more vigorously by rubber but are less hydrophilic than soaps, may protect the uncharged and partially "stripped" (owing to desorption of soaps) particles of the coagulated latex from coalescence. Hydroquinone is evidently such a substance. If the amount of hydroquinone is insufficient, coalescence is not excluded but merely hindered, and other steric conditions are set up, so that the coagulum is looser.

Certain other nonelectrolytes exert an influence analogous to that of hydroquinone on the second stage of coagulation. Especially interesting results were obtained with phenol. The action of the latter was even more dependent on the concentration than the action of hydroquinone, and it also greatly depended on the concentrations of the latex and NaCl. In particular, it was found that in presence of 0.8% of phenol (on the weight of the latex) complete coagulation of the latex can be effected by addition of one third of the amount of NaCl prescribed in the formulation, and the blanket formed from the coagulum is fully satisfactory and is dried more easily than the usual blanket obtained by NaCl coagulation of the latex.

The complex nature of the effects produced by the addition of different amounts of phenol to the latex can be explained by its twofold role. It seems that phenol, on the one hand, assists coagulation of the latex, and on the other, hinders coalescence of the coagulated particles. It seems possible that phenol molecules are not only adsorbed on the soap-free regions of the surface of the globules and their primary aggregates (or are solubilized in the soap film), but also partially displace the soap molecules from this surface. This is confirmed by variations of the soap concentration in the dispersion medium of the coagulated latex. It was shown by a conductometric titration method developed by Maron, et al. [9] that serums of latexes to which 0.8% phenol had been added before coagulation by NaCl contained much higher concentrations of soap than control serums, formed under the usual coagulation conditions.

SUMMARY

1. It is shown that the absolute values of the coagulation thresholds of SKS-30A latexes diluted down to 0.01% correspond to the usual values for lyophobic sols. The values for NaCl are 200 times those for $CaCl_2$, and increase with the latex concentration. The complete coagulation concentration for NaCl is 30 times that for $CaCl_2$, and does not depend on the dilution of the latex.

2. It was shown by a nephelometric method that the volume of the primary particles formed in coagulation of the latex by sodium chloride is about 10 times the volume of the uncoagulated latex globules, irrespective of the latex concentration.

3. Consideration of the experimental data, in conjunction with facts reported in the literature, leads to the concept of two stages in the coagulation of latex by electrolytes: the first is the consequence of a decrease of the zeta potential, leading to the formation of primary particles, and the second leads to coalescence of these particles. The secondary aggregation processes can be prevented or modified by introduction of certain additives (nonelectrolytes) into the latex.

4. In addition to an explanation of the mechanism of latex coagulation by electrolytes, and a demonstration that this process can be controlled, indications are given of means of an approach to development of conditions for the production of a good blanket by coagulation of latex by sodium chloride, with a much decreased consumption of the latter.

The Saratov State University

Received October 3, 1956.

LITERATURE CITED

[1] S. S. Voyutsky and R. M. Panich, Progr. Chem., 25, 57 (1956).

[2] E. M. Aleksandrova and P. V. Mochalov, Colloid J., 16, 161 (1954). *

[3] M. Ardenne and D. Beischer, Kautschuk 5, 55 (1940).

[4] A. Yurzhenko and S. Mints, Proc. Acad. Sci. USSR, 55, 339 (1947).

[5] B. Zwicker, Ind. Eng. Chem. 44, 774 (1952).

[6] V. Balandina, K. Berezan, A. Dobromyslova, B. Dogadkin and M. Lapuk, Bull. Acad. Sci. USSR, Chem. Ser., 2, 397 (1936).

[7] A. I. Yuzhenko and V. P. Gusyakov, Colloid J., 16, 72 (1954).*

[8] E. P. Korchagina and S. A. Glikman, Sci. Mem. Saratov State Univ. Chem. Ser. (in the press).

[9] S. H. Maron, I. N. Ulevitch and M. E. Elder, Anal. Chem. 21, 691 (1949).

---

* Original Russian pagination. See C. B. translation.

ANALYSIS OF THE FORMS OF MOISTURE BONDING IN POROUS ADSORBENTS WITH THE AID OF DRYING THERMOGRAMS

M. F. Kazansky

In Lykov's theory of drying [1] it is shown that the drying of colloidal capillary-porous bodies is a complex thermal and physicochemical process, the laws of which are determined by the forms of bonding of the moisture being removed, and its state within the pores of the body. By studies of the kinetics of the drying of moist porous bodies it is possible to carry out a quantitative analysis of the forms of moisture bonding. The present paper gives descriptions of experiments on the drying of powdered silica gels of various structural types and of activated charcoal, moistened with water and methyl alcohol, carried out in order to establish a new method for the analysis of the forms of moisture bonding in porous bodies. The experiments were carried out at constant surrounding air temperature.

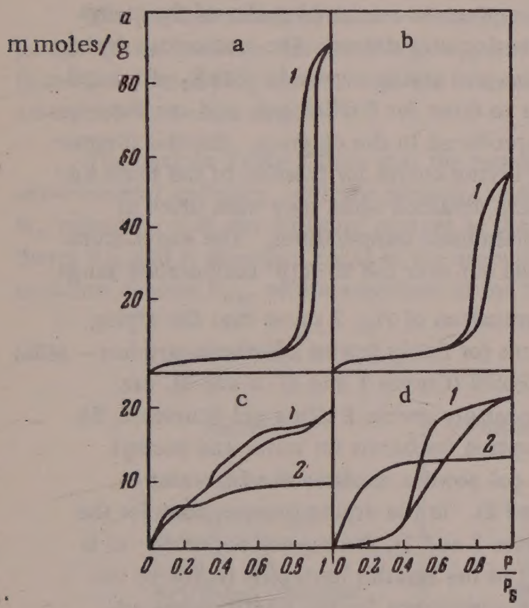

Fig. 1. Adsorption isotherms for water (1) and methyl alcohol (2) vapors on silica gels: a) E; b) VKhK$_2$ [6]; c) MSM; d) activated charcoal.

Of all the curves which illustrate graphically the kinetic relationships of the drying of porous bodies, in our opinion the most suitable for solution of the problem in question is the curve representing the temperature variations of a porous body during drying at constant surrounding air temperature. The important advantage of such a curve, which we have named the drying thermogram, is that it represents a direct experimental result and can be automatically recorded by means of suitable apparatus.

Silica gels and activated charcoal were chosen for the investigation because they are typical capillary-porous bodies, the structure of which have been studied fairly fully by a number of independent methods [2], while the contents of moisture bound in different forms can be determined from isotherms for water vapor adsorption.

With the aid of an automatic laboratory apparatus [3], the drying thermogram, the weight variation curve (drying curve), and a control curve for the surrounding air temperature were recorded automatically on the ribbon of a recording potentiometer. The experiments were performed with powder fractions > 0.25 mm of three silica gels: uniformly coarsely porous silica gel E, prepared in the Institute of Physical Chemistry, Academy of Sciences Ukrainian SSR; homogeneously coarsely porous silica gel VKhK$_2$; finely porous silica gel MSM from commercial samples of the Voskresensk Chemical Combine; the activated charcoal was a finely porous sample from the Molotov Chemical Works. The adsorption isotherms for water and methyl alcohol vapors are given in Fig. 1.

Before the experiment, the adsorbent powder was put into the cell of the laboratory apparatus [3] in a layer 1-2 mm thick. The cell was then put into the thermostat of the same apparatus, where the powder was dried at 110°. The cell was then placed in a desiccator where the powder was cooled over P_2O_5, and then moistened with water or methyl alcohol from a buret inserted in the neck of the desiccator lid.

The isothermal drying thermograms and the drying curves for the moistened adsorbent powders were recorded on the ribbon of a recording potentiometer while they were dried in the thermostat. The air temperature in the thermostat was kept constant by means of an electronic thermoregulator.

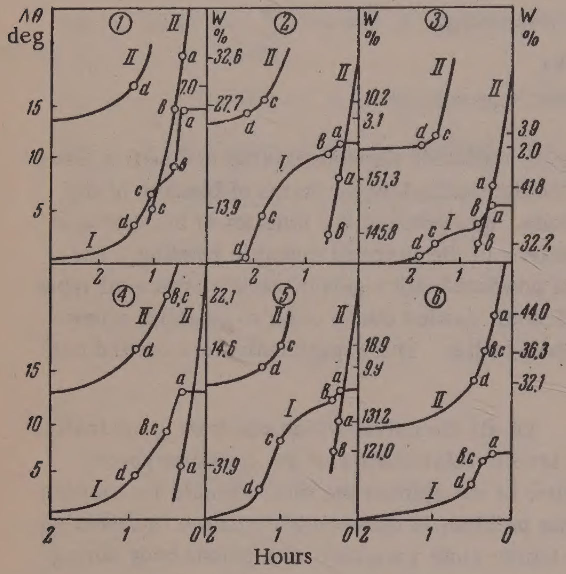

Fig. 2. Isothermal drying thermograms (I) and drying curves (II) at different temperatures for silica gel powders moistened with water: 1) MSM, 72°; 2) E, 75.4°; 3) activated charcoal, 51°, and moistened with methyl alcohol: 4) MSM, 75.4°; 5) E, 75.5°; 6) activated charcoal, 55.1°.

The powders were weighed automatically during the experiments by means of a photoelectric balance, the weight variations being recorded in the form of drying curves. The powder temperature was measured by means of a thermopile consisting of 32 thermocouples made from thin copper and constantan wires. One group of the thermopile junctions was in the cell with the adsorbent, and the other in the air over the powder. Thus the drying thermograms for the powders, recorded on the ribbon, show variations of the temperature difference between the powders and the constant temperature of the surrounding air during drying. The upper part of Fig. 2 shows thermograms (I) and drying curves (II) for MSM silica gel, E silica gel, and activated charcoal, moistened with water; in the lower part the corresponding thermograms and drying curves for the same adsorbents moistened with methyl alcohol are given. The graphs shown are copies, on a reduced scale, of the traces on the potentiometer ribbon. The isothermal drying thermograms and drying curves for $VKhK_2$ silica gel are similar to those for E silica gel, and are therefore not reproduced in the diagram. Similar thermograms and drying curves for powders of the same adsorbents were obtained when they were dried at different thermostat temperatures. The experiments were carried out over the 25-110° temperature range.

Examination of Fig. 2 shows that the drying thermograms for finely porous adsorbent powders – MSM silica gel and activated charcoal, moistened with water or methyl alcohol (Curves 1 and 4; 3 and 6), are similar in character, but differ from the drying thermograms for the coarsely porous E silica gel (Curves 2, 5). Corresponding to the presence of a large hysteresis region in the adsorption isotherms for water and methyl alcohol vapors on E silica gel, the drying thermograms for this silica gel powder, moistened with water or methyl alcohol, have considerable convex regions (b–c; Curves 2 and 5). In the drying thermograms for the finely porous adsorbents, MSM silica gel and activated charcoal (Curves 1 and 3), the convex region (b–c) is considerably smaller than in the curves for E silica gel, corresponding to the smaller hysteresis region of the water vapor adsorption isotherms. The methyl alcohol vapor adsorption isotherms for the finely porous adsorbents – MSM silica gel and activated charcoal – do not have a hysteresis region, and the thermograms for these powders, moistened with methyl alcohol (Curves 4 and 6) do not have a convex region (b–a); the point b on the thermogram coincides with the point c.

The moisture contents of the powders corresponding to the critical points a, b, c, and d on the thermograms, were determined from the drying curves. The moisture contents expressed as percentages on the weight of the dry powder, corresponding to the critical points on the thermograms, are indicated (in Fig. 2) for each adsorbent along the moisture axis.

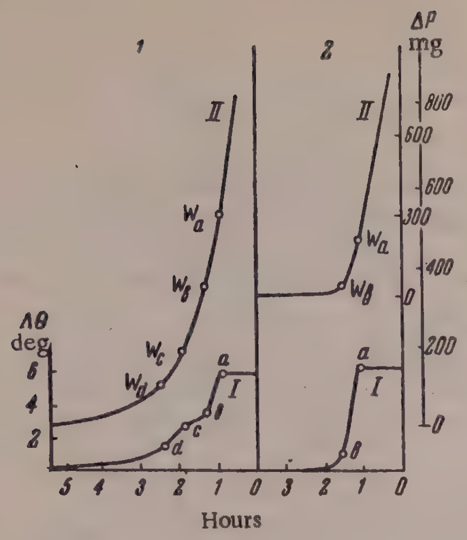

Fig. 3. Thermograms (I) and drying curves (II) at 50° for similar < 0.25 mm fractions of: 1) MSM silica gel powder; 2) quartz sand.

Figure 3 gives thermograms (I) and drying curves (II) at 50° for similar fractions of MSM silica gel powder (Fig. 3, 1) and quartz sand (Fig. 3, 2), moistened with water. The thermogram for quartz sand has two critical points, a and b, while the thermogram for the silica gel powder has four critical points, a, b, c and d. The upper part of the thermogram for the silica gel, above the point b, resembles the part of the thermogram for quartz sand above the point b.

We showed earlier [3] that the upper region of the drying thermogram for silica gel powder, limited by the position of the critical point b, and the corresponding region of the drying thermogram for sand, both correspond to the removal, from the macropores of the powder ($r > 10^{-5}$ cm), of capillary moisture in different states – capillary, "rope", and "joint".

Thus, the critical point b divides the drying thermograms for powdered adsorbents into two regions: the upper region corresponds to the period of moisture removal from the macropores of the body in the so-called moist state, and the lower, to the period of moisture removal from the body in the hygroscopic state from pores less than 10^{-5} cm radius, removed at relative vapor pressures less than unity.

The physicochemical nature of the points b, c and d on the drying thermograms was elucidated by comparison of the moisture contents, W_b, W_c, and W_d of the powders at the critical points of the thermograms, found from the drying curves, with the moisture contents of the same adsorbents at the inflection points of the adsorption isotherms at 20°.

The data in Table 1 show that the moisture content W_b of the adsorbents coincides, within the limits of experimental accuracy, with the moisture content P of the maximum hygroscopic state; the moisture content W_c coincides with the moisture content at the point of the start of the hysteresis region of the adsorption isotherm P_{sh} and it therefore equal to the amount of adsorbed water; and the moisture content W_d is equal to the moisture content P_{ma} of the adsorbent at the point at which monomolecular layer adsorption is completed.

TABLE 1

Adsorbent	Moistening agent	Moisture content, % of wt. of dry powder at 20°					
		P	W_b	P_{sh}	W_c	P_{ma}	W_d
MSM silica gel	Water	32.6	31.8	13.9	14.1	7.2	8.3
$VKhK_2$ silica gel	Water	93.6	87.0	7.0	6.6	2.6	3.0
E silica gel	Water	170.0	172.0	10.0	9.8	3.4	3.0
Activated charcoal	Water	37.8	35.2	3.6	4.5	—	—
MSM silica gel	Methyl alcohol	28.2	29.5	—	—	14.4	18.2

The moisture contents of the powders at all the critical points of the thermograms were determined for different temperatures from the thermograms and drying curves recorded during drying at different air temperatures. The results of these experiments were used to plot the curves in Fig. 4, which show the variations, with the temperature, of the moisture content at the maximum hygroscopic state (Curves 1b – 4b) and the amount of adsorbed water (Curves 1c – 4c) of MSM, $VKhK_2$, and E silica gel powders and of activated charcoal moistened with water, and of MSM silica gel (Curve 5bc) moistened with methyl alcohol.

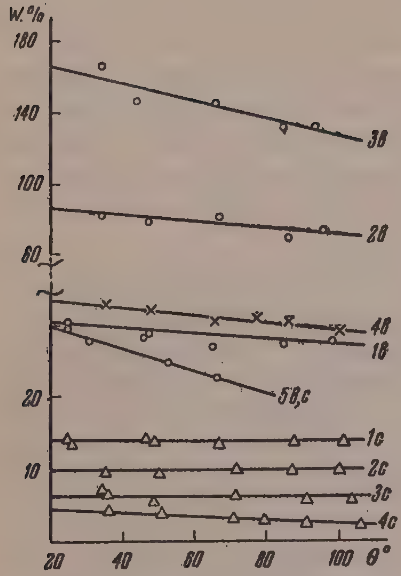

Fig. 4. Moisture contents at the critical points b and c of the isothermal drying thermograms for water-moist silica gel powders at various temperatures: 1b and 1c) MSM; 2b and 3c) VKhK$_2$; 3b and 2c) E; 4b and 4c) activated charcoal; 5b,c) MSM silica gel moistened with methyl alcohol.

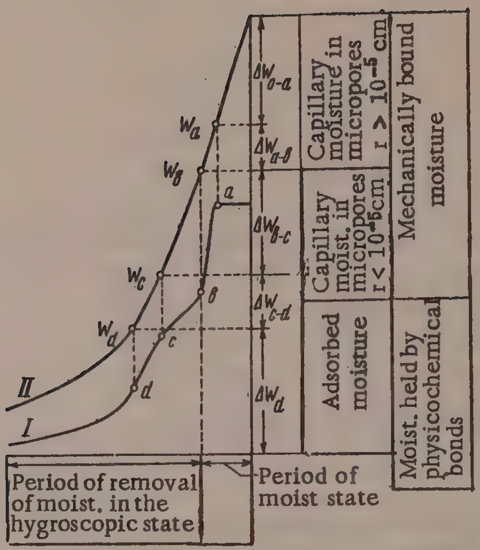
Wa
Wв
Wc
Wd
a
в
c
d
II
I
ΔW0-a
ΔWa-в
ΔWв-c
ΔWc-d
ΔWd
Capillary moisture in micropores r > 10⁻⁵ cm
Capillary moist. in micropores r < 10⁻⁵cm
Adsorbed moisture
Mechanically bound moisture
Moist. held by physicochemical bonds
Period of removal of moist. in the hygroscopic state
Period of moist state

Fig. 5. Diagram of the kinetics of the removal of moisture in different forms of bonding and states in the pores, during drying of fine capillary-porous bodies in isothermal conditions.

It is seen Fig. 4 that the moisture content of the maximum hygroscopic state of different silica gel powders decreases with increase of temperature, whereas the amounts of water adsorbed by silica gels remain constant; the amount of moisture in the hygroscopic state and the amount of adsorbed water in activated charcoal powder (Curves 4b and 4c) decrease with increasing temperature.

On the basis of the foregoing considerations concerning the nature of the critical points and the drying thermograms, in accordance with the modern theory of the drying of porous bodies, the kinetics of the consecutive removal of moisture during drying of adsorbent powders in isothermal conditions can be schematically represented as shown in Fig. 5. In Fig. 5, ΔW_{0-a} represents moisture in the capillary and "rope"*states, evaporating from a water-saturated surface; ΔW_{a-b} is moisture in the "joint"*state in the macropores, $r > 10^{-5}$ cm; ΔW_{b-c} is capillary condensation moisture in the pores, $r < 10^{-5}$ cm; ΔW_{c-d} is multimolecularly adsorbed moisture; ΔW_d is molecular adsorption moisture in monomolecular layers.

The diagram in Fig. 5 is based on the thermogram I and the drying curve II, for isothermal conditions, of a heterogeneously porous silica gel powder moistened with water to its full moisture capacity by contact with the liquid. By projecting the critical points of the thermogram I onto the drying curve II, and then projecting the corresponding points on the drying curve onto the moisture axis, we find the amounts of differently bonded moisture progressively removed during drying. In the interval from the start of drying to the critical point a, at constant temperature of the body and a constant drying rate, the moisture ΔW_{0-a} of the capillary and "rope" states is evaporated from the water-saturated surface of the porous body. In the time interval between the critical points a and b, moisture of the "joint" state ΔW_{a-b} is removed. Up to the critical point b moisture is evaporated at relative vapor pressure equal to unity; the porous body loses capillary moisture from the macropores, moisture of the so-called moist state of the body.

Starting from the critical point b, the body loses moisture of the hygroscopic state at a relative vapor pressure less than unity. Here, in the time interval between the critical points b and c the body loses capillary moisture present in pores of less than 10^{-5} cm radius, including moisture corresponding to the hysteresis loop

---

* [The significance of this terminology is not clear; it is apparently the terminology used in [3]— Translator].

of the adsorption isotherm. The moisture removed from the porous body from the start of drying to the instant corresponding to the position of the critical point c is moisture bound mechanically with the solid phase of the body. Beyond the critical point c removal of adsorbed moisture – moisture held by physicochemical bonds – occurs. First is removed moisture of the multimolecular layers ΔW_{c-d}, corresponding to the linear region c–d in the thermogram. Then, from the critical point d, moisture ΔW_d of the monomolecular layer is removed.

The durations of these drying periods for thin specimens of porous bodies may vary according to the pore structure and the physicochemical properties of the body and of the liquid removed. If a particular bond form is absent, the corresponding section of the thermogram vanishes, as was the case for the drying of MSM silica gel and activated charcoal moistened with methyl alcohol.

We verified the above scheme in numerous experiments on the drying of other capillary-porous powders containing moisture bound in various forms to the solid phase. Therefore the scheme in Fig. 5 can be used as the basis for a new kinetic method for analyzing the forms of moisture bonding in capillary-porous bodies by means of drying thermograms for thin specimens.

SUMMARY

1. Thermograms and drying curves have been obtained for moistened silica gel powders of various types and for activated charcoal.

2. The moisture contents of powders at the critical points in the thermograms correspond to the limits of removal of moisture differing in the forms of bonding and state in the pores of the body during drying.

3. A kinetic scheme has been drawn up for the consecutive removal of moisture bound in different ways during drying of capillary-porous bodies; this is recommended as the basis for a new kinetic method of analyzing the forms of moisture bonding in porous bodies by the use of drying thermograms for thin specimens.

The A. M. Gorky State Pedagogic Institute, Kiev
Laboratory of Molecular Physics

Received September 8, 1957.

LITERATURE CITED

[1] A. V. Lykov, Colloid J., 10, 289 (1948).

[2] Coll.: Methods of Investigation of the Structure of Highly Disperse Bodies (Acad. Sci. USSR Press, Moscow, 1953).

[3] M. F. Kazansky, Sci. Mem., Phys.-Math. Ser., Kiev State Pedagogic Inst. 19, 155 (1956).

[4] O. M. Dzhigit, A. V. Kiselev, and I. E. Neimark, J. Phys. Chem., 28, 1804 (1954).

STUDY OF GELATION PROCESSES IN FRUIT CANDY MASSES BY MEANS OF THE CONE PLASTOMETER

L. S. Kuznetsova and A. L. Sokolovsky

For improving the technology of fruit gel production, it is important to develop an objective method for determining the gel strength and to establish the optimum gelation conditions. Our investigations have made it possible to determine the influence of a number of factors on gelation of candy masses containing pectin: sugar and moisture contents, pH, additions of various buffer salts. The gelling power of the raw fruit materials and confectionery masses was evaluated in terms of the strength of the gel, which depends on the presence of a structure in the gel. The strength was determined by means of the cone plastometer devised by Rebinder [1]. By means of this apparatus it was possible to study the kinetics of gel formation fairly simply, by the variation of the plastic strength with time. The cone plastometer is generally used for determining the least value of the acting force balanced by the plastic strength of the structure at the instant when the cone stops. In determinations of the plastic strength of candy jellies a creep effect was observed, consisting of a very slow immersion of the cone after it had apparently stopped. This shows that candy masses do not have true flow limit (elastic limit) forming a boundary between the regions of elastic and residual deformations. The stress corresponding to the abrupt change of the flow rate is the practical flow limit. Since we were interested in variations of the strength of confectionery jellies with time, the duration of the experiment had to be as short as possible. We selected a time interval of 1 minute, corresponding to immersion of the cone at the maximum speed.

Since it seems likely that the plastic strength values given by this method are too high, to determine the correction factor for conversion to true values the strength of the candy masses was determined by means of the Volarovich viscosimeter and by the plate shearing method.

In the first case the effective viscosity of the jellies was determined at various velocity gradients. Small forces, and therefore small velocity gradients, corresponded to high viscosities. Increase of the stress resulted in a decrease of effective viscosity owing to breakdown of the structure. The viscosity fell most sharply at stresses determined by extrapolation of the linear regions of the $\eta - P$ curves, indicating almost total breakdown of the structure. The stress determined in this way can be regarded as the strength of the gel. Comparison of the values for the strength of candy masses determined by this method ($5.05 \cdot 10^3$ and $2.54 \cdot 10^4$ dynes / cm^2) with the results found by means of the cone plastometer ($10 \cdot 10^3$ and $5 \cdot 10^4$ dynes/ cm^2) and by tangential displacement of a plate showed, as expected, that the cone plastometer gives high strength values. The factor for converting the plastic strengths to the true values is close to 0.5.

The nature of the strength increase in candy jellies as determined by these methods is the same in each case. The strength variation curves resemble the gel formation curves for pectin solutions. Therefore the cone immersion method, which gives the correct qualitative and quantitative characteristics of the strength properties of the structure (if the conversion factor is used), can be regarded as a convenient method both for studying the kinetics of gel formation in candy masses, and for production control.

By means of the cone immersion method it proved possible to determine the optimum strength of candy jelly over the range of $2 \cdot 10^4$ to $3 \cdot 10^4$ dynes/cm^2. The optimum strength of candy jellies is determined by correct formulation (contents of sugar, moisture, acid, and pectin). The data obtained on the effect of sugar on gelation processes in candy masses are of interest. Increase of the sugar content in fruit candy from 80 to 140 parts by weight (per 100 parts of fruit mixture) results in a decrease of jelly strength and a shorter gelation

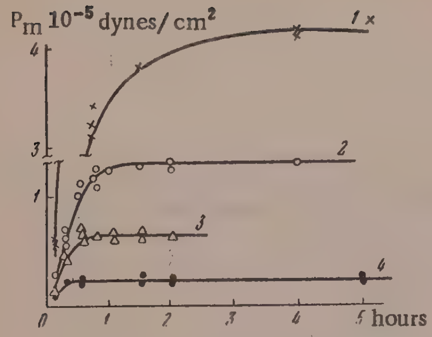

Fig. 1. Variation of candy jelly strength with moisture content: 1) moisture content 9.2%; 2) 14.0%; 3) 19.2%; 4) 23.6%.

time; this is in agreement with the existing views concerning the nature of sugar as a dehydrating agent in the formation of confectionery jellies, by decreasing solvation of the particles. The structural skeleton is formed by cohesion of individual pectin particles at regions free from solvate layers.

The strength of candy jellies is lowered not only by an increase of the sugar content but also by an increase of the moisture content, as is shown by the data in Fig. 1. (The recipe of the candy mass was sugar, plum puree, and apple puree in 1:0.7:0.3 ratio). In addition, the gelation time of candy masses is shortened with increase of moisture content. This is probably caused by accelerated orientation of the pectin chain molecules as the result of the decrease in the viscosity of the dispersion medium.

The active acidity plays a decisive role in the gelation of fruit candy masses. Two factors make it necessary to ensure the optimum active acidity in the gelation of candy masses: 1) at the optimum hydrogen ion concentration complete substitution of the metal ions in the carboxyl groups of the pectin molecules takes place, to give pectic acids, capable of gel formation; 2) increase of hydrogen ion concentration may lead to depolymerization of the pectin molecule, a decrease of the molecular weight of the pectin, and deterioration of its jellying power. The lower pH limit for a fruit candy jelly should be not less than 3.0, and the upper, ~ 4.

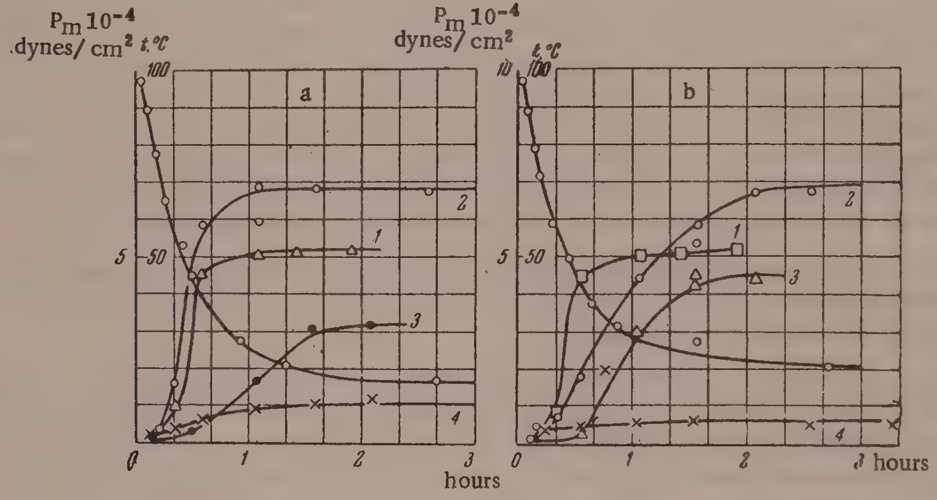

Fig. 2. Gelation kinetics of candy masses containing sodium tartrate (a) and sodium formate (b) in amounts: 1) 0%; 2) 0.2%; 3) 0.6%; 4) 1.0%.

The gelation processes can be regulated by addition to the candy masses of various buffer salts [2] of organic acids (tartaric, acetic, lactic, citric, and formic). Small amounts of the sodium salts of these acids (0.2% on the weight of the sugar and fruit puree) added to candy masses strengthen candy jellies (see Table). The sodium salts of the different organic acids can be arranged in the following sequence of their effects on the gelation of candy masses (increase of strength), which depend in this case on the anion: sodium citrate – sodium formate – sodium acetate – sodium tartrate – sodium lactate.

Small amounts (0.2%) of sodium tartrate and citrate accelerate the start of gelation (Fig. 2). On the

Effects of Sodium Salts of Organic Acids, and of Secondary and Tertiary Sodium Phosphates on the Physicochemical Properties of Candy Jellies.

Candy mass recipe	Salt	Salt, content, wt %of sugar – puree mixture	Moisture content, %	Acidity as % malic acid	pH	Reducing sugars, %	Jelly strength in dynes/cm²
Apricot puree, apple puree, sugar (0.5 : 0.5 : 1)	—	—	20.0	0.9	2.9	58.0	$5.2\cdot10^4$
Ditto	Sodium tartrate	0.2	20.0	0.9	3.3	54.75	$6.8\cdot10^4$
	Ditto	0.6	21.0	0.88	3.6	39.9	$3.1\cdot10^4$
		1.0	30.5	0.36	3.94	28.8	$1.0\cdot10^4$
	Sodium formate	0.2	20.0	0.86	3.5	41.25	$6.9\cdot10^4$
	Ditto	0.6	20.5	0.81	—	37.3	$4.5\cdot10^4$
		1.0	21.0	0.80	4.21	26.4	$6.0\cdot10^4$
	Sodium acetate	0.2	21.0	0.86	3.2	50.4	$6.8\cdot10^4$
	Ditto	1,0	20.0	0.79	3.5	37.2	$4.0\cdot10^4$
	Sodium lactate	0.2	19.8	1.06	—	—	$4.4\cdot10^4$
	Ditto	0.6	18.5	0.89	2.9	56.5	$4.6\cdot10^4$
		1.0	22.0	0.88	3.29	47.75	$7.4\cdot10^4$
Apricot puree, apple puree, sugar (0.7 : 0.3 : 1)	—	—	20.5	1.05	3.49	49.0	$2.8\cdot10^4$
Ditto	Sodium citrate	0.2	20.5	—	3.39	35.0	$1{,}07\cdot10^5$
	Ditto	0.6	20.7	0.74	—	34.5	$3.0\cdot10^3$
Apricot puree, apple puree, sugar (0.3 : 0.7 : 1)	—	—	20.0	0.92	3.22	65.7	$5.50\cdot10^4$
Ditto	Na_2HPO_4	0.4	19.6	0.9	3.47	55.8	$7.01\cdot10^4$
	Na_2HPO_4	0.6	19.4	0.87	3.49	44.2	$8.0\cdot10^4$
	Na_3PO_4	0.2	19.4	0.80	3.55	50.8	$8.0\cdot10^4$
	Na_3PO_4	0.5	17.4	0.77	4.09	38.5	$2.3\cdot10^4$
	Na_3PO_4	1.0	19.4	0.65	4.92	7.28	$0.8\cdot10^4$

other hand, sodium acetate, sodium lactate, and especially sodium formate retard gelation at the start, by lowering the temperature at which gelation begins. This makes it possible to extend the range of fruit materials used, and to make greater use of apple puree, which gives, under the ordinary boiling conditions without addition of salts, very viscous masses with a high temperature for the start of gelation. Secondary and normal sodium phosphates added to the candy masses in small amounts (0.2-0.6% on the weight of the puree and sugar) also have a favorable effect on gelation, increasing jelly strength.

Increase of the salt content, resulting in an increase of pH to 3.9-4.0 and over, has an adverse effect on the gelation of candy masses (the strength is decreased sharply). Not only salts containing the univalent Na^+ cation influence the formation of candy jellies. Several multivalent ions are known which have a favorable effect on the strength of pectin jellies; these include Ca^{2+}, Ba^{2+}, Al^{2+}; their role consists of the formation of new secondary bonds at the carboxyl groups of the polygalecturonic chains. This is fully confirmed by the results of our study of the effects of calcium lactate, chloride and phosphate; small additions (0.2-0.6%) of these salts increase gel strength and lower the gelation temperature. The quantitative differences between their effects are probably to be explained by the differences between the anions; these can be arranged in order of effectiveness as follows: PO_4, $CH_3CHOHCO_2$, Cl_2.

SUMMARY

1. It has been shown that the cone plastometer can be used for studying gelation processes of candy

masses and for control of the technological production processes.

2. The effects of the contents of sugar, moisture, active acidity, buffer salts, and salts containing multivalent ions on the gelation of fruit candy masses have been determined:

a) an increase of the sugar content from 80 to 140 parts by weight per 100 parts of the fruit mixture results in decreased jelly strength and a shorter gelation time;

b) increase of the moisture content of the jellies results in a decrease of strength and shortening of the gelation time;

c) an optimum active acidity must be maintained for normal gelation of fruit candy masses. The power pH limit of a fruit candy jelly must be not less than 3.0, and the upper limit, ~ 4;

d) addition various buffer salts to the candy masses results in changes of active acidity, and may be utilized for regulation of the gelation processes;

e) addition of small amounts of salts (lactates, chlorides, phosphates) containing bivalent ions (Ca^{2+}) has a favorable effect on the strength of candy jellies owing to formation of secondary bonds.

The Moscow Technological Institute for the
Food Industry

Received November 5, 1956.

LITERATURE CITED

[1] P. A. Rebinder, Summary of a General Course of Colloid Chemistry (Moscow State University Press, 1950). [In Russian].

[2] N. A. Gildebrandt, New Technology of Molded Marmalade Production (Food Industry Press, 1955). [In Russian].

THE ADSORPTIVE ACTIVITY OF CADMIUM HYDROXIDE IN RELATION TO THE CONDITIONS OF ITS FORMATION

S. A. Levina and N. F. Ermolenko

Of the papers which have been published in recent years on studies of the structure and the adsorptive and catalytic activity of metal hydroxides and oxides [1], only a few deal with cadmium oxide [2-3]. Nevertheless, studies of the influence of preparation conditions on the composition, structure, and adsorptive properties of cadmium hydroxide are of undoubted interest both in relation to the further conversion of the hydroxide into a more active catalyst, and for elucidation of the composition and structure of the hydroxide itself, prepared from different salts. The tendency of cadmium halides to complex formation is well known [4-7]. It is also known that when the hydroxide is precipitated from salts by the action of alkalies complexes are formed, the composition of which depend on the concentration of the components [8]. Iodine salts of cadmium have a considerable tendency to complex formation [9].

The purpose of the present work was to study the adsorptive activity of calcium hydroxide precipitated from the nitrate, and of the complex compounds of basic cadmium iodides formed by precipitation from cadmium iodide solutions at different pH values of the medium, in relation to their composition and structure.

Experimental procedure. Cadmium hydroxide was precipitated from cadmium nitrate solution by KOH solution. The precipitate was washed thoroughly and dried in air. To prepare basic cadmium salts, definite amounts of KOH solution were added to solutions of cadmium iodide. The precipitate was filtered off, washed with water to a negative reaction for I^- with $AgNO_3$, and dried in air. After the precipitate had been filtered off, the pH of the filtrate was determined (potentiometrically with a glass electrode) and a fresh portion of KOH was added. The precipitated fraction was again washed and dried in air. In this way the following 5 fractions were obtained in the air-dry state from 500 g of CdI_2:

Fraction No	I	II	III	IV	V
pH	4.22	6.25	7.20	8.20	11.24
Weight of precipitate, in g. .	7	10	11	70.0	32

The hydroxide samples and complex salt fractions were ground in a mortar and sifted through a sieve of 52 mesh. All the fractions were analyzed gravimetrically for moisture content and for cadmium and iodine. Cd was determined as the carbonate, and I as AgI. The particle size and surface were determined by Figurovsky's sedimentation method. The porosity was calculated from the apparent and true specific gravities. The adsorptive activity was determined from the adsorption of benzene vapor, of dyes from aqueous solutions, and of salicylic acid from benzene solutions.

Table 1 gives the analytical data for the moisture, cadmium, and iodine contents of the fractions.

These data show that the moisture contents of all the fractions are low, in contrast to the previously studied hydroxides of Al, Cr, and Fe, which contain from 25 to 37% moisture in the air-dry state. The precipitation of the hydroxide by the action of alkali solution on cadmium nitrate solution differs from the precipitation of basic salts from cadmium iodide: in the former case it occurs at constant pH 6.44, while in the latter it begins at pH 4.2 and continues with considerable variation of the pH of the medium. During drying at 100° the basic salts do not decompose, but the hydroxide begins to turn brown, passing into CdO. The fairly high iodine content of the fractions obtained from CdI_2 should be noted. Spectroscopic data indicate absence of potassium in the fractions (the iodine was not adsorbed in the form of KI). Neither is the iodine adsorbed molecularly; this is shown by a negative reaction with starch even when the hydroxide is dissolved in dilute sulfuric or nitric acids. In view of the known ability of cadmium halides to form complexes [3-8], we believe that in this case complex formation occurs, analogous to that observed by Urazov and Kirakosyan [8] in the preparation of hydroxides from $CdSO_4$ by the action of alkali. The composition of the complex of the type $n\,Cd(OH)_2 \cdot CdSO_4 \cdot mH_2O$ varied, in the opinion of these authors, with the concentration of the components.

TABLE 1

Characteristics of the Individual Cadmium Hydroxide Fractions

Fractions	pH of medium	Moisture, %	% Cd	% I
Hydroxide	6.44	0.78	72.5	—
I	4.22	0.50	53.96	33.82
II	6.25	0.40	54.70	32.53
III	7.20	0.40	53.10	32.18
IV	8.20	0.10	54.70	32.07
V	11.24	0.70	65.60	16.2

The compositions of our fractions based on the analytical data are given in Table 2.

A complex in which there is one CdI_2 molecule per 8 $Cd(OH)_2$ molecules is formed only in an alkaline medium (pH 11.24). In the remaining cases, according to our analytical data, the complex consists of three molecules of $Cd(OH)_2$ to one molecule of CdI_2. However, further investigations showed that despite the same composition, the fractions differ in structure and adsorptive activity. Studies of the sedimentation of the hydroxide at the instant of formation showed that the content of particles between 5 and 8 μ in radius increases sharply when the reaction of the medium is changed from acid to neutral. Subsequent transition from a neutral to an alkaline medium is accompanied by an increase in the number of large particles, as is clearly seen in Fig. 1.

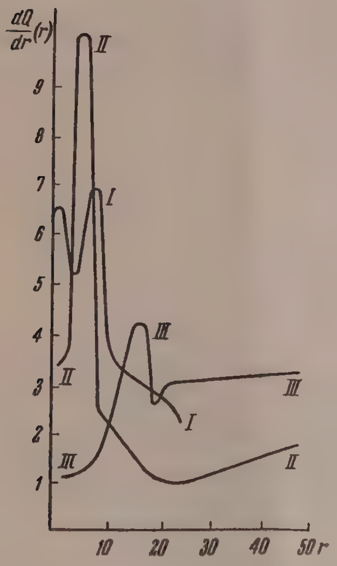

Fig. 1. Sedimenation analysis of calcium hydroxide suspensions at the instant of formation of different fractions: I) at pH 4.25; II) at pH 7.2; III) at pH 11.24.

The total surface area of the particles decreases in accordance with the increasing particle size as the pH of the medium rises. Table 3 gives the total surface areas of different cadmium hydroxide fractions, calculated from sedimentation analysis data obtained at the instant of formation of these fractions.

Sedimentation analysis of air-dry samples of the precipitated fractions also shows that the number of larger particles increases with rising pH of the medium.

The size of the precipitated particles depends to a considerable extent not only on the pH of the medium but also on the precipitation temperature. It is shown in Table 4 that, at a given solution pH (7.2-8), the content of larger particles increases with rise of temperature.

The porosity of the precipitates was determined from their apparent and true densities. The true and apparent densities and porosities of the precipitated fractions are given in Table 5.

The data in Table 5 show that Fractions I and IV have the highest true and apparent densities and also the lowest percentage porosities. They evidently have a dense structure of low porosity. It is to be expected that these fractions, especially Fraction IV, have a low adsorptive activity toward substances of high molecular weight. In fact, a study of

TABLE 2

Composition of Different Cadmium Hydroxide Fractions

Fraction	pH of medium	Composition of fractions	Calculated, %		Found, %	
			Cd	I	Cd	I
Hydroxide	6.44	$2\ Cd(OH)_2 \cdot H_2O$	72 3	—	72.5	—
I	4.22	$3\ Cd(OH)_2 \cdot CdI_2$	55,8	31.5	53.9	33.8
II	6.25	$3\ Cd(OH)_2 \cdot CdI_2$	55.8	31.5	54,7	32.5
III	7.20	$3\ Cd(OH)_2 \cdot CdI_2$	55.8	31.5	53,1	32.9
IV	8.20	$3\ Cd(OH)_2 \cdot CdI_2$	55 8	31.5	54.7	32.0
V	11.24	$8\ Cd(OH)_2 \cdot CdI_2$	65.8	16.5	65.6	16.2

TABLE 3

Total Surface Area of Particles in the Different Cadmium Hydroxide Fractions

Fraction No	I	II	III	IV	V
Total particle surface, in m^2	15	12	11	8	5

TABLE 4

Effect of Cadmium Hydroxide Precipitation Temperature on the Particle Size of the Main Bulk of the Sedimented Particles

Precipitation temperature, °C	5	10	20	25	30
Particle size, μ	2-8	3-10	3-12	4-8	4-11

TABLE 5

Variation of the Structure of Separate Fractions of Cadmium Hydroxide with the Precipitation Conditions

Fraction No.	Density		Porosity, %
	True	Apparent	
Hydroxide	4.8200	0.7746	83.9
I	5.4193	1.6398	69.8
II	4.3804	1.2978	70.6
III	4.8569	1.3246	72.7
IV	6.180	2.1694	64.9
V	4.4525	1.1728	73.6

the adsorption of dyes on the cadmium hydroxide fractions showed Fraction IV to be the least active.

The dyes used for the adsorption experiments differed both in nature and in degree of dispersion. The adsorption of the following dyes was studied: 1) methylene blue (a basic dye, molecularly dispersed); 2) Acid Blue (an anthraquinone dye), and 3) Congo Red (a coarsely disperse direct dye). In all cases normal adsorption isotherms were obtained, as shown in Fig. 2.

The values of the maximum surface saturation of the cadmium hydroxide fractions, calculated from the adsorption isotherms, are given in Table 6.

The data in Table 6 show that dye sorption depends not only on the structure of the adsorbent, but also on the nature and the degree of dispersion of the dye. Thus, the adsorption of the acid dye was greater than that of the basic dye in all cases.

Methylene blue is adsorbed better than the coarsely disperse Congo Red on all the fractions with the exception of cadmium hydroxide (which does not adsorb methylene blue at all) and Fraction V, where the basic nature of the compound evidently plays an important role in addition to the structure factor. The fact that Fraction IV has the lowest adsorptive power for the coarsely disperse Congo Red confirms that this fraction has a finely porous structure.

The active surface of the fractions was determined from the adsorption of benzene vapor and of salicylic acid from benzene solutions (Table 7).

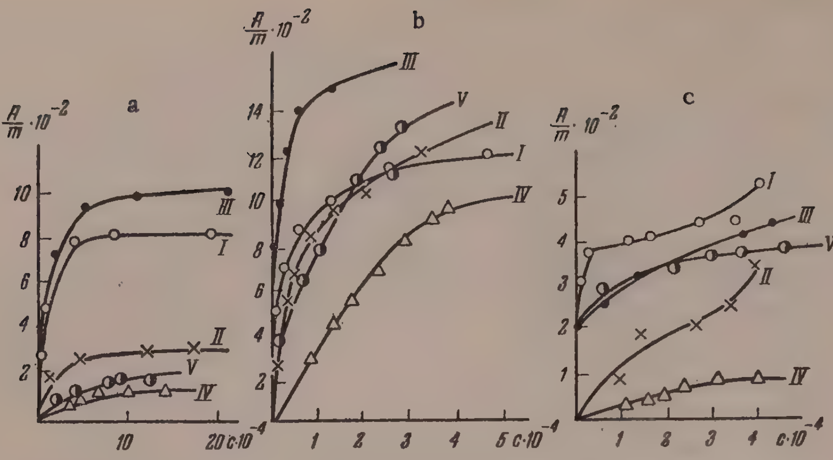

Fig. 2. Adsorption isotherms for methylene blue (a), Acid Blue (b), and Congo Red (c) on cadmium hydroxide fractions I-V.

The data in Table 7 show that the fractions have a fairly large active surface. As was to be expected, Fraction IV is the least active. It is interesting to note that nonpolar benzene is adsorbed very little on fractions containing iodine, and the value of the surface determined from benzene adsorption approaches to the value determined from adsorption of salicylic acid only for Fraction V and cadmium hydroxide. Fraction III is probably coarsely porous, and its active surface is therefore less than that of the other fractions (with the exception of IV). Owing to the presence of large pores, Fraction III adsorbs more of large dye molecules than do the other fractions. Therefore the adsorption of dyes is greater on this than on the other fractions.

TABLE 6

Maximum Surface Saturation of Cadmium Hydroxide Preparations by Dyes

Fraction No.	Amount of dye, in mg per g adsorbent		
	Methylene blue	Acid Blue	Congo Red
Hydroxide	—	86	57
I	90.9	142	45
II	50.0	125	55
III	108.0	180	55
IV	31.4	166	25
V	21.7	173	40

TABLE 7

Adsorptive Characteristics of Different Cadmium Hydroxide Fractions in Terms of the Active Surface

Fraction No.	Adsorbent surface, in m²/g	
	From adsorption of benzene vapor	From adsorption of salicylic acid
Hydroxide	385	426
I	77	399
II	110	366
III	110	320
IV	82	149
V	404	426

SUMMARY

1. The structure and composition of cadmium hydroxide and of complex compounds of cadmium hydroxide and iodide have been studied.

2. It is shown that the complex formed in an alkaline medium contains less iodine than the complexes formed in acid or neutral media.

3. Complexes of the same composition but precipitated at different pH differ in structure and therefore

in adsorptive activity.

4. The particle size of precipitated cadmium hydroxide fractions increases with increasing pH and precipitation temperature.

Institute of Chemistry, Academy of Sciences,
Belorussian SSR Minsk

Received November 19, 1956.

LITERATURE CITED

[1] Z. Ya. Berestneva, T. A. Koretskaya, and V. A. Kargin, Proc. Acad. Sci. USSR 70, 1121 (1948); Colloid J., 13, 323 (1951); 12, 338 (1950); 6, 369 (1949); N. F. Ermolenko and S. A. Levina, Bull. Acad. Sci. Belorussian SSR 1, 107 (1954); Colloid J. 17, 287 (1955);* Trans. 3rd All-Union Conf. Colloid Chem. (Izd. AN SSSR, 1956) p. 276.

[2] F. H. Healey, J. C. Fetsko, and A. C. Zettlemoyer, J. Phys. Chem. 57, 186 (1953).

[3] O. V. Krylov, S. Z. Roginsky and E. A. Forina, Proc. Acad. Sci. USSR 96, 1183 (1954).

[4] G. Urbain and E. Corner, Bull. Soc. Chim. 25, 131 (1919).

[5] P. Job, Ann. Chim. 9, 11 (1923).

[6] S. A. Shchukarev, L. S. Lilich and V. L. Latysheva, J. Inorg. Chem. 225 (1956).

[7] A. G. Bergman and E. L. Bakulskaya, J. Gen. Chem. 26, 625 (1956).*

[8] G. G. Urazov and A. K. Kirakosyan, Ann. Sector Phys.-Chem. Analysis, Inst. General and Inorganic Chem. Acad. Sci. USSR 25, 268 (1954).

[9] A. I. Golub, Ukrain. Chem. J., 19, 205 (1953).

---

* [Original Russian pagination. See C. B. translation].

A STUDY OF CHANGES IN THE STRUCTURAL AND MECHANICAL PROPERTIES OF PHOTOGRAPHIC EMULSIONS DURING DRYING

L. A. Lepilkina

Studies of the structural and mechanical properties of photographic emulsions are of great theoretical and practical importance, as in their physicochemical structure these emulsions constitute a new class of substances, distinct not only from such colloidal materials as clay and dough, but also from gelatin, which is one of the main constituents of photographic emulsions. The question involves the solution of a number of practical problems, foremost among which is the correct choice of optimum drying procedures and conditions. One of the causes of structural changes in photographic emulsions during drying is the stressed state resulting from irregular shrinkage which is the consequence of the existence of considerable moisture gradients along the surface and through the thickness of the emulsion layers. In consequence, stress concentration occurs at individual points of the emulsion layer during drying, leading to changes in the structure of the emulsion, pore formation, and warping of the layer.

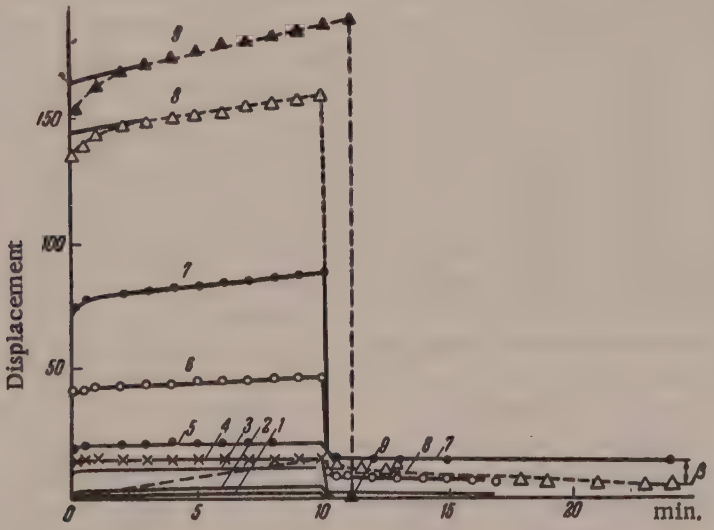

Fig. 1. Curves for the deformation kinetics of a positive emulsion at 450% moisture content and 18° at various stresses ($\tau \cdot 10^3$ kg/cm^2): 1) 0.160; 2) 0.323; 3) 0.668; 4) 1.18; 5) 1.68; 6) 3.06; 7) 6.07; 8) 11.6; 9) 17.3; ρ) degree of structural breakdown; β) degree of structural reinforcement.

The main purpose of the present investigation was to study the structural and mechanical properties of emulsion layers in order to reveal the peculiarities of their physicochemical structure and to determine the rheological characteristics necessary for calculation of the optimum drying conditions. Lykov's investigations [1] showed that the complex structural changes which occur during the drying of moist materials – local destruction, pore formation, changes in the forms of bonding between moisture and the material, transition of the structure from the amorphous into the crystalline state, and others – are caused by tangential stresses. For this reason the structural and mechanical properties of the emulsion layers were studied in shear conditions by means of a modified Gorazdovsky's apparatus [2]. The deformation kinetics under constant load, and the relationship between the tangential stresses and the relative shearing deformations under load applied according to a definite law were studied. The rheological characteristics were calculated by Rebinder's method [3, 4]. The following were studied: a diapositive emulsion with various contents of ammonium and potassium bromides, a positive emulsion, and an emulsion of the "ultrarapid" type with a high silver content. The rheological characteristics were determined at various moisture contents of the materials, from 1030 to 140%, and at 18 and 25°. Figure 1 gives curves for the deformation kinetics at 18° of the positive emulsion at 450% moisture content, which are typical for all the emulsions studied. The rheological characteristics of the diapositive emulsion, determined at 18° and with 816 and 350% moisture contents are given in Table 1. Analysis of the experimental data shows that photographic emulsions are elasticoplastic bodies, with considerable elasticity.

TABLE 1

Variations of the Rheological Parameters of a Diapositive Emulsion with 816 and 350% Moisture Contents at 18°, with the Tangential Stress

τ, kg/cm²	E_1, kg/cm²	E_2, kg/cm²	$\eta_1 \cdot 10^6$	θ, hours	ρ, 50 mm	β, 50 mm
Moisture content 816%						
0.160	0.046	0.069	—	—	4	4
0.276	0.027	0.118	—	—	4	—
0.669	0.038	0.286	—	—	0	—
1.175	0.063	0.503	—	—	0	—
3.090	0.059	0.885	1.58	—	0	—
4.160	0.068	1.780	4.97	20.2	2	—
5.550	0.079	2.370	5.70	20.0	0	—
8.260	0.058	7.110	1.69	8.1	14	—
10.800	0.064	1.160	1.11	4.8	0	—
13.500	0.061	1.650	3.48	15.9	—	27
16.300	0.073	1.990	4.20	16.0	—	18
19.200	0.083	5.820	1.65	5.5	—	20
22.100	0.137	3.160	2.84	5.7	—	80
25.300	0.136	4.350	2.17	4.4	—	84
28.300	0.123	2.700	3.64	8.3	—	46
34.400	0.150	1.970	2.52	4.6	—	38
Moisture content 350%						
3.08	0.266	0.88	—	—	3.5	—
5.99	0.342	2.57	—	—	0	—
8.65	0.370	4.90	—	—	2.0	—
12.80	0.305	3.65	—	—	2.0	—
22.40	0.305	3.19	5.74	5.3	—	1.0
32.40	0.327	3.46	2.08	1.8	—	4.0
42 80	0.307	18.40	2.45	2.2	—	2.0
53.50	0.327	6.54	3.92	3.4	—	0
64.00	0.320	6.85	2.19	2.0	—	8.0
75.00	0.316	9.20	2.56	2.3	—	0
86.50	0.316	14.90	1.27	1.1	—	26.0

At low loads, residual stresses arise in the emulsion layers and the diagrams do not coincide. The magnitude of the deviations, denoted here by ρ, represents the breakdown of the structure. In contrast to other colloidal materials, photographic emulsions have fairly large relaxation times. Consequently a considerable part of the energy used for deformation of the material is concentrated within the emulsion layer, causing complex structural changes. As a result, at certain tangential stresses not only is the emulsion structure completely restored, but it is also reinforced.

A characteristic feature of photographic emulsions is that at a definite stress and a definite moisture content they pass from the elasticoplastic into the elastic state. This indicates that under the influence of the stressed state a qualitatively different structure is formed. The elastic moduli of the emulsion in this new state are 5-10 times as high as in the original state; the relaxation time decreases considerably. The differences between the structures of the emulsion in these states are clearly seen in Fig. 2, which shows electron micrographs with × 10,000 magnification. Figure 2, b is a micrograph of the structure of a positive emulsion after a stressed state has been set up in it. This figure shows that under the influence of the stressed state an entirely new structure is formed in the emulsion layer, different from the original structure shown in Fig. 2, a. It seems likely that owing to the heterogeneous structure of the photographic emulsion stresses are concentrated at individual points in it during drying, leading to displacement of the silver halide grains with formation of groups containing from 2 to 10 grains. It is presumed that part of the moisture passes from the free into the bound state in the process. This new structure has not only different structural and mechanical properties, but evidently also different photographic properties. Similar studies of structural and mechanical properties were also carried out on diapositive emulsions with different ammonium and potassium bromide contents. Table 2 gives the rheological parameters of a diapositive emulsion containing excess potassium bromide at 18° with 400 % moisture content. It is seen from Table 2 that the strength and modulus of elasticity of this emulsion are much lower than those of an emulsion with lower ammonium and potassium bromide contents. With increase of ammonium and potassium bromide contents the structural transition from the elasticoplastic to the elastic state occurs at a higher moisture content. Consequently, these substances are surface-active, and as their content in the system increases the number of bonds at which adsorption of gelatin molecules occurs decreases, leading to weakening of the bonds between the silver bromide crystals and the dispersion medium. The emulsion with the higher potassium bromide content is nearer to gelatin in its structural and mechanical properties. Table 2 gives the rheological characteristics of an "ultrarapid" emulsion, calculated from data obtained at 330% moisture and 20°. Table 2 shows that the strength, elasticity, and plasticity moduli of the "ultrarapid" emulsion, containing 3 times as much silver as the diapositive emulsion, are one third of the corresponding values for the latter. This emulsion, in contrast to the diapositive and positive emulsions, does not show a transition of structure from the elasticoplastic to the elastic state with increase of tangential stress, at any moisture content. This emulsion shows considerable reinforcement at 430% moisture content.

Consequently, the bonds between the individual crystals and the dispersion medium are weaker in emulsions with higher silver bromide contents.

The structural and mechanical properties of these emulsions were also studied at 25°. The rheological characteristics of a diapositive emulsion at 25° and 930% moisture are given in Table 2. Increase of temperature results in a considerable change of the structural and mechanical properties; the elasticity moduli are decreased 3 to 5-fold, and the relaxation time is decreased 5 to 10-fold. The rheological characteristics of an emulsion previously held in the stressed state at 25° were also determined. The determinations were made at 18° and 785% moisture content. An emulsion which had previously been heated in the stressed state has considerably lower elasticity and a shorter relaxation time than an untreated emulsion. A characteristic feature of the diapositive emulsion is that β becomes zero with increase of temperature. The value of β characterizes reinforcement of the emulsion layer, probably by formation of groups of crystals of a complex compound of silver bromide. In this case reinforcement may occur under the influence of the stressed state by formation of a porous structure. A particularly large decrease of strength and elasticity with increase of temperature is found in the "ultrarapid" emulsion. For this emulsion the degree of structure reinforcement (β) at 25° is greater than the reinforcement at 20°. The probable explanation for this is that the mobility of the structure increases with rise of temperature, which leads to an increase in the number of possible groupings of silver bromide crystals when their content in the structure is high. To confirm the validity of the results obtained and to determine the rheological characteristics needed for calculation of the optimum drying conditions for emulsion layers, a study was made of the dependence of the tangential stress on the relative shearing deformation under definite loading conditions which apply during the drying of emulsion layers.

For the diapositive emulsion, the elasticity modulus increases with increasing stress down to 400% moisture content; this indicates considerable reinforcement of the structure. At lower moisture contents the reverse is

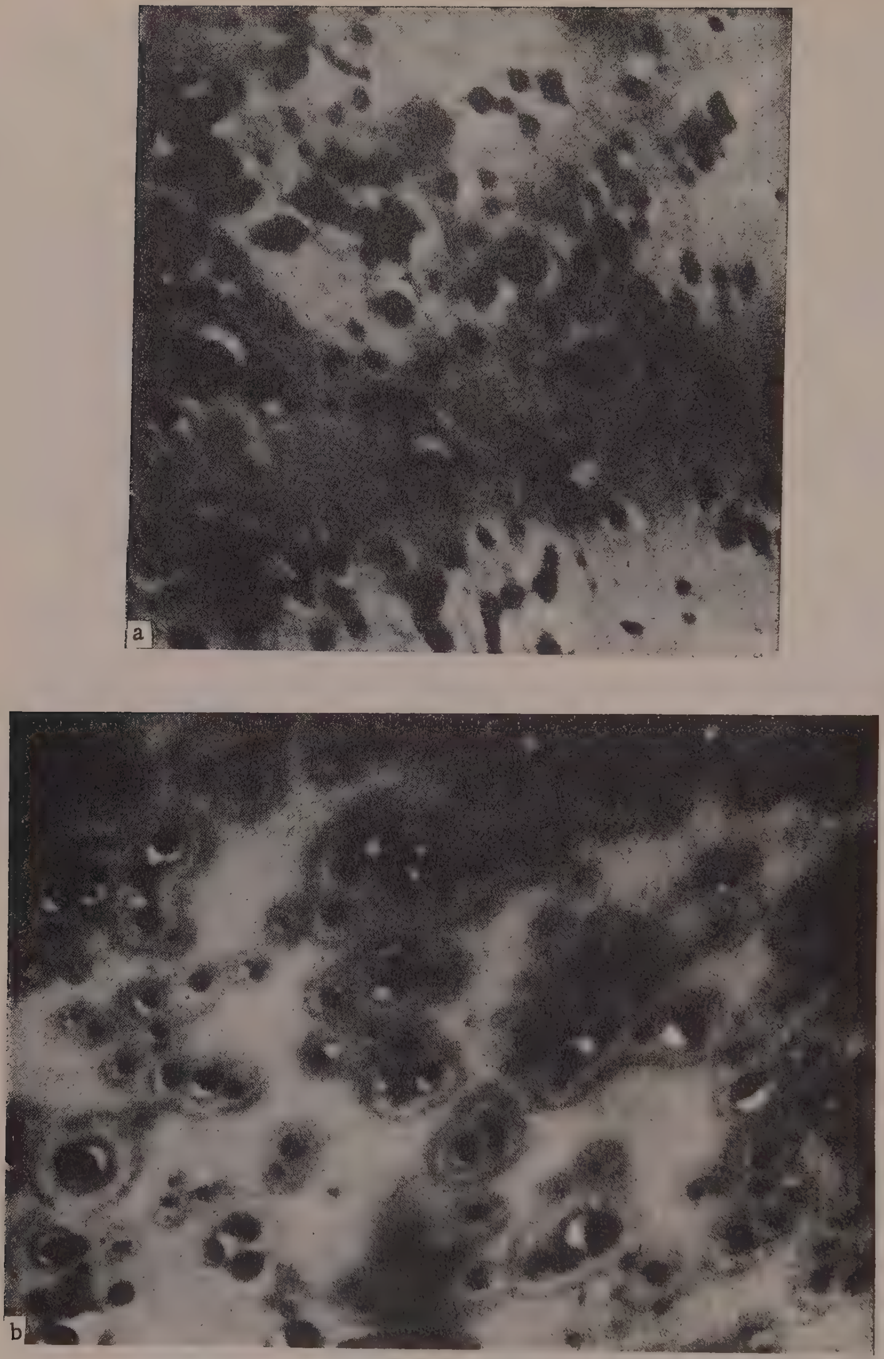

Fig. 2. Electron micrographs of the structure of a positive emulsion: a) before the stressed state; b) in the stressed state.

TABLE 2

Variations of the Rheological Parameters of Different Photographic Emulsions with the Tangential Stress

τ, kg/ cm^2	E_1, kg/ cm^2	E_2, kg/ cm^2	$\eta_1 \cdot 10^6$	θ, hours	ρ 50 mm	β, 50 mm
Diapositive emulsion, 930% moisture at 25°						
0.16	0.0197	0.046	—	—	9	—
0.32	0.0106	0.145	—	—	12	—
0.88	0.0240	0.475	—	—	9	—
1.11	0.0227	0.472	—	—	0	—
2.31	0.0238	0.997	0.198	2.3	8	—
3.33	0.0200	2.840	0.189	2.6	20	—
4.82	0.0186	0.830	0.146	2.2	20	—
6.35	0.0171	0.410	0.146	3.3	5	—
7.85	0.0165	1.680	0.144	2.4	104	—
9.40	0.0159	0.672	0.342	5.9	12	—
Diapositive emulsion with excess potassium bromide, 400% moisture at 18°						
3.06	0.131	13.10	—	—	2	—
5.66	0.121	16.20	—	—	4	—
8.65	0.134	18.50	2.17	4.5	6	—
12.80	0.132	18.30	4.30	9.1	4	—
18.00	0.133	3.86	1.54	1.1	—	7
23.50	0.124	10.00	1.30	2.9	3	—
34.00	0.129	2.93	1.44	3.1	34	—
44.50	0.136	6.35	0.95	1.9	—	60
50.00	0.124	3.57	1.17	2.6	—	26
54:00	0.154	1.93	1.74	3.1	—	25
"Ultrarapid" emulsion, 330% moisture at 20°						
0.16	0.175	—	—	—	4	—
0.32	0.030	1.39	—	—	4	—
1.80	0.057	3.10	1.85	9.1	8	—
3.23	0.054	5.54	0.24	1.2	5	—
5.73	0.051	7.00	0.42	2.3	12	—
8.40	0.051	1.79	0.54	2.3	8	—
10.90	0.053	1.88	0.40	2.1	0	—
16.50	0.057	0.95	0.60	2.9	10	—
21.70	0.056	1.16	0.56	2.8	10	—

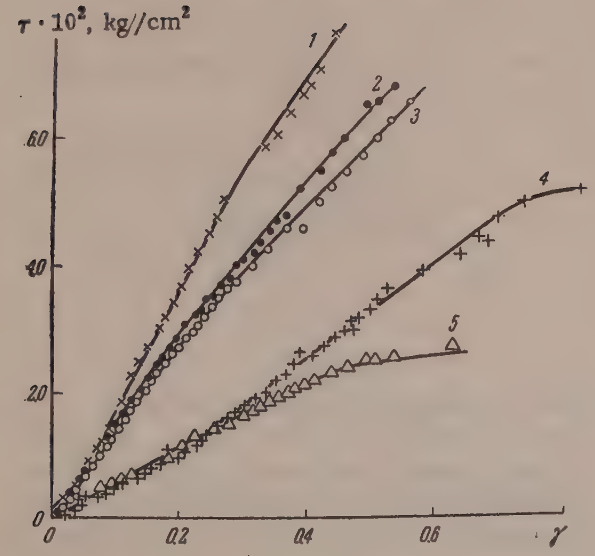

Fig. 3. Variation of tangential stress (τ) with relative shearing deformation (γ) for "ultrarapid" emulsion at 20° and at moisture contents: 1) 140%; 2) 229%; 3) 255%; 4) 440%; 5) 515%.

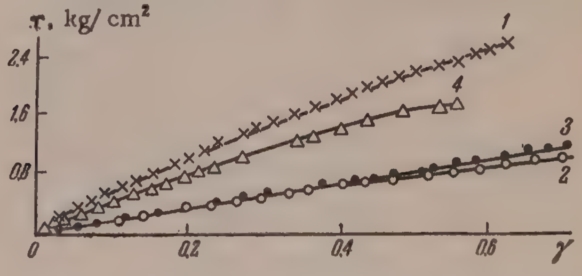

Fig. 4. Variation of tangential stress with relative shearing deformation for "ultrarapid" emulsion at 25° and at moisture contents: 1) 110%; 2) 180%; 3) 350%; 4) 500%.

the case. Figure 3 shows variations of the tangential stress with the relative shearing deformation for "ultrarapid" emulsion at 20° and various moisture contents. It is seen in Fig. 3 that the structure of this emulsion is reinforced only at 440% moisture content; on further decrease of the moisture content the elasticity modulus decreases with increasing stress. These results show that complex structural changes occur in the emulsion layers during the first period and at the start of the second period of drying. On further decrease of moisture content, probably with increasing local stresses, gradual breakdown of the structure takes place. The relationship between the tangential stresses and the relative shearing deformations was also studied for the above emulsions at 25° and with various moisture contents.

Such data for "ultrarapid" emulsion are given in Fig. 4. It is seen that at 25° the degree of structure reinforcement does not increase, as is the case at 18-20°, but decreases with increasing stress; a strength decrease is found even at relatively small loads. There is a sharp decrease of strength with increasing stress at moisture contents below 400%; this is a sign of breakdown in the structure formed at the beginning of the drying process.

SUMMARY

1. A new structure, different from the original structure, is formed during drying of emulsion layers under the influence of the stresses which arise. At a definite moisture content the formation of the new structure is accompanied by transition of the emulsion from the elasticoplastic into the elastic state, characterized by increased strength of the structure and different rheological properties.

2. The rheological characteristics necessary for calculation of the optimum drying conditions of emulsion layers have been determined.

In conclusion, the author expresses her gratitude to Professor A. V. Lykov for valuable guidance and advice during the work.

Scientific Research Institute of Motion
Picture Photography

Received October 1, 1956.

LITERATURE CITED

[1] A. V. Lykov, Heat and Mass Transfer in Drying Processes (State Power Press, 1956). [In Russian].

[2] L. A. Lepilkina, Colloid J. 18, 3, 302 (1956).*

[3] P. A. Rebinder et al., Proc. Acad. Sci. USSR, 72, 85 (1950); 49, 354 (1945); Colloid J., 9, 67, 381 (1947); 10, 223, 466 (1948); 12, 79 (1950).

[4] L. V. Chumakova and P. A. Rebinder, Proc. Acad. Sci. USSR 81, 239 (1951); L. V. Ivanova-Chumakova and P. A. Rebinder, Colloid J., 18, 540, 682 (1956).*

---

* [Original Russian pagination. See C. B. translation].

THE SWELLING OF ION-EXCHANGE RESINS AND THE NATURE OF THEIR SELECTIVITY

V. P. Meleshko and O. N. Myagkoĭ

Studies of the ability of ion exchange resins to change their volume with changes of the ionic composition or concentration of the solution in contact with them are of undoubted interest in relation to the theory of ion exchange chromatography. Many papers published recently are devoted to this question.

The results of investigations carried out in order to determine the laws governing the swelling of ion exchange resins are given below. Variations in the specific volume of a cation exchange resin on swelling in solutions of hydrochloric acid and of alkali and alkaline earth chlorides were studied.

The investigations were carried out with SDV-3 cationic resin, which is a sulfonated polymer of styrene with divinylbenzene containing one type of functional group, SO_3H, in its structure. The specific volume of the swollen resin was determined by measurement of a spherical particle of the resin in contact with the solution in a special cell, with the aid of a microscope. The cell was a compartment made from transparent Plexiglas through which the liquid flowed. The grain of resin was fixed in the cell in a constant position by means of two nickel-plated needles which could be moved by means of screw threads. Grains of strictly spherical shape ~ 1.5 mm in diameter were chosen for the experiments. A diagram of the apparatus is shown in Fig. 1.

The saturating solution was passed slowly through the cell. The grain diameter was measured after a time interval sufficient for equilibrium to be established in the system; this was determined by experiments on swelling kinetics (Fig. 2). After each determination the cell was washed out with distilled water and a fresh portion of the saturating solution was passed through.

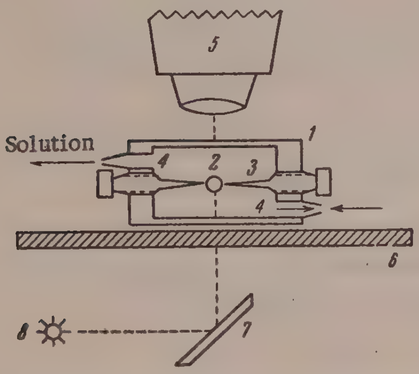

Fig. 1. Scheme of apparatus for microscopic measurement of the volume of swollen ion exchange resin grains: 1) cell; 2) spherical resin sample; 3) nickel-plated needles; 4) orifices for solution; 5) microscope objective; 6) microscope substage; 7) reflecting mirrors; 8) light source

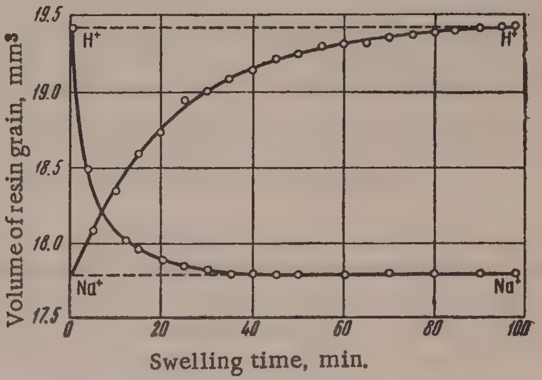

Fig. 2. Rate of swelling of spherical samples of SDV-3 cationic resin in relation to the initial and final ionic states.

All the determinations were performed with the cell in the same position and with a constantly focused microscope objective. The results of the measurements were checked by duplicate experiments, the average results being given in this paper.

Some of the experiments were conducted with artificial grains ~ 3 mm in diameter made from the same resin, which made greater accuracy possible. The grains were made by mixing the powdered resin with a small amount of adhesive made from butyl methacrylate film dissolved in a mixture of equal volumes of ligroin and benzene. It was shown in special experiments that the volume of a butyl methacrylate film remains unchanged even when immersed for a long time in water.

It was possible by the above method to carry out the measurements rapidly in conditions in which the resin is in contact with the saturating solution. This was expected to give results in closer agreement with the true state of the resin in use than any other method, including the pycnometric [1].

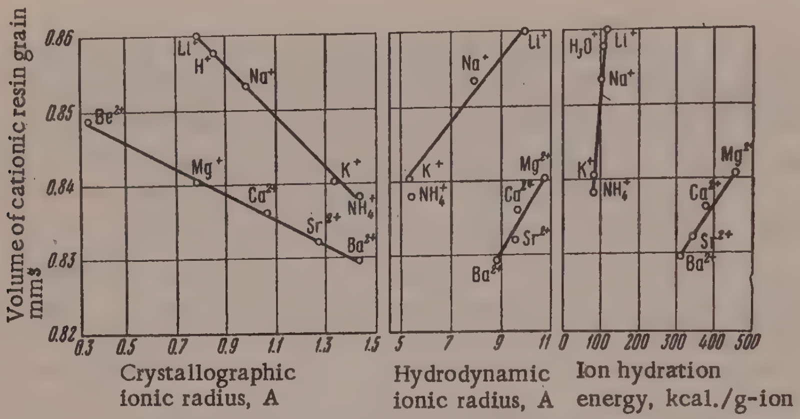

Fig. 3. Variation of the volume of a spherical sample of a swollen cationic resin with the radii of the saturating ions and their hydration energies.

The saturating solutions used for determinations of the effects of the kind of ion present on the volume of the swollen resin grain were 0.1 N solutions of alkali and alkaline earth metal chlorides. The grain volumes in different ionic forms were measured in the following sequence: R – Li, R – H, R – Na, R – K, R – NH_4, and the measurement sequence was then reversed: R – NH_4, R – K, R – Na, R – H, R – Li. The volumes of the cationic resin grain saturated with cations of bivalent metals: R – Be, R – Mg, R – Ca, R – Sr, R – Ba and R – Ba, R – Sr, R – Ca, R – Mg, R – Be, were determined in the same way. The reverse order of saturation served to check both the reproducibility of the results, and the reversibility of the volume change of the swollen resin.

The experiments showed that the specific volumes of the swollen resins form the following sequences:

$$RLi > RH > RNa > RK > RNH_4 \text{ and } RBe > RMg > RCa > RSr > RBa.$$

It is seen that these sequences are the reverse of the known adsorption series [1]:

$$Li^+ < H^+ < Na^+ < K^+ \text{ and } Mg^{2+} < Ca^{2+} < Sr^{2+} < Ba^{2+}.$$

The volume of the resin as a function of the crystallographic and hydrodynamic ionic radii and of the hydration energy of the saturating ions is shown graphically in Fig. 3. The cation hydration energies are taken from Mishchenko's data [2], the ionic radii from Goldschmidt's data [3], and the radii of the hydrated ions from Jenny's data [1]. It is seen from Fig. 3 that, in the alkali and alkaline earth metal series, the specific volume of the swollen resin is an inverse linear function of the radii of nonhydrated ions, and a direct linear function of their hydrodynamic radii and hydration energies.

This law for the volume change of the swollen resin, and its agreement with the adsorbability sequence of the cations studied, accounts for the affinity differences of these cations for a strongly acid cation exchanger such as SDV-3. It is evident that these differences are determined only to a small degree by the forces of chemical bonding between the cations and the active groups of the resin. In the present instance easily dissociated compounds are formed both in the resin phase and in the solution phase [4]. Consequently, the decisive role is played by the hydrated exchange ions.

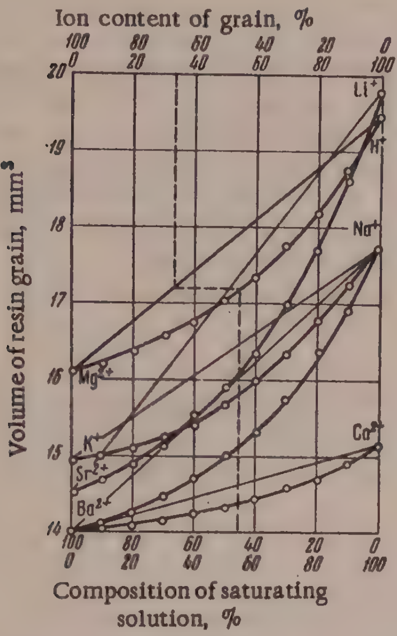

Fig. 4. Variation of the volume of a spherical sample of swollen resin with the composition of a solution of the chlorides of two cations.

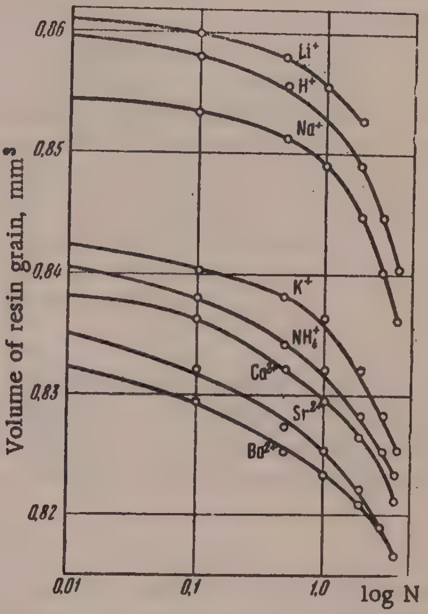

Fig. 5. Variation of the volume of a spherical sample of swollen resin with the concentration of the external solution.

In the absolutely dry resin the spatial network is in a state of least tension. Water entering the particle extends it. Entry of less hydrated ions into the resin is more favorable from the energy aspect than the entry of more highly hydrated ions. This is confirmed by the relationship between the volume of a resin particle in 0.1 N solutions of the chlorides of two cations and the composition of the mixture (Fig. 4). The concave curves in Fig. 4 show the variation of the volume of the swollen particle with the composition of the external solution. The straight lines correspond to the percentage contents of the ions in the resin phase at a given volume. The less the hydrate shell of the ion, the more of it enters into the resin phase. This is seen even more clearly by an examination of the kinetics of swelling of the resin in its conversion into various salt forms (Fig. 2). The process leading to a decrease in the volume of the resin is nearly three times as rapid in the system RH + Na^+ as in the saturation of the Na resin by hydrogen ions.

The effect of the concentration of the saturating solution on the volume of the swollen resin was studied next. The same method as before was used for these experiments. The curves in Fig. 5 show that the volume of the resin grain diminishes regularly with increasing concentration of the external solution. However, the differences between the specific volumes of the resin saturated with different cations persist even at high solution concentrations (up to 4 N). The sequence of the ions in order of their affinity for the resin also remains unchanged.

From the results of these investigations it is possible to draw conclusions concerning the nature of the forces acting in the resin—solution system.

As is known [5], the swelling of ion exchange resins is the result of hydration of active groups and of the gegenions neutralizing these groups, and also of the osmotic pressure which arises at the boundary between the resin particle and the solution. The swelling process and the behavior of the resin can be represented as follows. From the moment when water enters the resin phase, the particle begins to resemble a limited volume of electrolyte solution, and an osmotic pressure is set up between it and the free liquid. The organic framework of the resin, which retains the active groups in a limited volume, acts as a semipermeable membrane toward them, which is, however, permeable to other ions. The membrane action of the spatial resin network is analogous to the action of the semipermeable membranes in living cells, as its elastic forces restrict the amount of water entering the resin phase.

It is seen in Fig. 4 that equal volumes of particles saturated with different ions correspond to different concentrations of the external solutions. For example, the resin has a volume of 0-84 mm^3 in 0.1 N KCl solution and 3.0 N NaCl solution. Evidently under these conditions the elastic forces of the resin framework and the osmotic pressures of the internal solutions will be equal.* It follows from this that the volume of the swollen sample is determined not only by the magnitude of the osmotic pressures of the internal and external solutions and the elastic forces of the spatial network of the resin, as is the case in the swelling of gelatin [6], but also by the magnitude of the hydration energies of the adsorbed ions. Then the volume of a swollen resin sample in contact with a saturating solution will be the function of a number of parameters: π_i, the osmotic pressure of the internal solution; π_a, the osmotic pressure of the external solution; E_a, the energy of hydration of the active groups; E_u, the hydration energy of the gegenions; and *u*, the elastic forces of the spatial resin network. The distribution of the forces on which this volume will depend is determined by the equation

$$\pi_i + Q(E_a + E_u) = \pi_a + CV,$$

where C is the elasticity modulus of the spatial network of the resin; V is its volume increase; and Q is a constant which takes into account the commensurability of the quantities in this equation. The left side of the equation contains factors increase of which favors swelling; the right side contains factors increase of which results in a decrease of the specific volume of the swollen resin.

SUMMARY

1. The volume variations of small spherical samples of SDV-3 cation exchange resin in contact with solutions of alkali and alkaline earth metal chlorides of various concentrations have been studied.

2. It is shown that the volume of the swollen cation exchange resin increases regularly with decreasing crystallographic radii of the ions saturating the resin, and with increasing hydration energy of these ions. The action of the ions strictly corresponds to their positions in the adsorption series for strongly acid cation exchangers.

3. Curves for the variations in the volume of the cation exchange resin in contact with a solution (a mixture of two cations in various proportions) and curves for the rate of volume change in the conversion of the resin from one ionic form into another show that ions, the sorption of which leads to a decrease of volume of the swollen cation exchange resin, are the ions which are preferentially adsorbed.

4. The decreased differences between the volumes of the swollen resin with increasing concentration of the external solution correspond to the decreased selectivity of the ion exchangers found in such cases.

5. The investigations confirmed that the main cause of selectivity in the adsorption in the series of ions which form highly ionized compounds with the active groups of the resin lies in differences between the forces exerted from the exchanging ions against the elastic forces of the spatial resin network.

The Voronezh State University, Chair of
Inorganic Chemistry

Received November 26, 1956.

LITERATURE CITED

[1] R. Kunin and R. Myers, Ion Exchange Resins (IL, Moscow, 1952) [Russian translation].

[2] K. B. Yatsimirsky, Thermochemistry of Complex Compounds (Izd. AN SSSR, Moscow, 1954).

[3] Chemist's Reference Book, vol. 1 (State Chem. Press, Leningrad–Moscow, 1951) p. 288.

---

* Apart from certain concentration differences of the internal solutions with equal volumes of the sample, due to the Donnan effect.

[4] D. I. Ryabchikov, in coll.: Investigations in the Field of Chromatography (Izd. AN SSSR, Moscow, 1952) p. 234.

[5] H. P. Gregor, J. Am. Chem. Soc. 70, 1293 (1948).

[6] W. Bauman, in coll.: Ion Exchange (IL, Moscow, 1951) p. 49. [Russian translation].

THE ~~SOLUTION~~ STATE OF DIRECT DYES AND THEIR DIFFUSION IN A CELLOPHANE FILM

B. N. Mel'nikov and P. V. Moryganov

We have shown [1, 2] that the activation energy of diffusion of a number of direct dyes depends to a considerable extent on the neutral electrolyte concentration in the dye bath. For some dyes which tend to aggregate, there is an abrupt change in the activation energy in the transition from low temperatures (40-60°) to higher temperatures (70-100°). Addition of dispersing agents to the dye bath increases the diffusion coefficients and decreases the activation energy of diffusion, i.e., facilitates penetration of the dyes into the fiber. To explain these facts, we suggested that a relationship exists between the aggregation state of dyes in solution and their rate of penetration into the fiber. The purpose of the present investigation was to confirm this hypothesis experimentally. The work was accordingly divided into two parts:

1. Study of the diffusion of a number of direct dyes in solution over a wide range of temperatures and electrolyte concentrations.

2. Study of the diffusion of the same dyes in Cellophane in presence of dispersing agents in the system.

The diffusion of direct dyes in solution has been studied before [3, 4] for determination of particle size, but the investigations were mainly confined to 25°. At higher temperatures, diffusion in solution has been studied for five dyes: Benzopurpurine 4B and its meta isomer (Lenher and Smith [5]), Chicago Sky Blue 6B (Valko [6]), Chrysophenine, and Direct Fast Orange SE (Holmes and Standing [7]). It is difficult to use the results of these investigations for solving the present problem, owing to the great differences in the experimental procedures used.

We used the method of Northrop and Anson [8] for determining the diffusion coefficients of dyes in solution. In this method the two solutions between which diffusion occurs are separated by a porous sintered glass plate. If in the steady state the solution concentrations on the two sides of the porous plates are c_1 and c_2 respectively, the diffusion in this plate can be represented by the equation

$$\frac{dm}{dt} = {}_{c_2}\overline{D}_{c_1}\,\frac{\overline{A}}{L}\,(c_2 - c_1), \tag{1}$$

where ${}_{c_2}\overline{D}_{c_1}$ is the average coefficient of diffusion; L is the effective thickness of the plate; $\overline{A}$ is the effective average free surface of the plate.

In this method the diffusion coefficient is found from the increase in the dye solution concentration on one side of the plate, i.e., the dye concentration changes continuously during the experiment. A solution of Equation (1) with these concentration changes taken into account was given by Holmes and Standing [7]

$$\overline{D}\alpha = \frac{2\lambda}{(\lambda+1)\tau}\cdot\log\frac{c_1}{c_1-(\lambda+1)\,c_2}, \tag{2}$$

where α is a calibration constant for the diffusion cell; τ is the time during which the diffusion was observed; λ is the ratio of the solution volumes on the two sides of the plate; c_1 is the concentration of the dye in the inner vessel at the start of the experiment (when the dye concentration in the outer solution is zero); c_2 is the dye concentration in the outer solution after time τ.

In our studies of the effect of dispersing agents on the diffusion rates of direct dyes in Cellophane film in stationary conditions the diffusion coefficients were calculated from Fick's equation

$$\frac{ds}{dt} = DA\frac{dc}{dx} \quad (3)$$

or

$$D = \frac{bP}{A(c_2 - c_1)}, \quad (4)$$

where P = ds/dt, the amount of dye in mg/minute diffusing through the film in unit time; b is the film thickness in cm; A is the area of the film in cm^2; c_2 and c_1 are the dye concentrations on either side of the film in mg/cc.

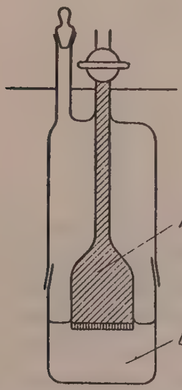

Fig. 1. Diagram of apparatus for determining the diffusion coefficients of dyes in solution.

The experiments on diffusion in solution were performed with three direct dyes; Direct Diazo Black C (CI 401), Direct Sky Blue K (CI 406), and Direct Diazo Black O (CI 395) at 25, 35, 60 and 80°. All the dyes were purified and analyzed by the method described previously [9]. The concentration of electrolyte, which was common salt, was varied from 0 to 20 g/liter for Diazo Black C and Sky Blue K, and from 0 to 0.5 g/liter for Diazo Black O. The reason for the lower electrolyte concentrations used for the latter dye is the possibility of its coagulation at high salt concentrations. The apparatus shown in Fig. 1 was used for determining the diffusion coefficients in solution.

The apparatus consists of the vessel A, terminating in a porous glass plate in the form of a disk 3 cm in diameter and ~ 0.2 cm thick. The approximate diameter of the pores in the plate is ~ 5-15 μ. The top part of vessel A is firmly closed by a well-ground stopcock. The vessel A was filled with the solution of dye and electrolyte and inserted into the vessel B, containing the electrolyte. The porous glass plate must only just touch the solution surface in vessel B. The whole apparatus was then put into a thermostat with the temperature kept constant to within ± 0.1°. At the end of a definite time, usually about 2-3 hours, required to establish thermal equilibrium and a concentration gradient in the plate, the solution was poured out of vessel B, and vessel A was very quickly transferred into another vessel B containing a solution of the same composition and temperature as in the first vessel B. The solution in vessel B was then analyzed at definite time intervals and the diffusion coefficients were calculated by means of Equation (2).

Equation (2) contains the calibration constant α, and therefore the apparatus was calibrated before the experiments with a substance of which the diffusion coefficient is well known. Chrysophenine dye was used for this purpose. The diffusion coefficients for this dye were determined very carefully by Holmes and Standing [7] who found, with the use of porous glass plates, that the calibration constants of the diffusion vessels changed gradually and irreversibly in the transition from lower to higher temperatures. We therefore repeated the calibrations by passing from lower to higher temperatures. However, we did not find any significant changes in the calibration constants. The changes did not exceed 5 % over the entire range studied. Some dyes, including Direct Diazo Black O, are adsorbed by the porous plate during the experiments. The apparatus was therefore washed thoroughly after each experiment. The results are given in Figs. 2, 3, and 4.

In studies of diffusion in Cellophane film, Direct Pure Blue (CI 518) was also used, in addition to the above dyes. The temperature in these experiments was varied from 25 to 85°. The dispersing agent used was pyridine, at concentrations of 80 and 200 g/liter. In addition, experiments were carried our for comparison

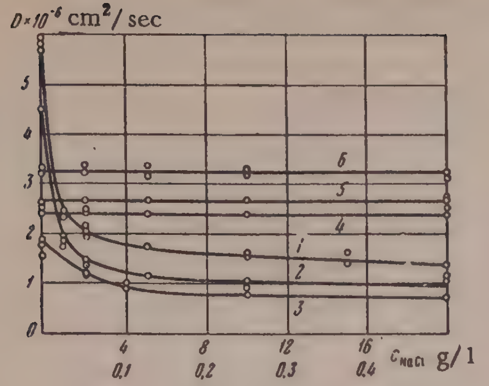

Fig. 2. Variation of the diffusion coefficients of direct dyes in solution with electrolyte concentration at 25°: 1) Direct Sky Blue K; 2) Direct Diazo Black C; 3) Direct Diazo Black O; 4,5,6) the same dyes, in presence of 200 g pyridine per liter.

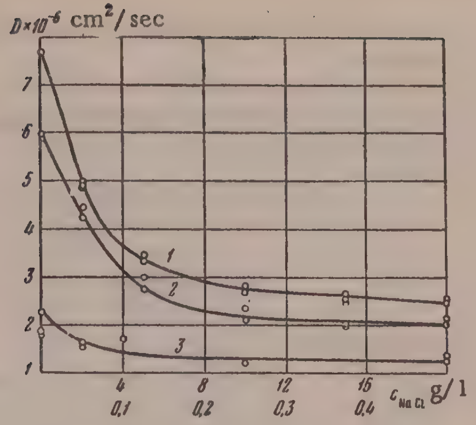

Fig. 3. Variation of the diffusion coefficients of direct dyes in solution with electrolyte concentration at 35°: 1) Direct Sky Blue K; 2) Direct Diazo Black C; 3) Direct Diazo Black O.

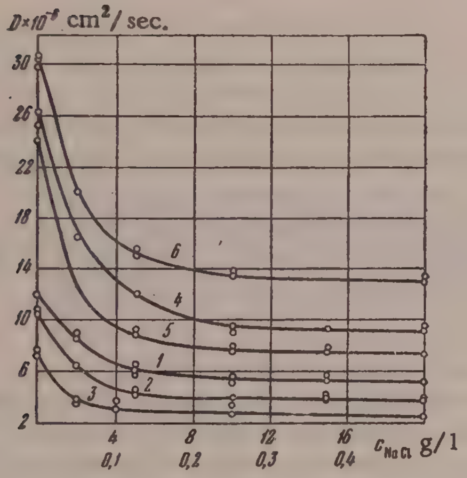

Fig. 4. Variation of the diffusion coefficients of direct dyes in solution with electrolyte concentration at 60 and 80°: 1,2, and 3) Direct Sky Blue K, Direct Diazo Black C, and Direct Diazo Black O at 60°; 4,5, and 6) the same, at 80°.

without addition of pyridine at 65, 75, and 85°. The experiments were carried out in U-shaped vessels, consisting of two parts separated by a Cellophane film. The thickness of the film was measured by means of a micrometer, and had the average value of 35 μ. The diameter of the film was 3.5 cm. Glycerol was carefully washed out of the film before the experiments. A solution containing the dye, common salt, and pyridine was put into one part of the vessel, and a solution containing the same components but without dye was put into the other. The apparatus was placed in a thermostat at a definite temperature. The temperature was controlled, as in the first series of experiments, to within ± 0.1°. The amounts of dye which passed through the membrane were then determined colorimetrically after definite time intervals. The time required to reach the steady state was determined by Barrer's method [10]. The diffusion coefficients of direct dyes in stationary conditions were calculated by means of Equation (4); the results are given in Table 1.

DISCUSSION OF RESULTS

The results in Figs. 2, 3, and 4 show that the coefficients of diffusion of direct dyes in solution greatly depend on the electrolyte concentration in the system. In pure water, owing to the action of the diffusion potential, the diffusion coefficients of dyes are abnormally high, and cannot be used for characterization of the state of dispersion of the system. Very small additions of electrolyte to the system greatly influence the diffusion potential and cause a sharp decrease in the diffusion coefficients of dyes. Increase of electrolyte concentration results in a further lowering of the diffusion potential and hence of the diffusion coefficients. However, as is seen in Figs. 2, 3, and 4, the subsequent fall of the diffusion coefficients is more gradual. This region of the curves can serve to characterize the dispersion state of dyes in solution, and can be used for calculations of the particle sizes of dyes by means

TABLE 1

Average Coefficients of Diffusion of Direct Dyes through Cellophane Film in Stationary Conditions

Pyrdine concentration in g/liter	Diffusion coefficient $D \cdot 10^{-7}$ cm²/min at temperatures						
	25°	35°	45°	55°	65°	75°	85°
				Direct Sky Blue K			
200	2.07	3.12	4.50	7.05	10.30	14.26	20.10
80	2.06	3.33	5.38	8 12	12.30	18.60	26.90
Without pyridine	—	—	—	—	1.22	2.80	6.11
				Direct Diazo Black C			
200	2.25	3.65	4.87	7.50	—	15.85	22.3
80	1.44	2.31	3.47	5.25	7.59	11.50	15.90
Without pyridine	—	—	—	—	1.02	2.57	5.50
				Direct Pure Blue			
200	—	3.32	4.96	7.50	10.90	14.90	21.11
80	2.46	3.47	—	9.30	14.40	19.90	30.00
				Direct Diazo Black O			
200	2.31	3.65	4.87	8.70	—	18.60	26.0
80	—	—	Coagulates		—	—	—
Without pyridine	—	—	Coagulates		—	—	—

of the Stokes–Einstein equation. The use of the Stokes–Einstein equation involves certain difficulties in this case because the dye particles are far from spherical in shape, and therefore the particle sizes as determined by this equation will not be absolute values, but can only serve as qualitative indications of changes in the degree of dispersion of dyes under particular experimental conditions. Nevertheless, this characterization of the dispersion state of the system is quite sufficient for solution of the problem in question. The values of the dye particle radii calculated from the average diffusion coefficients for the linear portion of the curves in Figs. 2, 3, and 4 are given in Table 2.

Table 2 shows that the dyes undergo progressive dispersion with increase of temperature, the process being fairly uniform over the whole temperature range studied in the case of Direct Sky Blue K and Diazo Black C. In contrast to this, in the case of Direct Diazo Black O the particle size decreases slightly in the range between 25 and 60°. At 60° the dispersion of the particles of this dye is accelerated, and the particle size is decreased sharply at 80°. It should be noted that the electrolyte concentration in solution at 80° in this case of this dye may be insufficient to eliminate the diffusion potential completely, and therefore the value of the diffusion coefficient in this case may be somewhat high. However, the fact that the diffusion coefficient of this dye increases sharply in the temperature range from 60 to 80° itself indicates that the particle size is sharply reduced as the result of the supply of heat from outside.

The results confirm our earlier hypothesis [1] that there is a relationship between the diffusion rate of a dye in the fiber and its state of aggregation in solution. Thus, we have shown [1] that in the temperature range between 70 and 100° there is a sharp increase of the coefficients of diffusion of Direct Diazo Black O in the fiber. For Direct Sky Blue K and Diazo Black C the coefficients of diffusion in the fiber increase without abrupt jumps, which is in full agreement with the observed behavior of these dyes in solution; the changes in their particle size occur smoothly and uniformly with a continuous reduction as the temperature increases. This is in all probability due to the higher degree of hydration of the anions of these dyes and hence to their greater stability in solution even at low temperatures.

The behavior of all these dyes in pyridine solution is somewhat different (Fig. 2). In this case the diffusion

TABLE 2

Effect of Temperature and Additions of Pyridine on the Particle Size of Direct Dyes in Solution

Dye	Temperature, °C	Particle radius x 10^8cm	
		Without pyridine	In presence of pyridine
Direct Sky Blue K	25	15.90	9.62
	35	11.95	–
	60	9.75	–
	80	8.51	–
Direct Diazo Black C	25	21.81	8.75
	35	15.50	–
	60	12.80	–
	80	10.35	–
Direct Diazo Black O	25	26.80	7.15
	35	21.90	–
	60	20.40	–
	80	5.98	–

coefficients do not decrease sharply on addition of electrolyte to the solution. The variation of the diffusion coefficients with electrolyte concentration remains linear over the whole range of NaCl concentrations studied. An explanation for this behavior of the dyes in presence of pyridine in solution is that in this case the influence of the diffusion potential is diminished by the cations of pyridine itself, and therefore when common salt is added to the solution the diffusion coefficients do not decrease as sharply as in experiments without pyridine.

Another interesting fact revealed in the study of dye diffusion in pyridine solutions is that the diffusion coefficients of all the dyes are increased sharply in this case. The size of the dye particles decreases accordingly, i. e., pyridine acts in the same direction as increase of temperature. The results once again confirm that there is a relationship between the diffusion rates of dyes within the fiber and their state of dispersion in solution. Thus, the experiments on the diffusion of dyes through Cellophane films (see Table 1) show clearly that when pyridine is present in solution the diffusion of dyes in the film is accelerated approximately 10-fold. It must be pointed out that in absence of pyridine the dyes do not diffuse through the film at all at temperatures below 65°, and therefore the difference between the diffusion rates will be very great. As the temperature increases, this difference diminishes and at 85° the diffusion rates of the dyes differ only by a factor of 2 to 3. The reason is that the effect of temperature on changes of the degree of dispersion of the dyes, and therefore on their rates of diffusion in the film, is most pronounced when pyridine is not present in the solution. The addition of pyridine itself greatly favors disaggregation of the dye particles, and therefore the influence of temperature is less pronounced in this case.

Fig. 5 gives the relationship between the temperature and the rates of diffusion of dyes through the film in $\log D - 1/T$ coordinates, in accordance with the Arrhenius equation

$$\log D = B - A/T.$$

The activation energies of diffusion of the dyes in the film, determined from the slopes of the straight lines in Fig. 5, are given in Table 3.

In full agreement with the foregoing, the activation energy of diffusion in presence of pyridine in the solution is only about one half of the activation energy of diffusion in absence of pyridine.

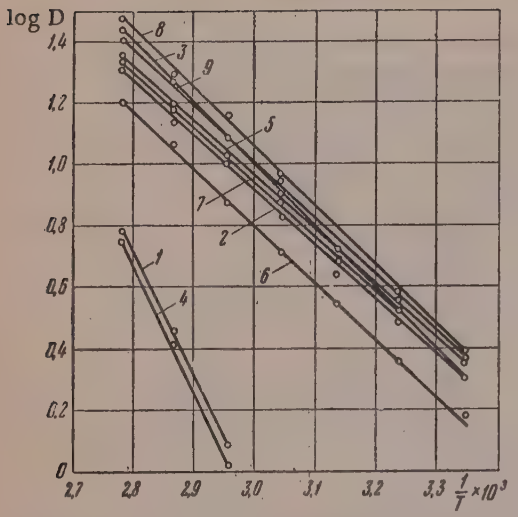

Fig. 5. Logarithmic relationship between the diffusion coefficients of direct dyes in the film and the reciprocal of the absolute temperature: 1) Direct Sky Blue K; 2) the same, with 200 g/liter of pyridine; 3) the same, with 80 g/liter of pyridine; 4) Direct Diazo Black C; 5) the same, with 200 g/liter of pyridine; 6) the same, with 80 g/liter of pyridine; 7) Direct Pure Blue with 200 g/liter of pyridine; 8) the same, with 80 g/liter of pyridine; 9) Direct Diazo Black O with 200 g/liter of pyridine.

TABLE 3

Energy of Activation of Diffusion of Direct Dyes in kcal /mole

Dye	Activation energy of diffusion at pyridine concentration		
	200 g/l	80 g/l	without pyridine
Direct Sky Blue K	8.09	9.20	18.70
Direct Diazo Black C	8.15	8.55	19.60
Direct Pure Blue	8.22	8.43	–
Direct Diazo Black O	8.38	–	–

A very remarkable fact is that the diffusion coefficients in the film of such dyes as Direct Sky Blue K and Direct Pure Blue are somewhat higher at pyridine concentration of 80 g/liter than at 200 g/liter. This indicates that the increase of the diffusion coefficients of dyes with increasing pyridine concentration in the bath is not unlimited, but passes through a maximum, after which the diffusion coefficients begin to decrease with increasing pyridine concentration. This relationship between the diffusion coefficients and the pyridine concentration in solution is probably the consequence of a decrease in the concentration of active water molecules at high pyridine concentrations in solution. The degree of hydration of the dye particles is therefore decreased, and their stability in solution is therefore less. These results show that by addition of suitable dispersing agents to the dye bath it is possible, without risk of aggregation, to increase very sharply the concentrations of the dye and neutral electrolyte and consequently to raise the dyeing rate. This is especially important in relation to acceleration of high-speed continuous dyeing processes.

SUMMARY

1. The coefficients of free diffusion in solution for three dyes over a wide range of temperatures and electrolyte concentrations, and also the diffusion coefficients of four dyes in Cellophane film with varying degrees of dispersion of the dyes in solution, have been determined.

2. A definite relationship exists between the degree of dispersion of the dyes in solution and their coefficients of diffusion in the film; in all cases the rate of penetration of the dyes through the film increases and the activation energy of diffusion diminishes with increasing degree of dispersion of the dyes in solution.

3. By addition of dispersing agents to the dye bath it is possible to increase considerably the concentrations of the dye and neutral electrolyte, and hence to raise the dyeing rate without the risk of producing surface dyeings which are not fast to rubbing.

The Ivanov Institute of Chemical Technology
Laboratory of the Chemical Technology of Fibrous Materials

Received November 2, 1956.

LITERATURE CITED

[1] B. N. Melnikov and P. V. Moryganov, Colloid J., 18, 566 (1956).*

[2] B. N. Melnikov and P. V. Moryganov, Colloid J., 18, 711 (1956).*

[3] E. Valko, Colloidochemical Principles of Textile Technology (State Light Industry Press, 1940) p. 369. [In Russian].

[4] T. Vickerstaff, The Physical Chemistry of Dyeing, (1954) p. 68.

[5] S. E. Lenher and J. E. Smith, J. Am. Chem. Soc. 57, 497 (1935).

[6] E. Valko, J. Soc. Dyers Col. 55, 173 (1939).

[7] F. H. Holmes and H. A. Standing, Trans. Faraday Soc. 41, 542 (1945).

[8] J. H. Northop and M. L. Anson. J. Gen. Physiol. 12, 543 (1929).

[9] P. V. Moryganov and B. N. Melnikov, Colloid J., 18, 49 (1956).*

[10] R. Barrer, Diffusion in and Through Solids (IL, Moscow, 1948) p. 33. [Russian translation].

---

* Original Russian pagination. See C. B. translation.

ELECTRON-MICROSCOPE STUDY OF THE STRUCTURE OF ALUMINOSILICATE HYDROGELS BY THE REPLICA METHOD

Ya. V. Mirsky

Many adsorbents and catalysts pass through the hydrogel stage in the course of preparation. Studies of the structure of such systems are of great interest, as they can yield data characterizing the formation of adsorbents and catalysts. Several papers dealing with electron microscopy of hydrogels have been published in recent years. Berestneva, Koretskaya, and Kargin [1] studied colloidal silicic acid; Ashley and Innes [2] investigated aluminum hydroxide and an aluminosilicate catalyst; and Levina and Ermolenko [3] studied the hydroxides of aluminum, chromium, and iron. All these investigations were carried out by direct observation of hydrogel samples in the electron microscope; the shape and size of the gel particles could be observed.

Nevertheless, the potentialities of electron microscopy for studies of hydrogel structure, i.e., of relative disposition and character of the bonds between the hydrogel particles, are limited, as the hydrogel undergoes shrinkage and deformation owing to drying of samples while the observations are being made and the photographs taken.

It is known that in studies of the structure of rubber mixtures [4] and collagen [5] it proved possible to obtain replicas reproducing the structure of the colloidal substances under investigation. It was therefore of interest to apply the replica method for studying the structure of hydrogels; this was done in the present investigation with a sample of pelleted aluminosilicate catalyst.

The procedure was as follows: the pellets of the aluminosilicate catalyst hydrogel, washed free from salts, were split into halves under slight compression; the cleavage surface was covered with a drop of a solution of nitrocellulose in amyl acetate, which flowed in an even and thin layer over the surface; after drying, the lacquer replica was cut along the edges and separated by immersion of the hydrogel into water; the replica was taken out of the water by means of the specimen holder screen of the electron microscope, shadowed with gold, and investigated.

It is known that amyl acetate has very low surface tension at interfaces with water; this is used in electron microscopy for production of structureless films from nitrocellulose solutions on water surfaces. It was therefore to be expected that amyl acetate lacquer would give a high degree of definition in the reproduction of the surface details on the replica. In all probability the nature of the microrelief of the split hydrogel surface is determined by the presence of a hydrogel framework and by the form in which water is bound to the gel substance; in particular, it is evident that free water cannot give rise to a microrelief. It is also quite probable that variations of the distance between individual elements of the hydrogel framework and the amount of adsorbed water should influence the dimensions of the microrelief details.

The replica method was used to study changes in the structure of the aluminosilicate catalyst during drying; replicas of the original hydrogel and of partially dried specimens were made.

Micrograph 1 is an electron micrograph of a replica from the surface of the original specimen, and 2, of a specimen formed by removal of ~ 75% of the water initially present in the hydrogel. Both replicas show a microrelief on the hydrogel surface, which is evidence for the existence of a hydrogel framework, to a certain extent differentiated from the intermicellar liquid. The details of the surface relief do not have clearly defined boundaries; this is probably due to the absence of a sharp boundary between the water of the hydrate shells of the micelles forming the hydrogel framework and the free water in the interstices of the framework.

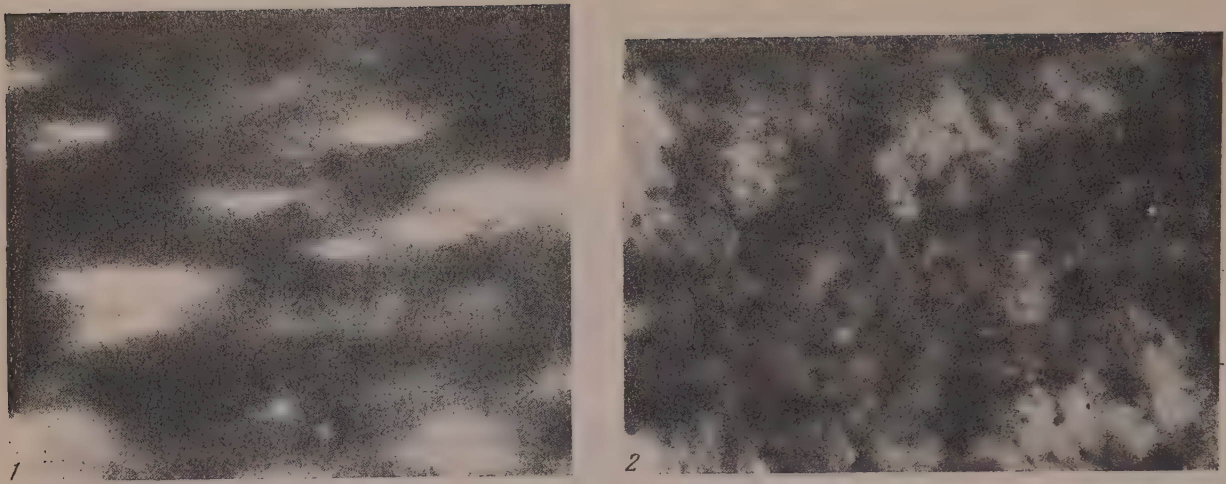

Electron micrographs (colloidion replica, magnification 15,000) of pelleted aluminosilicate catalyst with 90% moisture (1), and of the same specimen after removal of 75% of the water present (2).

Comparison of the two micrographs shows that the surface microrelief becomes finer and more complex as the hydrogel is dehydrated. While in Micrograph 1 considerable regions of the surface are almost entirely smooth (of the same shade), Micrograph 2 clearly shows an extensive microrelief structure, with individual details of several hundred angstroms in size. Replicas made from specimens with moisture contents intermediate between those of the specimens studied show an intermediate character of the hydrogel structure.

The closer approach of the micellar groups resulting from dehydration of the hydrogel cannot in itself be the cause of the observed structural changes. A change in the dimensions of the hydrate shells is also necessary. If this was not the case, the hydrogel surface would become smoother than before as the result of partial dehydration.

SUMMARY

1. Investigations of the structure of aluminosilicate hydrogel by means of the electron microscope showed the hydrogel has a microheterogeneous structure; this is direct evidence that it contains a micellar framework differentiated to some extent from the intermicellar liquid.

2. The micellar groups come closer together and the dimensions of the hydrate shells decrease with dehydration of the hydrogel.

The Grozny Petroleum Scientific Research Institute

Received July 23, 1956.

LITERATURE CITED

[1] Z. Ya. Berestneva, T. A. Koretskaya, and V. A. Kargin, Proc. Acad. Sci. USSR, 70, 1121 (1948); Colloid J. 13, 323 (1951).

[2] K. D. Ashley, and W. B. Innes, Ind. Eng. Chem. 44, 2857 (1952).

[3] S. A. Levina and N. F. Ermolenko, Colloid J. 17, 487 (1955).*

[4] K. A. Pechkovskaya, S. L. Pupko and B. A. Dogadkin, Colloid J. 12, 367 (1950).

[5] A. L. Zaides and S. L. Pupko, Proc. Acad. Sci. USSR 73, 379 (1950).

---

* Original Russian pagination. See C. B. translation.

GENERAL PRINCIPLES OF FORMATION OF METAL ALLOY ORGANOSOLS AT THE CATHODE IN A TWO-LAYER BATH

E. M. Natanson and N. N. Kozachek

It is known that simultaneous liberation of different metals at the cathode is possible only if their deposition potentials differ only slightly. Formation of alloys at the cathode then occurs mainly at fairly high cathode polarizations. Various surface-active agents, either of low or of high molecular weight, are usually added to the electrolyte in order to bring the deposition potentials of different metals closer together and to raise cathode polarization. The number of such additions is fairly large, and their effects on metal deposition and alloy formation at the cathode have been studied in detail.

However, no general laws have yet been established which would make it possible to classify the very considerable number of such substances into groups according to the nature of their action on electrode processes. Therefore at present they are usually selected on an empirical basis.

The formation of saturated layers of adsorbed surface-active substances on the cathode retards the discharge of predominantly those metal ions the equilibrium potentials of which correspond to the stability of these adsorbed layers. It is also necessary to take into account the depolarizing action of electropositve metals, which often decreases the deposition potentials of other, less positive components of the mixture.

The electrolyte composition has a significant influence on the deposition of alloys, Solutions of complex salts of the corresponding metals are generally used. This brings the equilibrium potentials of the different metals closer together. The proportions of the components in the alloy greatly depend on the nature and configuration of the polarization curve for each individual metal under the particular electrolysis conditions, and on the concentrations of these components in the electrolyte.

Apart from the above general considerations, in the electrolytic production of metal alloy organosols [1] it is also necessary to take into consideration the special circumstances when the electrolysis is carried out in a two-layer bath. The cathode which rotates horizontally in the upper oil layer touches the lower aqueous layer — the electrolyte solution — by only a part of its surface. Therefore the crystallization centers which form on its surface are rapidly transferred into the organic medium, which washes them off the cathode surface owing to the presence of surface-active substances. The cathode surface is thus continuously renewed and becomes coated with an adsorbed layer of surface-active substances and of the organic medium, which results in very strong cathode polarization, reaching 4-5 v in some cases. In such conditions the deposition potentials of a number of electropositive metals are increased so much that they become equal to or often even exceed the deposition potentials of typical electronegative metals (Zn, etc).

This sharp increase of cathode polarization in a two-layer bath occurs under the influence of a number of factors which cause continuous passivation of its surface. Thus, the discharge of ions on the cathode surface occurs at a considerable overvoltage, and only at individual places of the cathode surface, which are not covered with an insulating layer of surface-active substances and dispersion medium.

Electrocapillary effects [2] play a considerable role in electrolysis in a two-layer bath; they cause desorption of molecules of the surface-active agents and dispersion medium from the cathode surface when it is in the aqueous layer, and readsorption of these substances when this surface reenters the organic layer and leaves the zone in which metal ions are discharged. The ratio of the rates of these two processes determines the total cathode area at which metal ions are discharged during motion of the cathode. Under such conditions the true current density at individual regions of the moving cathode surface becomes especially high. In such regions the rate of metal ion discharge is very high; this greatly favors the formation of highly disperse particles of metal alloys. Adsorption of surface-active substances on the surface of such particles assists their removal from the cathode surface, protects them against aggregation, and to a considerable extent retards their oxidation.

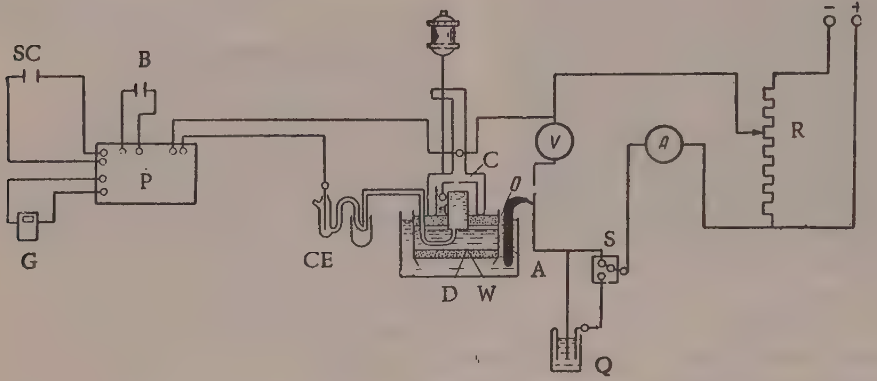

Fig. 1. Diagram of apparatus: C) rotating roller cathode; A) anode; O) upper organic layer; W) lower aqueous layer; D) ceramic diaphragm; CE) calomel electrode; P) potentiometer; B) battery; SC) standard cell; G) galvanometer; Q) coulometer; S) commutator switch; R) potential distributor.

In the preparation of alloys we were guided by the extensive experimental data accumulated in our laboratory (Institute of General and Inorganic Chemistry of the Academy of Sciences, Ukrainian SSR) over a number of years, on the cathodic deposition of colloidally disperse metal powders and on the formation of metal organosols.

In this paper we give the results of an experimental study of the cathodic formation of lead–tin, nickel–chromium, and nickel–iron alloys in a two-layer electrolytic bath, the upper layer of which is an organic medium containing dissolved surface-active substances, and the lower layer is an aqueous electrolyte solution. The apparatus is shown schematically in Fig. 1, and was described in detail in earlier publications [3].

Organosols of lead–tin alloys. In the electrolytic deposition of lead–tin alloys considerable difficulties arise mainly because of the limited number of anions which form soluble salts in the simultaneous presence of the cations of both metals. Fluoborate and fluosilicate electrolytes are the most commonly used. Deposition of lead–tin alloys has been studied by a number of authors [4, 5,-9], but all these studies dealt with the formation of dense compact deposits of lead–tin alloy at the cathode. The literature contains no data on the conditions for electrolytic deposition of highly disperse powders of these alloys.

As the result of numberous experiments on the selection of a suitable composition of the lower aqueous layer, we chose an alkaline electrolyte – a solution containing a mixture of plumbite, stannate, and stannite.

A production of powdered lead–tin alloys of a high degree of dispersion from electrolytes of this type does not present any special difficulties. In preparation of the plumbite we used the concentrations and lead oxide – caustic soda ratio established previously [10] (34 g of lead and 100 g of caustic soda per liter). The stannite was prepared from stannous chloride, 1 liter of the solution containing 36.2 g of $SnCl_2 \cdot 2H_2O$ and 100 g of caustic soda. The plumbite and stannite were kept separately and mixed in the required proportions immediately before electrolysis. The upper organic layer consisted of toluene with added surface-active agents. Considerable difficulties arose in selection of the composition of the upper organic layer owing to the presence of excess alkali in the aqueous layer. This reduced considerably the number of surface-active agents suitable for production of metal organosols without causing emulsification of the organic layer in the lower, strongly alkaline electrolyte layer.

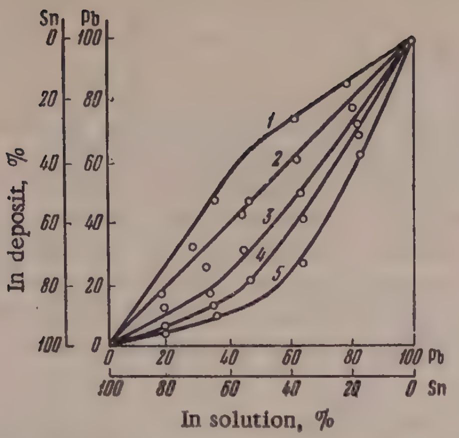

Fig. 2. Variation of the composition of the disperse phases of lead–tin organosols with the ratio of the component metals in the electrolyte. Current density: 1) 3; 2) 10; 3) 15; 4) 20; 5) 30 amp./dm^2.

Our selection of surface-active substances was based on the fundamental principles of lyophilization of disperse phases of metal organosols which had been established by one of us [3, 11]. Of the relatively large number of the substances surface-active with respect to the metal–organic medium interface, which were studied, the most suitable proved to be lead and tin oleates in the presence of a little octyl alcohol in the organic layer. The octyl alcohol plays a particularly important role in this case: it seems that its molecules interact with the hydrophilic groups of the lead oleate molecules dissolved in the organic phase (toluene) and adsorbed on the surface of the colloidal alloy particles, to form strongly hydrophobic compounds. This greatly diminishes the emulsifying power of lead oleate with respect to toluene and, despite the rotation of the cathode, toluene is not emulsified in the lower alkaline electrolyte layer.

In order to determine the optimum concentrations of these components in the organic layer, we made a more detailed study of the effects of lead oleate and octyl alcohol on the formation of cathode deposits of lead–tin alloys. The results of these experiments showed that the optimum concentration of lead oleate in toluene is in the range of 0.2 to 0.3%, and cessation of emulsification and good peptization of the deposit commence at 3% octyl alcohol concentration. Excess of octyl alcohol does not have any significant effects on these processes. The variations of the composition of tin–lead alloy cathode deposits and of the current efficiency with: a) the ratio of the components in the aqueous electrolyte solution under constant conditions of electrolysis, and b) current density at constant electrolyte composition, were determined. These results are given in Fig. 2. It is seen that as the current density increases from 3 to 30 amp./dm^2, the lead–tin ratio in the disperse phases of the organosols decreases in comparison with the value of this ratio in the electrolyte; at the beginning, at current densities from 3 to 10 amp./dm^2, it is higher than in the electrolyte; at 10 amp./dm^2 it becomes equal to the latter, and at higher current densities it is considerably less. The current efficiency with respect to the yield of powdered lead–tin alloy varied between 30 and 60%.

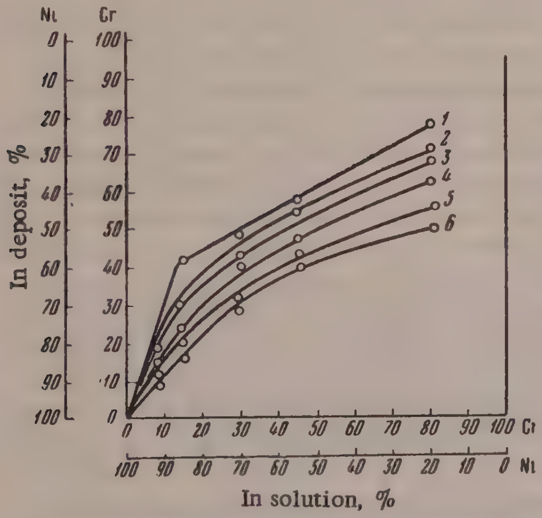

Fig. 3. Variation of the composition of disperse phases of nickel–chromium organosols with the ratio of the component metals in the electrolyte. Current density: 1) 5; 2) 10; 3) 20; 4) 30; 5) 40; 6) 50 amp./dm^2.

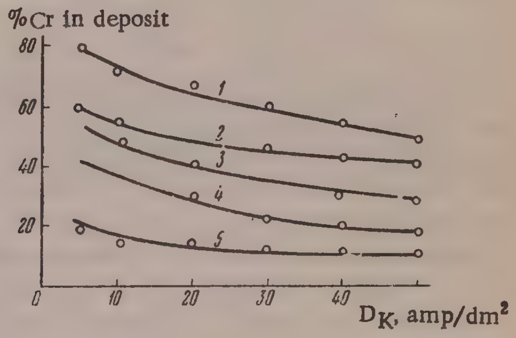

Fig. 4. Variation of the composition of disperse phases of nickel – chromium organosols with current density. Ratio of nickel to chromium in the disperse phase: 1) 1:5; 2) 1:1; 3) 2:1; 4) 5:1; 5) 10:1.

The results of detailed electron microscope and x-ray investigations of the disperse phases of lead–tin organosols obtained at various cathode current densities and with different component ratios in the aqueous layer of the electrolyte bath were published by us earlier [12].

Organosols of nickel–chromium alloys. As the result of a detailed examination of extensive experimental data on the question of the simultaneous electrolytic deposition of nickel and chromium at the cathode, and after numerous experiments, we reached the conclusion that the most suitable electrolytes for this purpose contain mixtures of nickel, chromium, and ammonium chlorides in the pure form and with additions of urea (30 g/liter) and hydrochloric acid (10-12 g/liter). Ammoniacal electrolytes containing, in addition to nickel and trivalent chromium salts, also ammonium tartrate, ammonium thiocyanate, and free ammonia are also of interest. With acid electrolytes, the upper organic layers consisted of toluene, xylene, or Diesel fuel, containing 0.5% oleic acid, while with ammoniacal electrolytes they contained oleates of heavy metals (lead, nickel, etc.) in concentrations from 0.25 to 0.5%. In the latter case 5% octyl alcohol on the volume of the upper layer was added to avoid emulsification.

Variations of the composition of the disperse phase of nickel–chromium alloy organosols with the ratio of the components in the acid electrolyte and cathode current density are shown graphically in Figs. 3 and 4. These results show that the chromium content of the disperse organosol phases increases with its content in the electrolyte. This is especially clearly seen for chromium concentrations not exceeding 50% in the electrolyte. With further increase of chromium concentration, its contents in the cathode deposits increase more slowly, especially at high current densities. For example, at D_k = 50 amp./dm^2 an increase of the chromium–nickel ratio in the electrolyte from 1 : 1 to 4 : 1 results in an increase of only 5-6% in the chromium contents of the deposits.

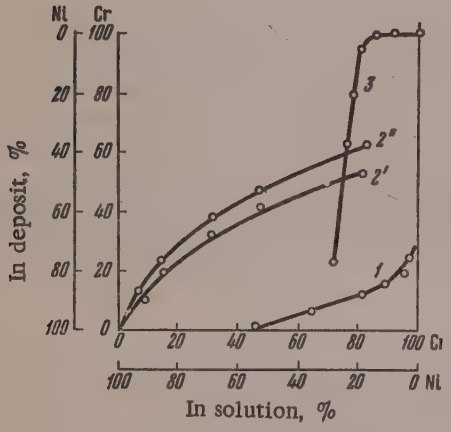

Fig. 5. Variation of the composition of cathode deposits of nickel–chromium alloy with the ratio of the components in the electrolyte, deposited from: 1) ammonium tartrate electrolytes; 2) acid electrolytes containing chromium and nickel chlorides; 3) acid electrolytes based on chromic anhydride [14].

Curves for the variation of chromium contents of the disperse phases of the organosols with the current density for given component ratios in the electrolyte, $c_{Cr} = f(D_k)$, show that a decrease of the chromium content occurs mainly as the current density increases from 5 to 30 amp./dm^2. Higher current densities (from 30 to 50 amp./dm^2) have no significant influence on the composition of the cathode deposits. The current efficiency in respect to the disperse organosol phases reaches 20% for these electrolytes; this can no doubt be increased if the experiments are carried out on a larger scale.

Variations of the composition of disperse phases of nickel–chromium alloy organosols deposited from ammoniacal electrolytes with various proportions of the components and at the same cathode current density (30-40 amp./dm^2) are shown in Fig. 5 (Curve 1). These results show that cathodic deposition of the alloy from ammoniacal baths begins at an atomic ratio of nickel to chromium close to 1 : 1. With lower chromium contents in the electrolyte, only nickel is deposited. For formation of a nickel–chromium alloy of the usual composition the atomic ratio of nickel to chromium in the electrolyte must be in the range between 1 : 20 and 1 : 50. It is probable that the excess of chromium relative to nickel brings their cathodic deposition potentials closer together and favors alloy formation. In addition to this relationship, Fig. 5 also shows, for comparison, curves for the variation of the composition of cathodic nickel–chromium deposits formed from acid electrolytes with various ratios of the components and at the same current density (30-40 amp./dm^2) (Curves 2 and 3). Comparison of these results shows that in the cathodic deposition of colloidally disperse nickel–chromium alloy powders, electrolytes based on nickel and chromium chlorides have considerable advantages with regard to composition variability and current efficiency.

Organosols of nickel–iron alloy. The electolytic production of nickel–iron alloys in compact form has been studied by many authors. However, very little information is available in the literature on the cathodic deposition of nickel–iron alloys of a colloidal degree of dispersion. We used the following electrolytes for the production of such alloys: ferrous chloride and nickel chloride in various proportions; ammonium chloride, 25 g/liter; urea, 30 g/liter; hydrochloric acid, 10-12 ml/liter; electrolyte pH 1.4-1.5. The use of such an acid electrolyte considerably simplifies the selection of the upper organic layer. For the latter, 0.5% solutions of oleic acid in toluene, xylene, Diesel fuel, MK oil, etc. were used.

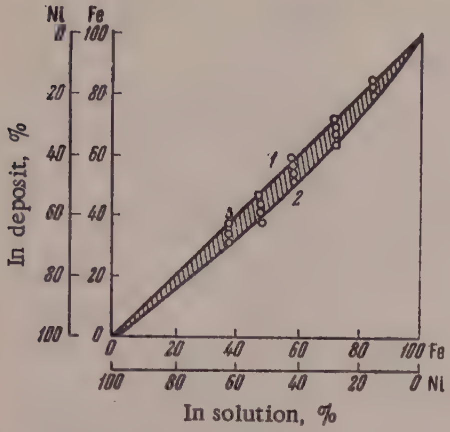

Fig. 6. Variation of the composition of disperse phases of iron–nickel organosols with the ratio of these components in the electrolyte. Current density: 1) 5; 2) 40 amp./dm².

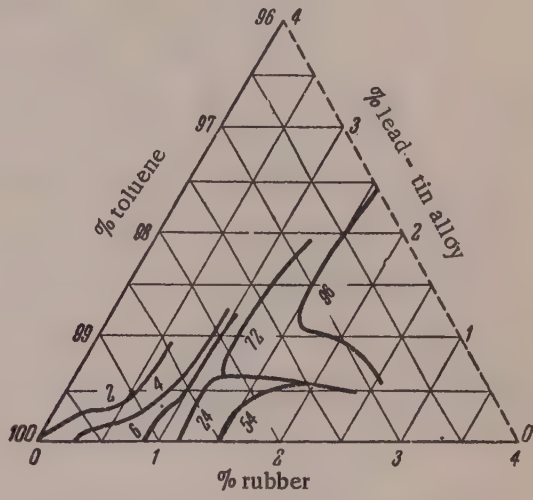

Fig. 7. Variations of the stability of lead–tin alloy organosols stabilized by rubber. Numbers on the curves represent hours.

Variations of the composition of disperse phases of nickel–iron organosols with the ratio of these components in the original electrolyte and with the cathode current density are shown in Fig. 6. In this case there is almost direct proportionality between the composition of the highly disperse cathode deposits and the electrolyte composition over a fairly wide range of current densities, from 3 to 40 amp./dm². The current efficiency with respect to the yield of nickel–iron alloy organosol varied from 60 to 80% in these experiments.

Stability of alloy organosols. The results of a study of the stability variations of organosols of lead–tin, nickel–chromium, and nickel–iron alloys in toluene in presence of a high polymer – rubber – are given in Figs. 7-9 in the form of triangular diagrams. The criterion of stability used was the time required for complete precipitation of the disperse phase of the alloy organosol from these systems at rest. Each system was observed systematically until the boundary of the disperse phase completely ceased to move toward the bottom of the cylinder.

Examination of the stability diagram for lead–tin alloy organosols stabilized with rubber (Fig. 7) shows that the stability of these sols depends on the concentration of the protective polymer (rubber) and on the ratio of the disperse phase of the organosol and the amount of rubber. At protective polymer concentrations from 0.1 to 1.2%, increase of the disperse phase – rubber ratio results in decreased stability of the organosols studied. At rubber concentrations from 1.2 to 1.8% increase of this ratio results in a considerable increase of the stability of these systems.

A similar situation is found in the stability diagrams for nickel–chromium and nickel–iron alloys stabilized by rubber (Figs. 8 and 9). This is especially pronounced when the nickel–chromium alloy concentration in the organosols is between 0.5 and 1.5%. In this case the stability increases from 3 hours for rubber concentrations of 0.1-0.4%, to 300-350 hours for rubber concentrations of 1.5-1.8%. With nickel–chromium alloy concentrations between 0.1 and 0.3%, the variations of stability with rubber concentration are less pronounced. The stability of nickel–chromium alloy organosols stabilized by rubber also depends on the quantitative ratio of the disperse phase of the organosol to the amount of rubber in these systems. As regards nickel–iron alloy organosols, the stability of these systems depends little on this ratio.

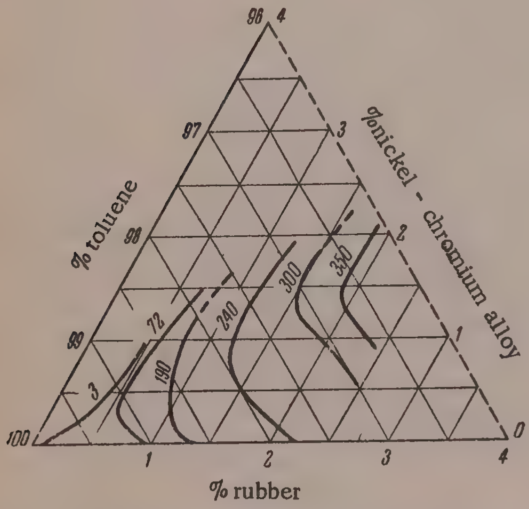

Fig. 8. Variations of the stability of nickel–chromium alloy organosols stabilized by rubber. Numbers on the curves represent hours.

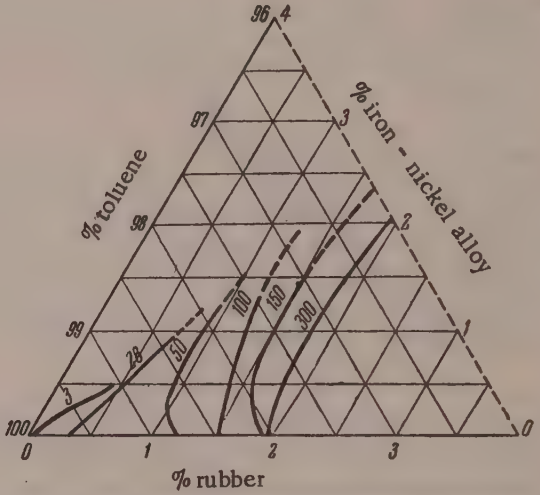

Fig. 9. Variations of the stability of iron–nickel alloy organosols stabilized by rubber. Numbers on the curves represent hours.

These results confirm the views, put forward by us earlier, concerning the significant influence of the quantitative ratio between the disperse phase and the protective polymer in a hydrophobic sol on the stability of such a sol [13].

The increase in the stability of the alloy organosols studied, found at higher concentrations of the protective polymer, is probably the result of the formation of a stable structural network from the rubber macromolecules and the colloidal alloy particles, which serve as the nodal points in such a network.

SUMMARY

1. The optimum conditions for formation of organosols of lead–tin, nickel–chromium, and nickel–iron alloys at a horizontal rotating cathode in a two-layer electrolytic bath have been determined.

2. The compositions of the disperse phases of organosols of these alloys have been studied in relation to the ratios of the component metals in the electrolyte and the cathode current density.

3. The stability of the organosols has been studied in presence of rubber, in relation to the concentration of the latter and to its quantitative ratio to the disperse phase of the organosol.

Institute of General and Inorganic Chemistry
Academy of Sciences Ukrainian SSR Kiev

Received May 24, 1956.

LITERATURE CITED

[1] E. M. Natanson, Colloid J. 9, 191 (1947).

[2] A. N. Frumkin, Electrocapillary Curves and Electrode Potentials (Odessa, 1919);* Naturwiss. 7, 235 (1928). A. N. Frumkin, V. S. Bagotsky, Z. A. Iofa and B. M. Kabanov, Kinetics of Electrode Processes (1952).*

[3] E. M. Natanson, Trans. 2nd All-Union Conf. on Colloid Chemistry, 1950, p. 113.*

[4] W. Blum and E. Haring, Trans. Amer. Electr. Soc. 40, 287 (1921).

[5] E. Raub and W. Blum, Metalloberflache 9, 4, A54 (1955).

[6] P. P. Belyaev and L. M. Berman, Technical News, No. 10 (1933).

[7] P. P. Belyaev and Ya. N. Birman, Bull. Metal Industry, No. 9, 88 (1937).

[8] M. A. Loshkarev and M. P. Grechukhina, J. Phys. Chem. 24, 1502 (1950).

[9] A. E. Carlson and J. M. Kane, Monthly Rev. Am. Electroplaters Soc. 33, 255 (1946); A. E. Carlson and C. Struyk, Metal Finishing Guide Book Directory, 24 (1956); N. J. Westwood, Finish Publ. Inc. 317 (1955).

[10] N. N. Gratsiansky and P. F. Kalyuzhnaya, Ukrain. Chem. J. 19, 380 (1953).

[11] E. M. Natanson, Colloid J. 9, 428 (1947).

[12] E. M. Natanson, V. P. Chalyi, N. N. Kozachek and A. P. Kaban, Colloid J. 19, 319 (1957). [See C. B. translation].

[13] E. M. Natanson, Proc. Acad. Sci. USSR 74, 517 (1950).

[14] M. F. Skalozubov and A. S. Vlasova, Bull. Novocherkassk Industrial Inst. Chem. Ser. 6, 15 (1940).

---

* In Russian.

INFLUENCE OF THE REACTION OF THE PRECIPITATION MEDIUM AND OF THE pH OF THE WASH WATER ON THE STRUCTURE OF CHALKY SILICA GELS

I. E. Neĭmark and I. B. Slinyakova

Silica gels prepared from solutions of sodium silicate and easily hydrolyzed salts are opaque or chalky. In contrast to glassy silica gels, in the precipitation of which silicic acid sols are first formed and then pass into gels, the formation of a chalky silica gel is accompanied by instantaneous formation of a flocculent precipitate consisting of silicic acid, metallic hydroxide, and possibly also of complex compounds. In addition, during the precipitation of a chalky silica gel the pH of the mixture varies over wide limits as the result of mixing of alkaline and acid components, and therefore the precipitate is heterogeneous in composition and degree of dispersion; this must undoubtedly influence the final pore structure of the chalky silica gel.

Therefore the formation of the pore structure of chalky silica gels (coagels) should be somewhat different from the structure formation of glassy silica gels (xerogels). While the pore structure of silicic acid xerogels does not depend on the history of the hydrogel formation, but is determined by the subsequent treatment and the dehydration conditions of the hydrogels [1], the porosity of coagels should depend on the conditions of their precipitation.

It was shown in our paper [2] that the reaction of the medium in a suspension formed from solutions of sodium silicate and nickel chloride has a considerable influence on the porosity of chalky silica gels. As the alkalinity of the medium decreases, the volume of the sorptional pores increases and the volume of the macropores diminishes. The purpose of the present investigation was to verify the applicability of these results to chalky silica gels precipitated from sodium silicate solutions by ferric chloride. We studied the influence of the precipitation medium and of the pH of the wash waters on the structure of chalky silica gels made from water glass and ferric chloride. An attempt was also made to elucidate the chemistry of chalky silica gel formation.

RESULTS AND DISCUSSION

Method. The method used for preparation of chalky silica gels from sodium silicate and ferric chloride was similar to that used previously [2]. A solution of $FeCl_3$ was added slowly, with vigorous stirring, to sodium silicate solution; an flocculent precipitate was instantly formed. This was aged for two days, filtered off, and molded into small cylinders. The cylinders were partially dried at room temperature for 18-20 hours to 70-80% moisture content. They were then treated with 6N HCl solution to remove ferric hydroxide, the acid was decanted off, and the gel washed with distilled water to a negative reaction for Cl^-. The hydrogel was dried for 24 hours at room temperature, for 6 hours at 100°, and for 6 hours at 200°.

The following were determined in order to obtain the structural and adsorptive characteristics of the chalky silica gels: bulk density, true and apparent densities from which the total pore volume was calculated, the maximum sorption volume of the pores for benzene at $p/p_s = 1$; methyl alcohol sorption isotherms were determined at 20° in a high vacuum apparatus with the aid of a quartz spring balance.

Influence of the reaction of the medium during precipitation of coagels on the structure of chalky silica gels. Several specimens were prepared, with different pH values of the suspension medium. In order to exclude the influence of silicic acid concentration, the sodium silicate solution used had the same density and the same modulus (d = 1.12, modulus 3.5), and was used in the same amounts in all the experiments. To obtain suspensions with different pH, the amounts of the 2N $FeCl_3$ solution added were varied. Specimens of the third series were prepared from more dilute water glass, sp.gr. 1.045 g/cc.

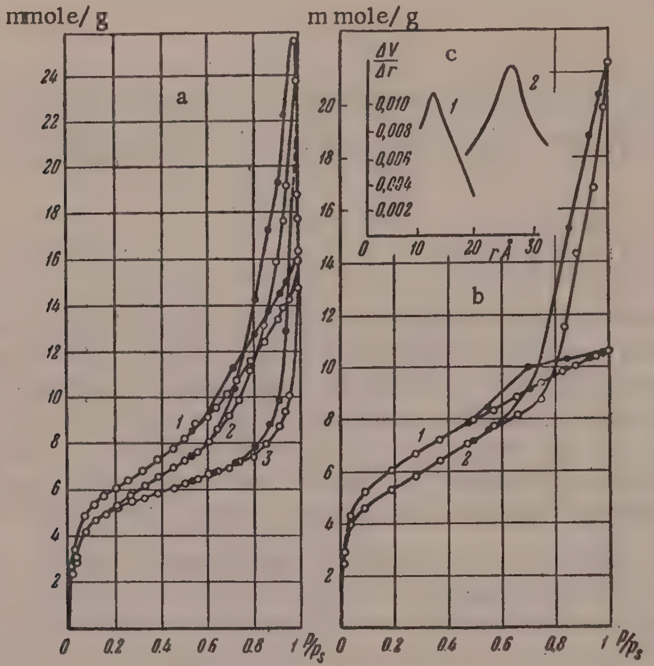

Fig. 1. Sorption isotherms for methyl alcohol vapor on chalky silica gels precipitated by $FeCl_3$ with different suspension pH: a. 1) pH 0.43; 2) pH 8.2; 3) pH 10.9; b. 1) pH 0.44; 2) pH 10.9; c. pore volume – effective radius distribution curves.

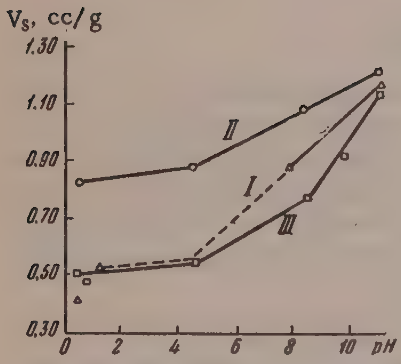

Fig. 2. Effect of suspension pH on the volume of benzene adsorbed by chalky silica gels from saturated vapor (I, II and III are series of experiments): I) Specimens 1-4; II) Specimens 5-9; III) Specimens 10-16 (see Table 1).

Table 1 gives the conditions for the preparation of three series of chalky silica gels specimens, and their sorption characteristics, and Fig. 1 shows isotherms for sorption of methyl alcohol vapor at 20° on specimens of the first (1, a) and second (1, b) series of experiments.

The variations of the volume of benzene taken up from saturated vapor with pH of the suspension are given in Fig. 2.

It follows from the data in Table 1 that the total pore volume, the limiting sorption volume of benzene at $p/p_s = 1$, and the volume of the macropores of chalky silica gels obtained from silicate and $FeCl_3$ increase with increasing pH of the suspension. Comparison of the sorption isotherms for specimens formed from an acid medium (Curves 1 in Fig. 1) with isotherms for silica gels precipitated in an alkaline medium (Curves 2 and 3 in Fig. 1) reveals considerable differences in the character of their porosity. In the first case the hysteresis loop is not large, indicating that the volume of the intermediate pores is not great. At low and moderate relative pressures Curves 1 lie above Curves 2 and 3. The specimens precipitated in an alkaline medium have a more coarsely porous structure. The isotherms show large hysteresis loops. The limiting sorptional volume of the pores of these silica gels at $p/p_s = 1$ is large.

TABLE 1

Preparation Conditions and Structural and Sorption Characteristics of the Silica Gels Studied

Series	Specimens	pH of suspension	$FeCl_3/Na_2SiO_3$ (by volume)	Apparent sp.gr. in g/cc	Total pore volume in cc/g	Benzene adsorbed at $p/p_s = 1$, in cc/g	Volume of macropores, cc/g	Specific surface, m^2/g
I	1	0.37	1:1	0.90	0.66	0.42	0.24	689
	2	1.2	3:4	0.76	0.85	0.52	0.33	—
	3	7.8	1:2	0,50	1.55	0.88	0.67	660
	4	11.0	1:3.3	0.39	2.11	1.16	0.95	638
II	5	0.43	1:1	0,40	2.05	0.84	—	762
	6	2,4	3:4	0.52	1.48	0.75	0.73	—
	7	4.4	3:5	0,48	1,63	0.88	0.75	732
	8	8,2	1:2	0,34	2.50	1.08	1,42	660
	9	10.94	1:3,3	0.31	2.75	1.21	1.54	682
III	10	0.44	1:2	1.12	0.44	—	—	768
	11	0,6	1:2,6	1.09	0.47	0.48	—	—
	12	2,5	1:3,3	0.96	0,59	0,65	—	—
	13	4.5	1:4	1.01	0.64	0.54	—	—
	14	8.4	1:5	0.86	0.71	0.77	—	—
	15	9.7	1:6	0.69	1.00	0.92	0,08	—
	16	10.9	1:8	0.54	1.40	1,06	0.36	688

Consequently, an acid medium leads to formation of chalky silica gels with highly developed microporosity, giving a large specific surface. These gels are either without macropores, or their macropore volume is low. The limiting sorptional volume of the pores (at $p/p_s = 1$) is 2-2.5 times smaller than that of specimens obtained from an alkaline medium.

For comparison, chalky silica gels were also precipitated by nickel chloride in the same conditions as the silica gels from $FeCl_3$, and their structure and sorptional properties were studied. The isotherms for sorption of methyl alcohol vapor on these specimens are given in Fig. 3. It follows from Fig. 3 that the sorption isotherms for chalky silica gels precipitated by $NiCl_2$ from acid media lie above the isotherms for silica gels prepared from alkaline media. The macropore volume of silica gels precipitated by $NiCl_2$ solution increases from 0.23 to 0.88 cc/g as the suspension pH increases from 0.5 to 10.5. However, in contrast to the silica gels precipitated by $FeCl_3$, the limiting sorptional volume of the pores decreases. The ratio of the sorptional pore volume to the macropore volume, V_s/V_{ma}, falls from 7.4 to 1.4. It seems that the increase of the total pore volume in silica gels precipitated by $NiCl_2$ is due to increased macropore volume, and in silica gels precipitated by $FeCl_3$ it is due to increased intermediate pore volume.

All the gels described above, precipitated at different pH values of the medium, were washed for prolonged periods with distilled water before being dried. It was of interest to determine the effect of the pH of the wash waters on the structure of chalky silica gels.

Influence of the pH of the wash water on the structure of chalky silica gels. Precipitates washed with distilled water to a negative reaction for Cl^- were divided into three portions; one was covered with a solution of pH 2.6, another, with a solution of pH 6.5, and the third, with a solution of pH 10.4; the specimens were then dried in a drying oven at 120°.

The structural and sorptional characteristics of these silica gels are given in Table 2, and isotherms for the sorption of methyl alcohol vapor on these specimens are shown in Fig. 4.

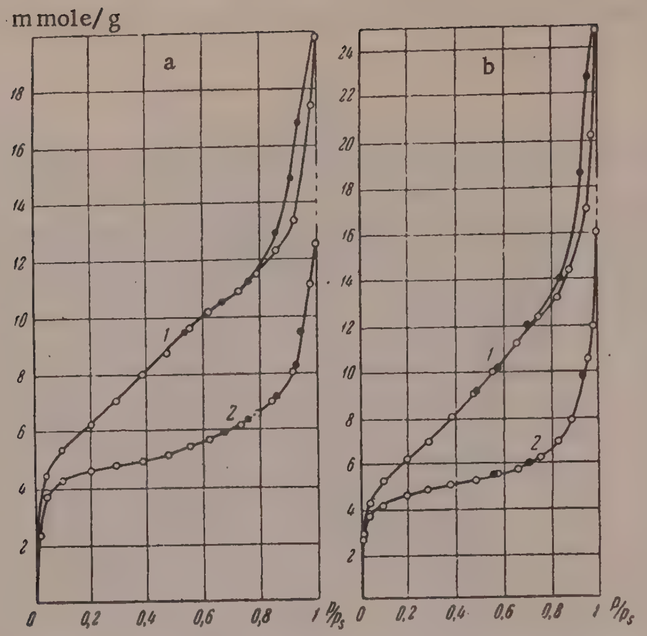

Fig. 3. Sorption isotherms for methyl alcohol vapor on chalky silica gels precipitated by $NiCl_2$ with different suspension pH: a. 1) pH 0.5; 2) pH 10.5; b. 1) pH 0.6; 2) pH 11.2.

TABLE 2

Structural and Sorptional Characteristics of the Silica Gels Studied

Specimen	pH of suspension	pH of wash water	Total pore volume, cc/g	Sorptional pore volume, cc/g	Volume of macropores, cc/g	Specific surface, m²/g
17	8.5	2.6	2.50	0.78	1.72	464
18	8.5	6.5	2.50	1.05	1.45	624
19	8.5	10.4	2.75	1.15	1.60	435
20	6.2	2.6	2.16	0.75	1.41	—
21	6.2	6.5	2.16	0.81	1.35	—
22	3.3	2.6	2.05	0.80	1.25	631
23	3.3	6.5	2.68	0.97	1.71	574
24	3.3	10.4	3.12	1.09	2.03	580

Comparison of the structural and sorptional characteristics of chalky silica gels covered with solutions of different pH values (see Table 2 and Fig. 6) showed that drying of precipitates at different pH values merely leads to some changes in the character of the pore distribution, and the structural differences consist only of changes in the volumes of the intermediate pores and macropores. The sorptional volume of the silica gel pores increases from 0.78 to 1.15 cc/ g as the pH of the precipitate is increased from 2.6 to 10.4. The specific surfaces of these specimens have similar values, 500-600 m^2/ g. It is evident that this method cannot be used for varying the porous structure of chalky silica gels over a wide range.

Some considerations of the chemistry of chalky silica gel formation. The chemistry of the formation of chalky silica gels from water glass and easily hydrolyzable salts is still obscure. Holmes [3] presumed that in the first instant of the reaction the heavy metal salt is hydrolyzed with formation of acid; the latter reacts with sodium silicate, forming silicic acid:

$$\begin{array}{c} MeCl_2 + 2H_2O = Me(OH)_2\downarrow + 2HCl \\ Na_2SiO_3 + 2HCl = H_2SiO_3\downarrow + 2NaCl \\ \hline MeCl_2 + Na_2SiO_3 + 2H_2O = Me(OH)_2\downarrow + H_2SiO_3\downarrow + 2NaCl. \end{array}$$

Patrick [3] showed, however, that a precipitate is not formed if hydrochloric acid is added to sodium silicate in an amount equal to the amount of acid liberated by hydrolysis of the salt. Therefore Holmes' scheme does not appear to be consistent with the facts.

Dubinin [4] assumed that sodium silicate is first hydrolyzed to form silicic acid and alkali, and the latter then reacts with the heavy metal salt, giving the hydroxide according to the scheme:

$$\begin{array}{c} Na_2SiO_3 + H_2O = H_2SiO_3\downarrow + 2NaOH \\ 2NaOH + MeCl_2 = Me(OH)_2\downarrow + 2NaCl \\ \hline NaSiO_3 + MeCl_2 + H_2O = Me(OH)_2\downarrow + H_2SiO_3\downarrow + 2NaCl. \end{array}$$

However, it is difficult to imagine that the metal hydroxide and silicic acid can be present in an unbound state in the precipitate in an alkaline medium. They are most likely to form complex compounds.

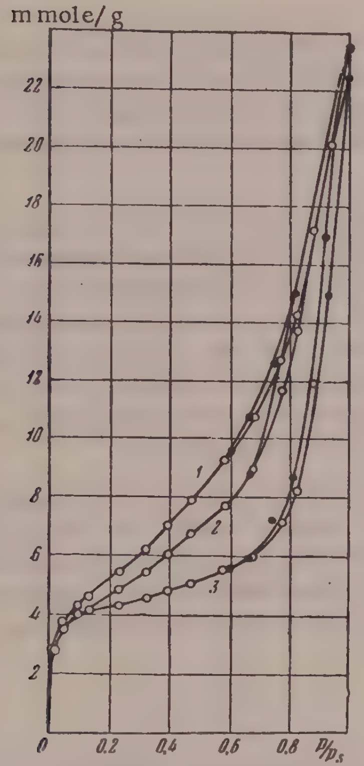

Fig. 4. Sorption isotherms for methyl alcohol vapor on chalky silica gels washed with solutions of different pH: 1) pH 2.6; 2) pH 6.5; 3) pH 10.4.

To verify this hypothesis, we prepared ferric hydroxide by the action of ammonia on $FeCl_3$ solution, and, for comparison, we precipitated a chalky gel by mixing solutions of sodium silicate and $FeCl_3$. In order to determine whether this precipitate contains $Fe(OH)_3$ in pure form, or whether it is chemically combined with H_2SiO_3, we tested the solubility of pure $Fe(OH)_3$ and of the chalky gel precipitate in acids.

It was found that fresh $Fe(OH)_3$ dissolved readily in 6 N hydrochloric and 8 N acetic acids, and with difficulty in 4 N acetic acid. The iron in the precipitate formed when $FeCl_3$ and Na_2SiO_3 solutions were mixed dissolved in 6 N HCl but was entirely insoluble in 6N acetic acid. It is likely that, in addition to $Fe(OH)_3$ in the pure form, the precipitate contains iron combined with silicic acid. After treatment of the precipitate with 6N HCl this compound is destroyed and only silicic acid gel remains in the precipitate. It is probable that Dubinin's scheme also fails to conform to reality.

Ray and Ganguly [5] measured the quantity of heat evolved in complete reaction of one mole of $FeCl_3$ with various solutions of alkali metal silicates; they found that the quantity of heat evolved per mole of $FeCl_3$ falls appreciably with increasing contents of silicic acid and constant Na_2O content in the solutions. If the only reaction product was $Fe(OH)_3$, the heat of reaction should be constant, and close to the heat of reaction between $FeCl_3$ and NaOH. The gradual decrease of the heat effects observed by these authors indicates the formation of complex silicate ions with increasing contents of silica in solution.

In our opinion, Grigorjew [6] was nearer to a correct view of the chemistry of chalky silica gel formation; he assumed that the reaction proceeds according to the equation:

$$MeCl_2 + Na_2SiO_3 = 2NaCl + MeO \cdot n\, SiO_2.$$

It is difficult to believe, however, that in an alkaline medium the sodium ions present will not take part in complex formation.

We represent the general reaction scheme as follows:

$$Na_2SiO_3\,(SiO_2)_n + aMeCl_2 = Na_2O \cdot a\,MeO \cdot b\,SiO_2 \cdot mH_2O + nNaCl.$$

Evidence in favor of this scheme is provided by our quantitative determinations of Na and Fe in ferrosilica gels prepared from alkaline media.

When the ferrosilica gels were precipitated with excess of Na_2SiO_3 in solution, sodium ions were always present in the finished dry ferrosilica gel. Na^+ ions were not found in chalky silica gels precipitated from alkaline media if the hydrogels had been treated with 2N HCl. It is probable that ion exchange of Na^+ for H^+ takes place in such treatment. If the gels are treated with 6N HCl, the complex is destroyed, and neither Fe^{3+} ions nor Na^+ ions can be detected in the silica gel.

Our results are in good agreement with the fundamental theoretical principles relating to the mechanism of hydrophilic adsorbent structure formation [7]. In precipitation of a chalky silica gel the precipitate is formed instantaneously as the precipitant is added to the sodium silicate. In neutral and alkaline media the most probable result is formation of silicic acid micelles, the outer layers of which consist of adsorbed cations from the solution. The possibility is not excluded that if the precipitation takes place in an alkaline medium the cations will also be present within the micelles, forming complexes. It is probable that in such cases the bonds between the micelles and water are weakened, resulting in further aggregation of the micelles into longer chains and clusters. Dehydration will result in a loose texture and the silica gel will be coarsely porous.

In an acid medium, adsorption processes involving ion exchange or complex formation are unlikely, the micelles will be hydrophilic, the packing of the particles as the result of dehydration will be compact, and the resultant silica gel will be finely porous. It is interesting to note that the limiting sorptional volume of the pores of chalky silica gels, like that of glassy silica gels, only begins to increase sharply after the pH of the precipitation medium exceeds 5 (see Fig. 2). It is probable that up to pH 5 ion exchange processes do not take place on the micelle surfaces.

SUMMARY

1. The reaction of the medium in precipitation has an important effect on the porous structure of chalky silica gels. The total pore volume and the macropore volume increase with increasing pH.

2. The effect of the reaction of the precipitation medium is largely independent of the nature of the easily hydrolyzed salt.

3. Adsorption processes associated with ion exchange on the surfaces of the silicic acid micelles do not take place in an acid medium. In an alkaline medium the outer shell of the micelles consists of adsorbed cations.

4. The chemistry of chalky silica gel formation is discussed.

The L. V. Pisarzhevsky Institute of Physical Chemistry
Academy of Sciences, Ukrainian SSR, Kiev

Received March 29, 1957.

LITERATURE CITED

[1] I. E. Neimark, M. A. Piontkovskaya and I. B. Slinyakova, Colloid J. 18, 61 (1956).•

[2] I. E. Neimark and I. B. Slinyakova, Colloid J. 15, 277 (1953).•

[3] H. Holmes and J. Anderson, Ind. Eng. Chem. 17, 280 (1925).**

[4] M. M. Dubinin, Physicochemical Principles of Sorption Technology [In Russian] (Goskhimizdat, 1932).

[5] R. Ray and B. Ganguly, J. Phys. Chem. 2, 396 (1931).

[6] P. N. Grigorjew, J. prakt. Chem. 118, 91 (1928).

[7] I. E. Neimark, Progr. Chem. 25, 748 (1956).

---

* Original Russian pagination. See C. B. translation.

** [The original did not contain any reference by Patrick, as cited in the text – Publisher].

GELATIN–GLYCEROL GELS AS MATERIALS FOR STUDYING STRESSES BY THE OPTICAL POLARIZATION METHOD

D. N. Osokina

Gelatin–glycerol gels are widely used for optical polarization studies of stresses in models in relation to problems of mining [1], soil mechanics [2, 3], geotectonics [4], etc.

Gelatin gels have not been sufficiently studied as optically active materials, although there have been numerous investigations of their properties. These investigations have followed two unrelated directions. In one type of investigation [5-10], purely physical and physicochemical, gelatin gels were studied for purposes which had nothing to do with modeling. In the second type [1-3, 11] gelatin gels were used as optically active materials for modeling phenomena in which volume forces play an important role. The most complete quantitative studies of gelatin gels as optically active materials were those carried out by Trumbachev [1].

Researches of the first type lead to the following conclusions:

1. The elasticity modulus of gelatin gels greatly decreases with increase of temperature and increases with the time which elapses after casting of the gel.

2. The temporary birefringence and deformation in a gel under constant load increase with time, at least for 20-30 minutes.

3. The magnitude of the temporary birefringence (optical effect) is evidently associated with the deformation and not with the stress acting on the specimen.

It has been shown [6, 13, 14] that Poisson's ratio for gelatin gels is 0.5. It should be pointed out that in studies of the mechanical properties of gelatin gels most authors referred to $E = \sigma/\epsilon$ (where σ is the applied force and ϵ is the deformation produced in the specimen) as Young's modulus or elasticity modulus, by analogy with ordinary solids. In the modern view [12], the elastic deformation produced in a gelatin gel at room temperature consists of a conventionally instantaneous component (ϵ_{ci}), and a high-elastic component (ϵ_e) which has developed at the instant of the determination, and hence

$$\frac{1}{E} = \frac{\varepsilon}{\sigma} = \frac{\varepsilon_{ci} + \varepsilon_e}{\sigma} = \frac{1}{E_1} + \frac{1}{E_e},$$

where E_1 is the conventionally instantaneous modulus; E_e is the elasticity modulus.

Since several days are required before equilibrium high-elastic deformation is reached in gelatin gels, generally not the total elastic deformation is measured, but only a certain part of it, and accordingly E_e is greater than the equilibrium elasticity modulus, and E is greater than the total equilibrium elasticity modulus. In this paper, for brevity, we term E the elasticity modulus, remembering that this is not the total modulus but an intermediate value between the conventionally instantaneous and the total equilibrium modulus.

Most of the investigators in the second type of studies ignored the specific nature of the high-elastic state of gelatin gels, and regarded them as ordinary photoelastic materials in which the optical effect (optical path difference) is a linear function of the principal stress difference; i.e., they did not take into account the variations of the gel properties with the time of action of the load, temperature of the experiment, and "age" of the material.

The investigations cited above provide much important and necessary information on the properties of gelatin gels. However, before gels can be used for stress investigation with all the factors influencing the experimental results taken into account, the following questions remain to be answered: 1) for how long do the optical path difference and deformation continue to increase under constant load, and do these quantities reach equilibrium values within a period of time suitable for carrying out the experiments, i.e., within the first few hours after application of the load (since gelatin models are very susceptible to drying, it is undesirable to keep them under load for longer than this before the start of the experiment); 2) can the material be characterized by an elasticity modulus and an optical stress coefficient, constant for all stresses, at any time after application of the load; 3) how do the stress-optical coefficient and the elasticity modulus of a gelatin gel vary with the preparation conditions and the nature of the test.

Methods of specimen preparation and measurements of deformation and optical effect. The specimens for compression tests were made in the form of prisms (5 × 3 × 2 cm), and for extension tests in the form of strips (11 × 1.6 × 1 cm) of rectangular section and with mirror-smooth faces, so that the specimens could be investigated in polarized light. For the extension tests, two horizontal lines 2 cm apart were marked with India ink in the middle of the strip. The ends of the strip were fixed in two clamps, the top one being connected to a stand, and a light pan for weights being attached to the lower one. The distance between the marks was measured to an accuracy of 0.1 mm by means of a traveling microscope rigidly connected to a vernier moving along a vertical steel scale fixed on the same base as the stand.

For compression tests, the prismatic specimen was placed between circular plates of a small press in which a load between 5 g and 5 kg, with an accuracy of 2-3 g, could be applied to the specimen. The deformations were read off to an accuracy of 0.1 mm from the displacement of a vernier pointer attached to the upper plate of the press, along a scale. The interference colors of the specimens indicated that the stress distribution within them was fairly homogeneous.

For the birefringence determinations, the specimen fixed in the loading device was placed between the polaroids of a coordinated synchronous KSP-5 polarimeter. The path difference in the region of the specimen between the marks was measured by means of Krasnov's compensator. To avoid drying of the specimens, they were removed from the molds immediately before the start of the experiments, while during lengthy tests they were placed in a transparent hermetically sealed box.

Behavior of the specimen with time under constant load. Figure 1 shows the variations of the path difference R in m μ, and of the relative deformation ϵ arising in the specimen under a constant tensile force, with time from the application of the load. The determinations were made both with the specimen under load, and after release of the load. The composition of the gel was 30% gelatin, 30% glycerol, and 40% water; the temperature was 21-22°; the time of action of the load was 3 hours 50 minutes. The longest period of action of the load in experiments of this type was 70 hours. It follows from these experiments that the path difference and deformation under constant load at room temperature increase with time, at a diminishing rate; they do not reach equilibrium values in 60-70 hours. On removal of the load, part of the path difference and deformation disappears abruptly; the remainder diminishes at a continuously decreasing rate. If the specimen is heated through a frew degrees, the rate of decrease of the "residual" path difference and deformation rises sharply, and these value drop almost to zero. All the deformation remaining after application of the load can therefore be regarded as reversible and elastic, and it may be assumed that plastic deformation of the gel in these conditions (temperature 22°, small stresses of 0.1-0.2 kg/cm^2) is negligible or entirely absent.

Consequently the deformation and path difference do not reach constant values in the time which can be devoted to experiments with models. It is therefore necessary to carry out the measurements before equilibrium deformation becomes established.

Variations of the birefringence and deformation with the stress with the determinations carried out immediately after application of the load (1-1.5 minutes after loading) were determined in extension and compression experiments. The load on the specimen was increased by 50 g steps; before each successive i-th loading the specimen was released and the distance L_{i0} between the lines (in compression experiments, the height of the specimen) and the path difference R_{i0} were measured. The load P_i was then applied, and the following were measured: L_i, the distance between the lines in extension experiments (or the height of the specimen in compression experiments), and the path difference R_i.

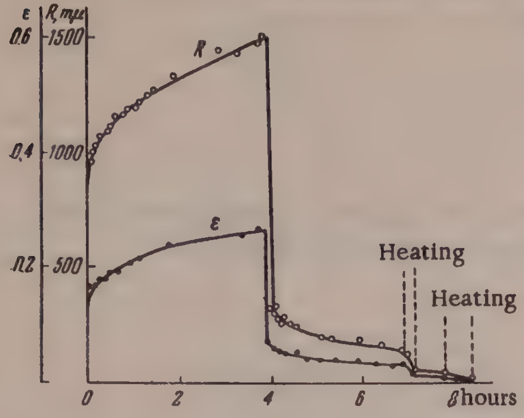

Fig. 1. Variations of the optical path difference R and relative deformation ε with time.

In the calculations, stress increases of $\sigma_i(\sigma_i = P_i/S_i)$, where S_i is the area of the specimen deformed under the action of the load (P_i), were correlated with $R = R_i - R_{i0}$ and $L = L_i - L_{i0}$, i.e., the increments of the path difference and of the length of the portion of the specimen in question, produced by the given stress increase. It was necessary to remove the load and to subtract R_{i0} and L_{i0} from the corresponding values of R_i and L_i in order to eliminate the influence of increases of R and L with time, which could distort the results of the determinations.

When the path difference changes by the value R, the difference between the principal refractive indices $\Delta n = n_1 - n_2$ changes by the value $\Delta n = R/d_i$, where d_i is the thickness of the specimen deformed by the load P_i; d_i was calculated on the assumption that the volume was constant

$$d_i = d_0 \sqrt{L_0/L_i};$$

S_i was calculated on the same assumption: $S_i = S_0L_0/L_i$; the relative deformation ε was determined as

$$\epsilon = (L_i - L_{i0})/L_{i0}.$$

Figure 2 shows variations of Δn and ε with the stress in extension and compression (1-1.5 minutes after

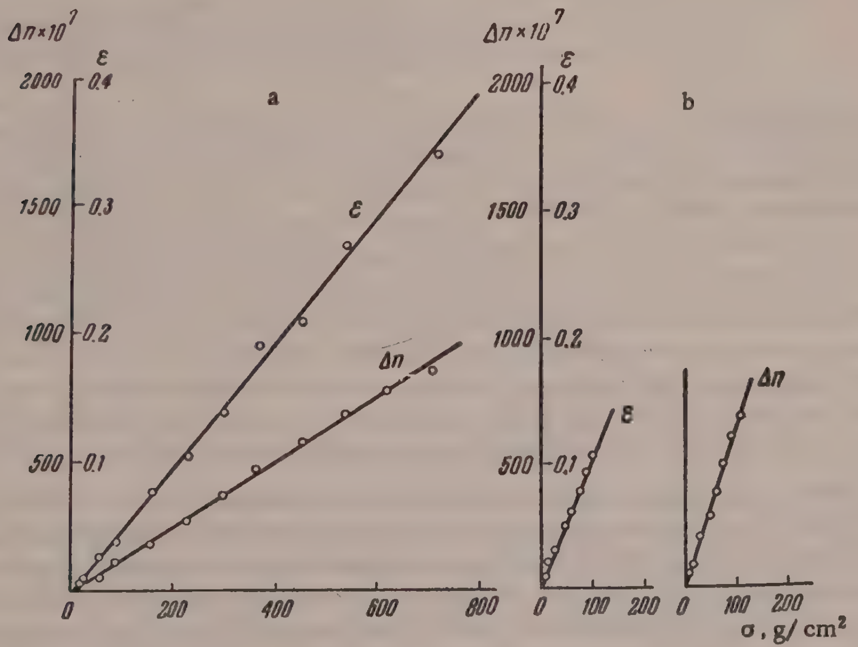

Fig. 2. Variations of birefringence Δn and relative deformation ε with stress: a) in extension (gel composition: 40% gelatin, 30% glycerol, 30% water); b) in compression (gel composition: 25% gelatin, 30% glycerol, 45% water).

application of the load); it is seen that at deformations not exceeding 25-30% Δn and ϵ are linear functions of σ.

It follows from the linear relationships between Δn and σ, and ϵ and σ, that 1-1.5 minutes after loading gelatin gels can be characterized by the optical coefficient C_{1M} and the elasticity modulus E_{1M}, constant for all stresses (at deformations not exceeding 25-30%). Since under uniaxial extension or compression $\sigma_1 = \sigma$, $\sigma_2 = 0$, $\sigma_1 - \sigma_2 = \sigma$, the values of C_{1M} and E_{1M} are given by the expressions

$$C_{1M} = \frac{R_{1M}}{\sigma d} = \frac{\Delta n_{1M}}{\sigma}, \quad E_{1M} = \frac{\sigma}{\varepsilon_{1M}},$$

where $\underline{d}$ is the thickness of the deformed specimen, and R_{1M}, Δn_{1M} and ϵ_{1M} are the path difference, birefringence, and deformation arising in the specimen 1-1.5 minutes after application of the load.

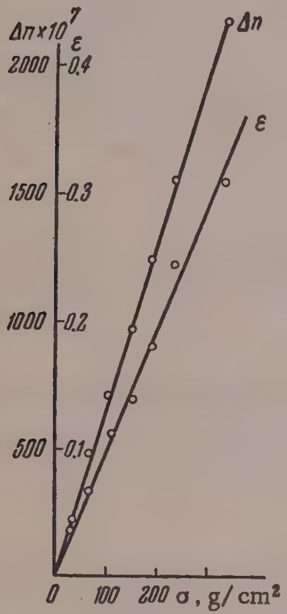

Fig. 3. Variations of briefringence Δn and deformation ϵ with stress 2 hours after application of the load.

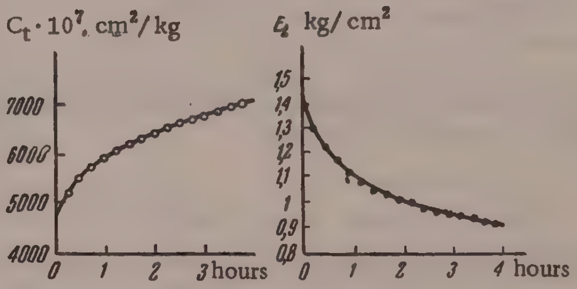

Fig. 4. Variation of the stress-optical coefficient C and elasticity modulus E with time under constant load.

Variations of the birefringence and deformation with the stress under prolonged action of the load. For determination of the variations of Δn and ϵ with σ for time intervals considerably greater than 1 minute, such as might be required for experiments with models (1.5-2 hours), a series of curves for the variations of R and ϵ with time under various constant loads was plotted. The gel contained 30% gelatin and 30% glycerol; the temperature of the experiment was 21-22°. Each curve was plotted for a separate specimen. The specimens all had the same composition and were prepared and tested under the same conditions. The curves were used to find R and ϵ for three different times – 1.5 minutes, 1 hour, and 2 hours after application of the load. With the loads used the maximum change of stress caused by decrease of the specimen area was not more than 6% 1 hour and not more than 10% 2 hours after application of the load. The variations of Δn and ϵ with the average true stresses were linear in all cases (Fig. 3).

Thus, at any time instant ($t \leq 2$ hours) after loading, the gelatin material can be characterized by values of the stress-optical coefficient C_t and the elasticity modulus E_t which are constant for the given time interval. The value of C_t increases, and that of E_t decreases with increasing time between the loading and measurement. Figure 4 shows variations, with time, of C_t and E_t calculated from the results of an experiment (Fig. 1) carried out under a constant load of 311 g; the true stress acting on the specimen was 229 g/cm² at the start and 251 g/cm² at the end of the experiment. The greatest changes in the values of C_t and E_t occur during the first hour, and subsequently the rate of change decreases considerably with time. During the whole time of action of the stress (3 hours 50 minutes) C_t increased by about 50%, while E_t decreased by 35% relative to the values of C_t and E_t 3 minutes after application of the load. During the same time the stress increased by only

10%. Therefore the increase of C_t cannot be attributed to increase of the stress. Thus, in determinations of stresses in gelatin models it must be taken into account that the stress-optical coefficient depends on the time elapsing after application of the load.

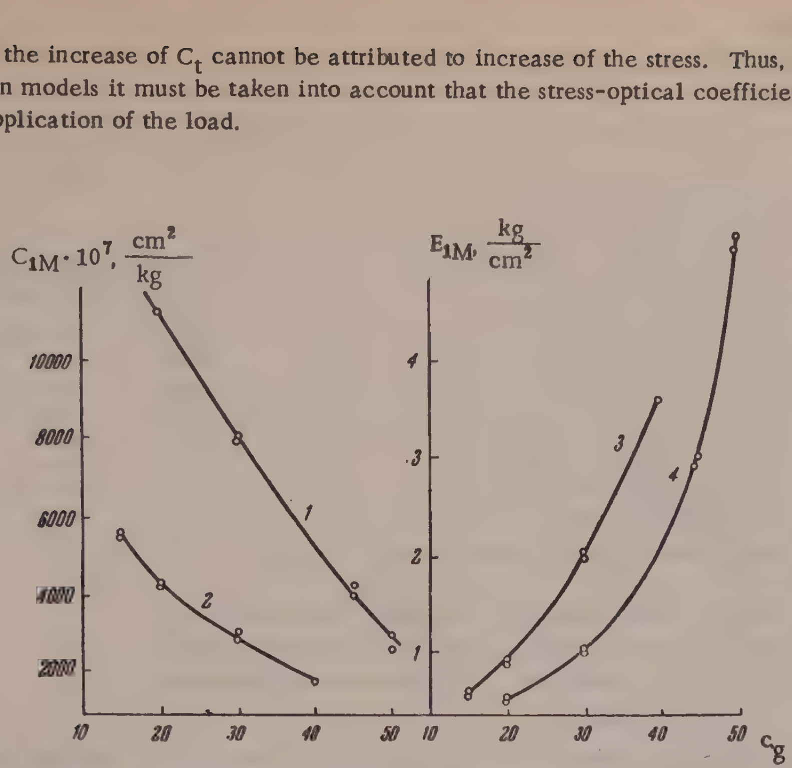

Fig. 5. Variations of the stress optical coefficient C_{1M} (1, 2) and elasticity modulus E_{1M} (3, 4) with gelatin concentration c_g at constant concentration of glycerol: 1 and 4) 10% glycerol; 2 and 3) 45% glycerol.

When the usual photoelasticity equation: $R = C(\sigma_1 - \sigma_2)d$ is applied to gelatin gels, the constant C must be replaced by the variable C(t), which depends on the time. For calibration of the material to be used for a model, curves for the variation of R and ϵ with time under constant load should be plotted for three or four different stresses; the results should then be used to calculate the values of C and E of the material for the time after application of the load at which the experiment was carried out.

Effect of gelatin concentration in the gel on optical activity and elasticity modulus. Specimens containing progressively increasing amounts of gelatin were tested. All the specimens were made and tested under the same conditions. Graphs for the variation of Δn and ϵ with σ (time after application of the load, 1-1.5 minutes) were plotted for all the specimens. The values of C_{1M} and E_{1M} determined from these graphs are shown in Fig. 5 as functions of the gelatin concentration in the gels. In another series of experiments (30% glycerol) the determinations were carried out under compression as well as under extension. It follows from the results that within the limits of experimental error $C_{1M} = E_{1M}$[*] for compression and extension; C_{1M} decreases and E_{1M} increases with increasing gelatin concentration (c_g) (Fig. 5).

In the c_g range from 15 to 35% the variations of C_{1M} and E_{1M} can be approximately represented by the expressions $C_{1M} = A/c_g$ and $E_{1M} = Bc_g^2$. Here A and B are constants for each curve, but their values vary with the glycerol concentration (see Leik's paper [7]).

It must be noted that specimens made from the same solution show small variations of C_{1M} and E_{1M} (on the average 5-6%) which may be wholly attributed to experimental error. Values of C_{1M} and E_{1M} for the same specimens made from different solutions sometimes differ by as much as 40%, which is several times the mean experimental error. These large differences must be ascribed to differences in the thermal history of these specimens. Therefore for calibration of the material the thermal conditions for the preparation of the model and the specimen must be identical.

---

[*] [As in original – Publisher].

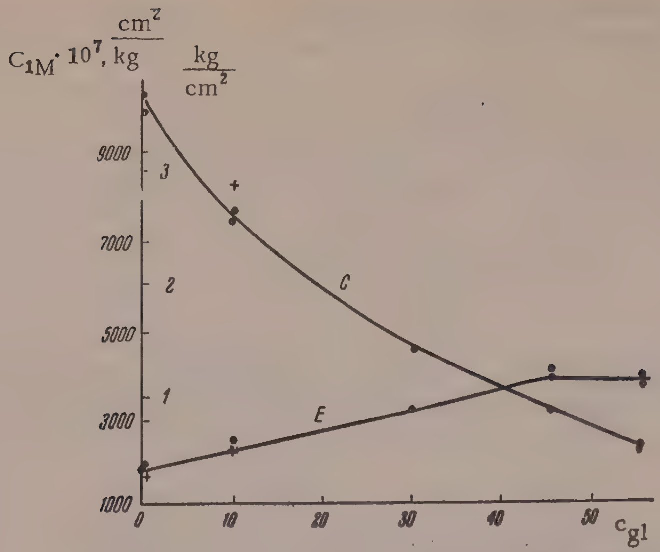

Fig. 6. Variations of the stress-optical coefficient C_{1M} and elasticity modulus E_{1M} with glycerol concentrations c_{gl} for 30% gelatin content. ●) extension, +) compression.

Effect of glycerol concentration. Variations of C_{1M} and E_{1M} with the glycerol concentration (c_{gl}) are shown in Fig. 6. It is seen that C_{1M} decreases while E_{1M} increases with increasing glycerol content. The decrease of C_{1M} is slower than that caused by increase of the gelatin content. As regards the value of E_{1M}, this increases almost linearly with c_{gl} up to about 40%, and then remains constant.

Effect of swelling time. The results of experiments with specimens differing only in the swelling time of the gelatin in the water–glycerol mixture showed that for specimens of two different compositions (30% gelatin and 30% glycerol, and 25% gelatin and 30% glycerol) the values of C_{1M} and E_{1M} remain unchanged, within the limits of experimental error, with increase of swelling time from a few minutes to 48 hours.

Effect of the dissolving time of gelatin in the water–glycerol mixture (heating time). Tests on specimens which differed only in the time during which they were "cooked" on the water bath showed that the stress-optical coefficient C_{1M} increases while the elasticity modulus E_{1M} decreases with increasing cooking time. The results are given in the Table. The specimens contained 30% gelatin and 30% glycerol; the "age" was 42 and 90 hours, and the test temperature was 19°.

It is seen from the Table that when the cooking time is increased from 2 to 7 hours C_{1M} increases by 20%, while E_{1M} decreases to about the same extent. A decrease of E_{1M} was observed previously by Fraas [6]; it can be attributed to degradation of the macromolecules during prolonged heating. Fraas recommended a cooking temperature of 60-70° in order to decrease degradation.

Effect of time elapsing after casting of the specimen (age). The test specimens differed only by the time they were left in the molds after casting. The tests were performed under compression. The gel contained 25% gelatin and 30% glycerol. The results in Fig. 7 show that E_{1M} increases and C_{1M} decreases with increasing time after casting. After four days C_{1M} diminished by nearly 20%, while E_{1M} increased by nearly 50%.

Variations of C_{1M} and E_{1M} during the first 20 hours after gelation are shown in Fig. 7,b. The less the "age" of the specimen, the higher is the rate of change of C_{1M} and E_{1M}. This change is especially rapid during the first 40 hours after casting. Therefore gels should not be used during the first few hours after gelation, when their properties change very rapidly; it is best to use them on the second day, 35-40 hours after casting.

Variation of birefringence with deformation. In publications [5] and [15] dealing with gelatin gels it has been suggested that the optical effect in gelatin gels is directly related to deformations and not to stresses.

TABLE

Variations of the Stress-Optical Coefficient C_{1M} and Elasticity Modulus E_{1M} in Extension with Cooking Time for Two Gel Specimens

Age of gel, hours	Cooking time, hours	$C_{1M} \cdot 10^7$ cm²/kg	E_{1M}, kg/cm²
42	2.7	3600	1.91
42	5.5	4200	1.70
42	7.7	4550	1.59
90	2	3750	2.21
90	5	4030	1.81
90	7	4280	1.65

The present investigation confirms this view by a number of facts: 1) the increase of the optical path difference with time under constant load (and almost constant stress) proceeds simultaneously with increase of the high-elastic deformation; 2) simultaneously with high-elastic after-effects there are path difference after-effects after removal of the load; 3) there is a close connection between the stress-optical coefficient C_{1M} and the elasticity modulus E_{1M}. Whenever the elasticity modulus E_{1M} of the gel increases (with increasing concentrations of gelatin or glycerol in the gel, and with increasing "age" of the specimen), the stress-optical coefficient decreases. If the elasticity modulus E_{1M} decreases (with increasing cooking time), the stress-optical coefficient C_{1M} increases.

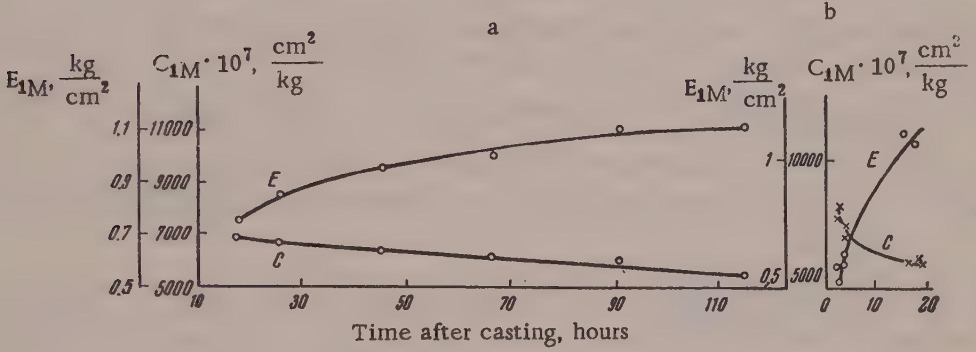

Fig. 7. Variations of the stress-optical coefficient C_{1M} and elasticity modulus E_{1M} with time after gelation at 22° ± 1°; a) during 5 days after casting; b) during the first 20 hours after casting.

All these facts can be satisfactorily explained on the hypothesis that the optical effect is directly related to the magnitude of the reversible elastic deformation, and therefore an increase of the modulus E_{1M}, which leads to a decrease of the deformation under a given stress, results in a decrease of the stress-optical coefficient.

The ratio of the birefringence Δn to the deformation ϵ may be termed the optical coefficient of deformation C_ϵ. The value of C_ϵ is obtained by multiplication of C by E

$$C \cdot E = \frac{\Delta n}{\sigma} \frac{\sigma}{\varepsilon} = \frac{\Delta n}{\varepsilon} = C_\varepsilon .$$

The behavior of C_ϵ differs in many respects from the behavior of C. When deformation and optical path difference increase with time under constant load, C_ϵ remains practically constant, decreasing by not more than 5-6% while C increases by nearly 50%. C_ϵ increases almost linearly with increasing gelatin content in the gel, and decreases linearly with increasing glycerol content. C_ϵ increases with increasing age of the specimen, the increase being particularly rapid during the first 20-40 hours after gelation.

SUMMARY

1. The value of the artifical birefringence and deformation produced under constant load at 22° in highly concentrated gelatin–glycerol gels increase with time for a least 60-70 hours.

2. The stress-optical coefficient C and the elasticity modulus E of the gels remain constant at different

stresses for equal times after application of the load (this has been demonstrated for time intervals of 1 minute to 2 hours after application of the load).

3. Variations C_{1M} and E_{1M} with the composition of the material and the preparation conditions have been studied.

4. The earlier view is confirmed that the birefringence depends directly on the deformation and not on the stress. The concept of the optical coefficient of deformation of gelatin gels is discussed and its behavior under the influence of various factors is shown.

5. The great influence of "thermal history" on the values of C_{1M} and E_{1M} has been confirmed.

In conclusion, the author expresses her deep gratitude to M. V. Gzovsky who supervised, to M. P. Volarovich and V. F. Trumbachev for guidance, to Yu. S. Lazurkin for valuable advice, and to V. V. Fedorova, who took part in the experimental work and analysis of the results.

Institute of Soil Physics Academy of
Sciences USSR Moscow

Received September 24, 1956.

LITERATURE CITED

[1] V. F. Trumbachev and N. A. Suvorov, Trans. Mining Inst. Acad. Sci. USSR 1 (1954); V. F. Trumbachev, ibid; G. A. Krupennikov and V. F. Trumbachev, Coal, No 3 (1954).

[2] F. B. Farquharson and R. G. Hennes, Civil Engineering, April, 10, No. 4, 211 (1940).

[3] D. C. John and B. C. Crisp, The Engineer, March, 465 (1953).

[4] M. V. Gzovsky, Bull. Acad. Sci. USSR, Geophys. Ser. No. 6 (1954); M. V. Gzovsky and E. I. Chertkova, op. cit. No. 6 (1953).

[5] P. Bjerken, Ann. phys. 43, 808 (1891).

[6] E. Fraas, Ann. phys. 53, 1074 (1894).

[7] A. Leik, Ann. phys. 14, 139 (1904).

[8] H. J. Pool, Trans. Faraday Soc. 21, 114 (1926).

[9] E. Hatschek, Trans. Faraday Soc. 29, 1109 (1933).

[10] R. I. Dulitskaya and S. I. Sokolov, Collected Papers of the Physicochemical Section of TsNIKL (1927) p. 138.

[11] L. D. Prokofyeva-Mikhailovskaya, Trans. Conf. on Control of Rock Pressure (Izd. AN SSSR, 1938).

[12] N. A. Mikhailov and P. A. Rebinder, Colloid J. 17, 107 (1955). [See C. B. translation].

[13] R. Maurer, Wied. Ann. 28, 628 (1886).

[14] E. Wiedemann, Verhandl. phys. Gesellschaft, Berlin, 24 October, 1884, p. 45.

[15] E. Coker and L. Filon, Optical Method of Stress Investigation (Leningrad–Moscow, 1936). [Russian translation].

THE SELECTION OF PLASTICIZERS FOR HIGH POLYMERS*

S. P. Papkov

The purpose of the present paper is to examine certain general principles of the selection of plasticizers for high polymers in relation to phase equilibrium in the plasticizer–polymer system. It is necessary to take this equilibrium into account because in most cases plasticizers, being solvents of low activity, are incompletely compatible with polymers. At definite component ratios and definite temperatures considerable changes occur in the properties of the systems as the result of microseparation which may sometimes go as far as macroseparation of one of the phases ("bleeding" of the plasticizer).

Some questions of plasticization of high polymers were considered in one of our earlier papers [1]. In particular, phase equilibrium diagrams were used for explaining the plasticizer–polymer compatibility limits, and it was shown that plasticizer–polymer compatibility is determined by the position of the equilibrium curve for separation of the system into two phases. Later, similar views were advanced by Spurlin [2] and Colborne [3].

It must be pointed out, however, that examination of the position of the phase equilibrium curve on the composition–temperature diagram is not sufficient for explaining the properties of a polymer–plasticizer system. This curve merely defines the limits of the permissible plasticizer concentrations, but does not show variations of the mechanical properties of the plasticized product at various component ratios. In Colborne's paper cited above, a curve for variations of the "melting" temperature as a function of composition is drawn on the phase equilibrium diagram, as a characterization of the mechanical properties. However, this curve by no means represents the principal properties of the plasticized polymer from the practical aspect. Moreover, Colborne's paper contains an error of principle; the point of intersection of the "melting" curve with the compatibility curve is taken as the critical temperature of mixing. It is known that phase equilibrium is not related to transitions of this type. As Kobeko [4] correctly pointed out, gradual softening of polymers cannot be regarded as a phase transition.

For a more complete characterization of the properties of a polymer–plasticizer system a suitable form of temperature–composition diagram is one which shows, together with a phase equilibrium curve for the components, a family of curves for isoviscous solutions. Additional justification for this is that the principal purpose of polymer plasticization is modification of its viscous properties so that the system is not prone to brittle fracture at a given frequency of load variation. As is known, brittleness depends mainly on viscosity. Under normal use conditions the viscosity limit of plasticized polymers (above which brittle fracture occurs) is of the order of 10^{10} - 10^{13} poises. Additions of plasticizers (formation of polymer solutions) lowers the viscosity of brittle polymers down to the limits set by the use conditions.

Figure 1 is a generalized diagram of this type for a polymer–plasticizer system. Before consideration of variations in the properties of the system, it is necessary to comment briefly on the general nature of the curves in the diagram.

The phase equilibrium curve ABC lies far on the side of high plasticizer concentrations; this is in accordance with practical data on equilibria in polymer–solvent systems [5]. In a plasticized polymer, the composition of one of the coexisting phases differs very little from that of the pure plasticizer; it is therefore sometimes justifiable to speak of the separation ("bleeding") of pure plasticizer in the case of a system which lies in the region of phase separation, although in theory the concentration of the high polymer in the separating liquid phase is not zero. The maximum on the curve also lies in the region of low polymer concentrations, whereas the second branch of the curve can lie at low temperatures, according to practical data on plasticizer–polymer compatibility, in the region of 25-75% plasticizer concentration (by weight).

---

* Communication II in the series "Phase Equilibria in Colloid Systems."

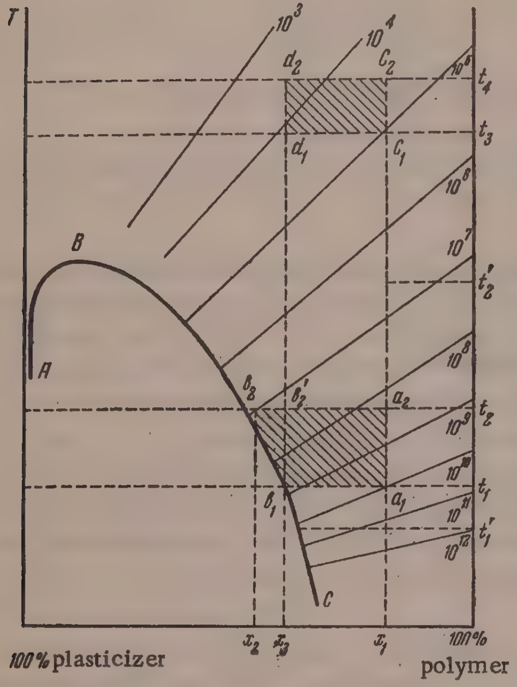

Fig. 1: Phase equilibrium diagram for a polymer–plasticizer system.

The position and form of the group of curves for isoviscous solutions as shown in the diagram are to some extent arbitrary, but they conform to the known fact that for solutions of equal concentration the viscosity increases with decrease of temperature according to an exponential law, the exponent being greater than unity. Nevertheless, the exact nature of the isoviscous curves is not important for the subsequent discussion. It is only important to note that these curves do not intersect. For convenience of analysis, these curves have been given values from 10^{12} to 10^3 poises, which represent the practical limits within which the viscosity of plasticized polymers varies during molding and in use.

Let us consider an example of the choice of the quantitative polymer–plasticizer ratio on the basis of this diagram. If the temperature range in which the polymer products are to be used is t_1-t_2, then the diagram shows that the unplasticized polymer will be unsuitable for use, as the brittle limit (viscosity 10^{10} poises) for the pure polymer lies within this temperature range. Addition of plasticizer to the polymer lowers its viscosity. We follow the dash line corresponding to the temperature t_1 (the lower temperature limit for use of the product) in the diagram until we reach the point a_1, at which the viscosity of the plasticized polymer is 10^{10} poises. This point corresponds to the composition x_1. This is the lower limit for the amount of plasticizer which must be added to the polymer. With lower plasticizer contents the product will not have the necessary plasticity in the conditions of use.

The upper limit for the plasticizer content can also be determined from the viscosity of the plasticized polymer. If the product is under load for considerable periods at the highest use temperature, the possibility of considerable irreversible deformations must be taken into account. Let us assume that on practical grounds the viscosity of the product must not be less than 10^7 poises to avoid appreciable residual deformations. Then the maximum permissible amount of plasticizer is determined by the position of the point b_2 (intersection of the t_2 temperature line with the 10^7 poise viscosity curve), which corresponds to the composition x_2. It is found, however, that for the case shown in this diagram this upper limit of plasticizer concentration is unacceptable, as with the composition x_2 the system enters the region of separation into two phases when the temperature falls to the lower limit t_1. If the product is used in the low temperature region, the plasticizer–polymer compatibility limit will be passed; this will influence the properties of the product and will result in "bleeding" of the plasticizer. The compatibility limit is determined by the phase equilibrium curve, and for temperature t_1 (point b_1) it corresponds to the composition x_3. The plasticizer content of the system cannot exceed this limit. Thus the region of temperatures and compositions satifying the given brittleness and flow conditions lies within the limits of the shaded area. In practice only the area confined between the points a_1, a_2, b_2, b_1 is used.

Let us consider other possible limitations in the selection of plasticizers. Suppose that the lower temperature limit for use of the product is t_1', while the character of the mechanical stresses remains the same, so that brittle fracture corresponds to a viscosity of 10^{10} poises. Examination of the diagram shows that the required degree of plasticization cannot be attained in this system, as with an increase of the plasticizer content at temperature t'_1 the compatibility limit is reached before the required plasticity. It is therefore necessary to choose another plasticizer, with the phase equilibrium and isoviscosity curves in other positions, such that the region of the required viscosities of the product does not overlap the region of phase separation of the system.

On the other hand, if the use temperature range is extended in the direction of higher temperatures and lies, for example, between t_1 and t'_2, then it is impossible to use the particular plasticizer if the minimum viscosity is 10^7 poises (to avoid irreversible deformation), since at temperature t'_2 and the lower plasticizer concentration limit the viscosity of the product will be below 10^7 poises. It is therefore necessary to choose another plasticizer, with a smaller change of viscosity with temperature.

Yet another limitation in the choice of plasticizers is the molding temperature. If the molding is effected by the casting process with subsequent evaporation of volatile solvent from the solution, the stability of the plasticizer and polymer at high temperatures is not significant. However, if the molding is a mechanical process involving heating, the temperature at which the system reaches the required viscosity must not exceed the decomposition temperature of the polymer or plasticizer. The temperature range for mechanical molding is determined by the lower and upper viscosity limits. If, for example, the lower viscosity limit is 10^5 poises, and the upper limit must not exceed $5 \cdot 10^3$ poises, the molding temperature range for the case considered above will be $t_3 - t_4$, which corresponds to the shaded area c_1, c_2, d_1, d_2 in the diagram. The plasticizer can be regarded as suitable if the system does not undergo thermal decomposition at temperature t_4.

It is of interest to follow the changes in the mechanical properties of a plasticized polymer with variations of composition and temperature. For this it is most convenient to determine total deformations under loads acting for relatively short times, as this corresponds to the most usual conditions in which plasticized products are used. In this paper we shall confine ourselves to consideration of "rigid" polymers, in view of the fact that plasticization of this group of polymers presents the greatest practical interest. Such polymers include cellulose esters or ethers, which do not have rubberlike elasticity under normal conditions.

Figure 2 shows, in simplified form, a phase equilibrium diagram for a polymer—plasticizer system with two isoviscosity lines: the lower line corresponds to transition of the system into the glassy (brittle) state, and the upper corresponds to transition into a state of high fluidity. As is known, both these limits are arbitrary, and in practice they cover viscosity ranges of 10^{10} - 10^{13} poises (glass transition) to 10^3 - 10^5 poises (high fluidity).

Let us consider variations of the total deformation with the temperature at constant polymer : plasticizer ratio. At concentration x_1, which is beyond the limit of phase separation, increase of temperature should produce a gradual increase of deformation (Curve 1, Fig. 2,a); until the glass transition limit is reached the deformation is elastic in character and does not exceed 1-2%, while above this limit irreversible deformation should increase considerably, and should reach very high values (flow) at the second viscosity boundary (temperature t_4).

The following situation should be found for a concentration x_2 lying in the region of phase separation of the system. The system separates into two phases; one of these, which determines the principal mechanical properties of the system, is a concentrated solution of the polymer in the plasticizer, and the other is the practically pure plasticizer. In most cases the conditions for separation of high polymer systems into two phases are such that the low-viscosity phase is liberated in the form of micro-inclusions in a continuous high-viscosity phase. The resulting system, with incomplete macroscopic separation, is a gel and therefore has increased elasticity [6]. With increase of temperature, when the viscosity of the concentrated phase passes beyond the brittle fracture limit, i.e., at t_1, this peculiar structure of the two-phase system begins to have an effect. Elastic bending of the thin "walls" (interlayers) of the viscous phase leads to a sharp increase of reversible deformation. This reversible deformation of a laminar system differs in principle, on the one hand, from the elastic deformation of a continuous solid, where changes of interatomic distances within the limits of the potential barriers play the principal role, and on the other, from rubberlike elasticity, in which the principal role is played by changes in the equilibrium length of the curved macromolecules. This type of reversible deformation could be conventionally termed the elasticity of a gel system, in contrast to rubberlike elasticity. As has already been stated [6], gel system elasticity is characteristic not only of high polymers, but of any substances which form gels. The maximum value of this type of deformation cannot in theory exceed 57% of the original length of the specimen.

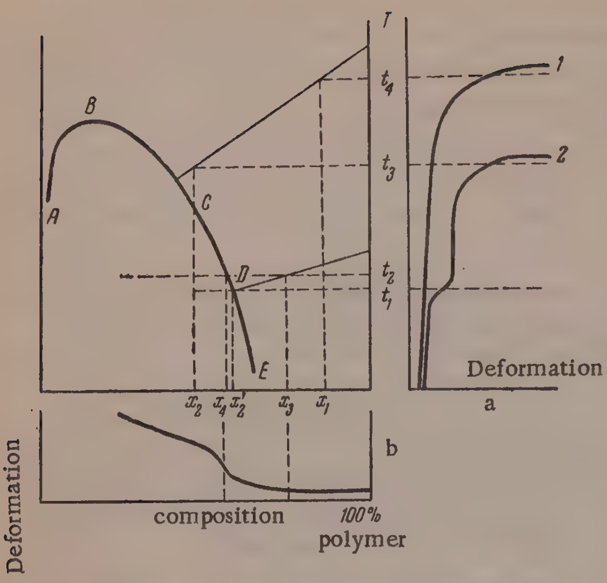

Fig. 2. Variations of the mechanical properties of a plasticized polymer with temperature (a) and composition (b).

The curve for variations of the total deformation for the concentration x_2 will have the following form (Curve 2, Fig. 2,a). Up to temperature t_1 elastic deformation will prevail; this will not exceed 1-2%, as the viscosity of the concentrated phase lies above the glass transition limit. The concentration of this phase varies along the phase equilibrium curve BCDE. At temperature t_1 the composition of the second phase will correspond to concentration x'_2 (point D) while its viscosity will reach the limit at which gel system elasticity begins to appear. At this point in Curve 2 (Fig. 2,a) there will be a sharp increase of total deformation, the greater part of which will consist of the gel system elasticity, since elastic deformation does not change greatly with temperature, while plasticity does not have time to develop to any appreciable extent during the brief action of the load. With further increase of temperature the system still consists of two phases, but the composition of the second phase shifts in the direction of lower polymer concentrations, and its plasticity begins to increase appreciably. Deformation due to plastic flow of the system begins to predominate in the total deformation. At the point C, a single phase is formed. Elasticity due to the gel structure of the system disappears at this point, but plasticity (fluidity) becomes considerable. Finally, at temperature t_3 a viscosity is reached at which the product becomes a liquid of relatively low viscosity. The general form of Curve 2 is characterized by the presence of a "plateau" which corresponds to the region of high reversible deformation.

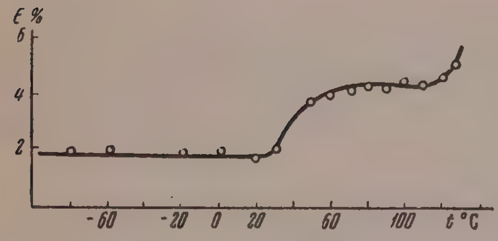

Fig. 3. Variation of deformation with temperature in the system nitrocellulose–dibutyl phthalate (after Kozlov and Russkova).

As an example, let us consider the experimental data obtained by Kozlov and Russkova [7] for the system nitrocellulose–dibutyl phthalate. Figure 3 shows one of their curves for the variations of the total deformation, over a wide temperature range, of a nitrocellulose–dibutyl phthalate composition in a molar ratio of 1:0.75. The general form of this curve is in agreement with the form of the schematic curve in Fig. 2,a (Curve 2).

Let us now consider in a similar way the variations of deformation with composition of the plasticized product at constant temperature. A schematic curve for the variation of total deformation at temperature t_2 is given in Fig. 2,b. It is seen in Fig. 2,b that the deformation remains practically constant and corresponds to the elastic deformation of an amorphous solid up to the composition x_3, which represents the limit of brittleness. With further increase of plasticizer content the viscosity of the system gradually decreases; this leads to some increase of total deformation owing to an increase of its irreversible component. At the point corresponding to composition x_4 the system separates into two phases with formation of a gel, and accordingly the total deformation increases considerably on account of an additional component – gel system elasticity. Further increase of plasticizer content produces an increase of total deformation because the amount of the second phase diminishes while the specific load on the specimen remains constant. No increase of the plastic component should be found above the concentration x_4. The deformation of the system will be predominantly reversible up to concentrations corresponding to the solubility limit of the polymer in the plasticizer (limit of gel formation). This region is not shown on the curve, as the deformation (fluidity) of plasticizer with low polymer content has very high values.

An experimental example is provided by data for the system nitrocellulose–dibutyl phthalate, taken from the paper by Kozlov and Russkova [8]. For temperatures of 40 and 60°, the total deformation curves show sudden rises at dibutyl phthalate–nitrocellulose ratios between 0.50–0.75:1 (Fig. 4). The dash line represents elastic and plastic deformations, extrapolated from the initial points. This curve also coincides in principle with the schematic curve in Fig. 2,b. Unfortunately, the paper [8] does not give points between 0.50 and 0.75 mole of plasticizer, which would make the curve more precise. However, its general nature is evident. *

A similar high elasticity effect for the same nitrocellulose–dibutyl phthalate system was found by Wadano [9], who found that at plasticizer concentrations above 40% (approximately 0.6 mole per 1 mole of nitrocellulose) the plasticized specimen tends to return to its original cross section after rupture under tension. At lower plasticizer concentrations the specimen exhibits ordinary plastic flow at break. Figure 5 gives a curve for the variation of the cross section of the specimen at break with the component ratio, based on Wadano's data.

It follows from this scheme for the variations of the mechanical properties of a polymer with additions of substances of low molecular weight that the same substance may produce both an increase of plasticity and large reversible deformations, according to the amount added. Until the compatibility limit is reached, a low-molecular substance increases the plasticity of the polymer; above this limit the plasticity of the system does not increase, but large reversible deformations arise.

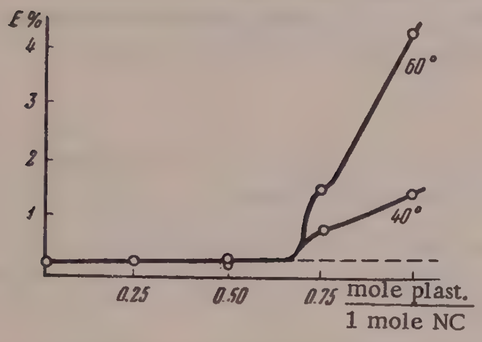

Fig. 4. Variations of deformation with nitrocellulose–dibutyl phthalate ratio (after Kozlov and Russkova).

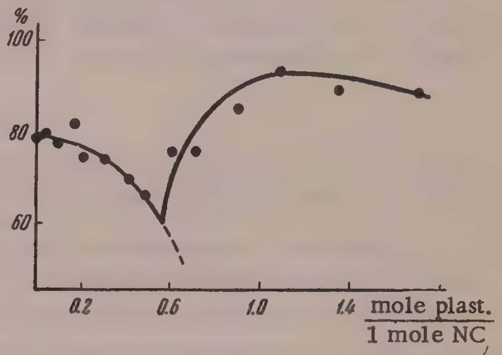

Fig. 5. Cross section of specimen at break (as % of original cross section) for the system nitrocellulose–dibutyl phthalate (after Wadano).

On these grounds, classification of low-molecular substances into plasticizers and elasticizers [10] according to their effects on the mechanical properties of polymers is inappropriate. By this classification a substance such as dibuyl phthalate is both a plasticizer and an elasticizer for nitrocellulose, since limited amounts of it decrease the viscosity of the system, while large amounts give rise to considerable reversible deformations.

In introducing the concept of elasticizers, Kozlov and Russkova assumed that certain substances can increase the flexibility of polymer macromolecules and thereby confer rubberlike properties to "rigid" polymers. It is difficult to believe, however, that the polar groups which hinder free rotation of adjacent polymer segments are shielded only when very large amounts of low-molecular substances are added, and that the effect is not produced by moderate additions. In fact, experimental data show that high reversible deformations in polymer–plasticizer systems are found only with considerable amounts of plasticizers, and the effect arises abruptly.

Moreover, the interacting polar groups which are the cause of polymer "rigidity" are situated at distances of the same order of magnitude as interatomic distances. Accordingly, increases of macromolecular flexibility should be more likely on addition of substances with small molecules, and in particular, on addition of the lower members of a homologous series. However, the "elasticization" effect is found primarily with the higher members of homologous series. For example, according to the data of Kozlov and Russkova, this effect is produced by dibutyl phthalate but not by dimethyl phthalate.

---

* The paper by Kargin et al. [11] contains an analogous diagram for the system polyvinyl chloride–dibutyl phthalate, which coincides in form with the schematic curve in Fig. 2,b.

According to the concepts of the mechanism by which the properties of a polymer are changed in plasticization, as developed in this paper, the difference between the behavior of dimethyl and dibutyl phthalates is entirely due to the higher compatibility of dimethyl phthalate with nitrocellulose. With very large additions of dimethyl phthalate, large reversible deformations should also be found; evidence for this is the formation of elastic gels with nitrocellulose concentrations of the order of 2-5% in dimethyl phthalate. On the other hand, solvents do not produce the "elasticization" effect.

In conclusion, let us consider possible practical methods for determining the limits of plasticizer–polymer compatibility. The plotting of phase equilibrium curves is made very difficult by the very high viscosity of one of the phases formed, so that complete hydrostatic phase separation is not attained in finite periods. Sorption of a plasticizer by a polymer is equally slow, and it is impossible to obtain equilibrium values in practice. Spurlin [2] refers to Mark's proposed method for determination of equilibrium concentrations in such systems from the vapor pressures of the low-molecular substances over the solutions. However, this method also involves exceptionally great experimental difficulties.

A suitable method for practical purposes is to make use of the fact, described above, that large reversible deformations arise at the point of phase separation of the system, for plotting phase equilibrium curves. The similarity of independent data obtained by Wadano (0.6 mole plasticizer per 1 mole nitrocellulose) on the one hand, and by Kozlov and Russkova (0.50-0.75 mole) on the other, shows that this is a suitable method for determining the approximate position of the phase equilibrium curve.

Examination of the relationship between the properties of the plasticized product and the molecular weight of the polymer is of undoubted interest. However, this involves a more detailed analysis of variations in the character of the phase equilibrium curve in relation to the degree of polymerization of the polymer.

SUMMARY

1. Phase equilibrium in the system polymer–plasticizer is discussed. The properties of such systems can be represented by phase equilibrium diagrams on which are plotted isoviscosity curves.

2. It is shown that the practical choice of an actual plasticizer and determination of the amount of it to be added to the polymer depend both on the nature of the group of the isoviscosity curves, and on the position of the phase equilibrium curve on the composition–temperature diagram.

3. Variations of the mechanical properties of plasticized polymers with the temperature and plasticizer content are briefly discussed. An attempt is made to explain the appearance of large reversible deformations at definite temperatures and polymer–plasticizer ratios; this is attributed to transition of the system into the region of separation into two equilibrium phases, with incomplete separation (gel formation).

4. It is pointed out that the same low-molecular substance can change both the plasticity and the elasticity of a polymer, depending on whether the amount of it is below or above the compatibility limit. Accordingly, the classification of low-molecular substances by their effects on polymers into plasticizers and elasticizers has no adequate basis.

5. The principle is proposed of a method for determining the phase equilibrium curve for a polymer–plasticizer system from the points at which increased reversible deformation begins to occur in the plasticized polymer.

Moscow

Received November 17, 1956.

LITERATURE CITED

[1] S. Papkov, Org. Chem. Ind. 6, 240 (1939).

[2] H. M. Spurlin, A. F. Martin and H. G. Tennet, J. Pol. Sci. 1, 63 (1947).

[3] R. S. Colborne, Brit. Plastics 20, 346 (1948).

[4] P. P. Kobeko, Amorphous Substances (Izd. AN SSSR, Moscow–Leningrad, 1952).

[5] S. P. Papkov, V. A. Kargin and Z. A. Rogovin, J. Phys. Chem. 10, 157,607 (1937); A. Dobry, J.

chim. phys. 35, 397 (1938); A. R. Schultz and P. J. Flory, J. Am. Chem. Soc. 75, 3888 (1953).

[6] S. P. Papkov, Colloid J. 19, 333 (1957).*

[7] P. V. Kozlov and E. F. Russkova, Proc. Acad. Sci. USSR 99, 105 (1954).

[8] P. V. Kozlov and E. F. Russkova, Proc. Acad. Sci. USSR 95, 583 (1954).

[9] M. Wadano, Koll.-Z. 93, 103 (1940).

[10] P. V. Kozlov and E. F. Russkova, High Polymers, No. 12, 44 (State Chemistry Press, 1952).

[11] V. A. Kargin, G. L. Slonimsky and L. Z. Rogovina, Colloid J. 19, 142 (1957).*

---

* Original Russian pagination. See C. B. translation.

EXCHANGE OF SODIUM AND CALCIUM IONS ON SWELLING SULFONIC AND CARBOXYLIC RESINS

G. V. Samsonov, A. A. Vasilyev, and V. A. Orestova

It was established by a thermodynamic method [1] that in the exchange of ions of any valency the selectivity of ion sorption (determined by the exchange constant) should diminish with increasing swelling of the resins.

The ion exchange constant in the equation

$$\frac{m_1^{1/z_1}}{m_2^{1/z_2}} = K \frac{c_1^{1/z_1}}{c_2^{1/z_2}} \tag{1}$$

(where m_1 and m_2 are the amounts of sorbed ions in mg-equiv./g; c_1 and c_2 are the concentrations of the ions in solution; z_1 and z_2 are the ionic charges) for resins of different degrees of swelling depends on the change of thermodynamic potential ($n_s \Delta \Phi_s$) during swelling or shrinkage of the resin during ion exchange

$$K = e^{r - n_s \Delta \Phi_s}, \tag{2}$$

where r can be regarded as a constant for any given pair of exchanging ions; n_s is the number of moles of solvent transferred into or out of the resin in the exchange of 1 mg-equivalent of ions.

Since $n_s \Delta\Phi_s > 0$ if sorption of the first component (see Equation (1)) leads to shrinkage of the resin, it follows, according to Equation (2), that the ion exchange constant will decrease with increasing swelling of the resins. If, in addition, the component the sorption of which causes shrinkage of the resin is sorbed more selectively, it follows that selectivity of ion sorption diminishes with increasing degree of swelling of the resins.

Since these relationships are of considerable theoretical interest, it was desired to verify them experimentally by a study of the exchange of metal ions on swelling resins.

The swelling resins used were KFU carboxylic resins supplied to us by A. A. Vansheidt and N. N. Kuznetsova, and SNF sulfonic phenolic resins prepared by us by the method described by A. A. Vansheidt and A. A. Vasilyev.

The carboxylic resins are polymers of phenoxyacetic acid

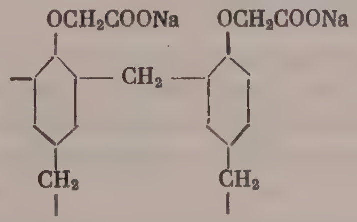

The structure of the SNF cation exchange resins can be represented as

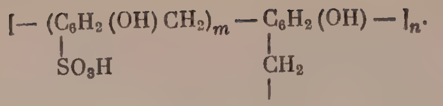

$$[-\underset{\underset{SO_3H}{|}}{(C_6H_2(OH)CH_2)_m}-\underset{\underset{\underset{|}{CH_2}}{|}}{C_6H_2(OH)}-]_n.$$

The sulfo group content of the resin was determined by the action of an excess of neutral salt solution on the resin in hydrogen form, followed by titration of the solution in presence of the resin, with methyl orange indicator [2].

The total sulfur found in SNF resins by elementary analysis is usually somewhat greater than the "active sulfur" content of the sulfo groups. The "inactive" sulfur is most probably present in the form of sulfones, which can also take part in cross bonding.

The degree of swelling of a cation exchange resin depends on the amount of formaldehyde present and on the heat treatment conditions of the insoluble sulfonation product. SNF sulfonic resins can be recommended as cation exchangers of fairly high exchange capacity with considerable swelling coefficients, which retain satisfactory mechanical strength.

The action of formaldehyde on the soluble sulfonation products is accompanied by a decrease of sulfo group content and additional cross bonding. An increase of the amount of added formaldehyde produces a considerable decrease of the swelling coefficient and exchange capacity and a further increase of the mechanical strength of SNF resins.

The substances chosen for the investigation were three samples of SNF resins based on the same starting material with different amounts of cross-linking agent (formaldehyde). The properties of the SNF resin samples are given in Table 1.

TABLE 1

Properties of Samples of SNF Sulfonic Resins

Sample No.	g formaldehyde per 100 g of starting material	Coefficient of swelling of resin in H form	Exchange capacity (by titration of resin in presence of NaCl) in mg-equiv./g	Sulfur content, %	
				By titration	By elementary analysis
1	21.5	2.4	2.78	8.91	10.60
2	6.5	4.2	3.53	11.29	11.24
3	4.6	9.7	3.81	12.22	12.74

Determination of exchange constants for sodium and calcium ions on KFU carboxylic resins. Ion exchange was studied by the dynamic method. A solution containing sodium chloride and calcium chloride in known concentrations was passed through a column containing KFU resin previously converted into the sodium form. Two methods were used for determining the amounts of ions taken up.

The first method involved the plotting of an elution curve, i.e., the relationship between the ion concentration at the exit from the column and the volume of the solution passed through. These curves were used to calculate the amounts of ions taken up. In the second method, after complete saturation of the column, when the resin had reached equilibrium with the original solution, sodium and calcium were displaced from the resin by hydrochloric acid solution and determined quantitatively in the eluate. The results are given in Table 2. The total exchange capacity was also determined by a dynamic method, from the displacement of sodium ions by calcium ions.

It is clear from Fig. 1 and Table 2 that the exchange constant K decreases with increasing swelling of the resins. This is in agreement with the theory put forward earlier [1], as sorption of the first type of ions –

calcium ions — leads to shrinkage of the resins. The exchange constant decreases only slightly with a small increase of the swelling coefficient of KFU resins from 2 to 3.3. With a very strongly swelling KFU resin ($K_s = 11$) the exchange constant decreases sharply. It must be pointed out that the exchange constants were determined over a very wide range of sodium ion concentrations, up to 1 N. At the same time, the ion exchange law without activity coefficients taken into account, as expressed by Equation (1), was very strictly obeyed.

TABLE 2

Exchange of Sodium and Calcium Ions on KFU Carboxylic Resins with Different Degrees of Swelling (K_s); m is Total Exchange Capacity

K_s	m in mg-equiv/g	c_{Ca} in mg-equiv.	c_{Na} in mg-equiv.	m_{Ca} in mg-equiv/g	m_{Na} in mg-equiv/g	K
2.0	4.37	0.0050	0.50	2.56	1.81	6.25
2.0	4.37	0.0024	0.25	2.92	1.45	6.02
2.0	4.37	0.00108	0.10	3.45	0.92	6.16
2.0	4.37	0.00052	0.05	3.68	0.69	6.11
3.3	4.47	0.0107	1.00	2.15	2.32	6.11
3.3	4.47	0.00535	0.50	2.58	1.89	5.81
3.3	4.47	0.0026	0.25	3.0	1.47	5.75
3.3	4.47	0.00115	0.10	3.53	0.94	5.90
11	4.10	0.0108	1.0	1.23	2.87	3.72
11	4.10	0.00526	0.50	1.79	2.31	4.00
11	4.10	0.00266	0.25	2.24	1.86	3.90
11	4.10	0.00095	0.10	2.70	1.40	3.91

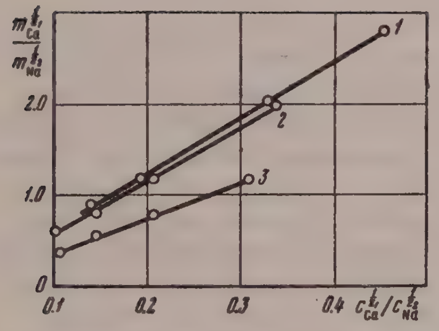

Fig. 1. Exchange of calcium ions with sodium ions on KFU carboxylic resins with different swelling coefficients: 1) 2; 2) 3.3; 3) 11.0.

All the determinations with KFU carboxylic resins were carried out at a constant concentration ratio of the exchanging ions, $c_{Na}/c_{Ca} = 100$. Table 2 shows that dilution of the solution leads to an increase in the sorbability of ions with the higher charge — calcium ions; this has been shown by a number of workers [3] for other systems.

Determination of the exchange constants of sodium and calcium ions on SNF sulfonic resins. The exchange constants of sodium and calcium ions on sulfonic phenolic resins with swelling coefficients 2.64, 4.44, and 10 were determined by the dynamic method described above. The results of determinations of the exchange capacity of the sulfonated resins (at the sulfo groups only — the exchange of Na^+ and Ca^{2+} ions took place in neutral solutions) and of the sorption capacity for sodium and calcium ions at definite equilibrium concentrations of the ions in solution are given in Table 3.

Comparison of the exchange constants of resins of different degrees of swelling (Table 3 and Fig. 2) shows that the exchange constant for calcium and sodium ions decreases with increasing degree of swelling of the resin, as sorption of calcium ions leads to a decrease in the degree of swelling of the resin. The exchange constant can be either greater or less than unity for resins of different degrees of swelling. Calcium ions are selectively sorbed on weakly swelling resins, and sodium ions on strongly swelling resins. Sulfonation is more complete at low degrees of cross linkage of the resin, which leads to an increase of the exchange capacity. However, this increase of the exchange capacity of swelling resins is not sufficient, as a sole factor, for practical utilization of strongly swelling resins for water softening, as the selectivity of calcium sorption and the total exchange capacity per unit volume decrease simultaneously with it.

TABLE 3

Exchange of Sodium and Calcium Ions on SNF Sulfonic Phenolic Resins with Different Degrees of Swelling (K_s); m is Total Exchange Capacity

K_s	m in mg-equiv/g	c_{Ca} in mg-equiv	c_{Na} in mg-equiv	m_{Ca} in mg-equiv/g	m_{Na} in mg-equiv/g	K
2.64	2.70	0.030	0.050	2.30	0.40	1.09
2.64	2.70	0.0100	0.050	2.02	0.68	1.05
2.64	2.70	0.0050	0.050	1.82	0.88	1.08
4.44	3.67	0.030	0.050	3.04	0.63	0.799
4.44	3.67	0.0100	0.050	2.60	1.07	0.753
4.44	3.67	0.0050	0.050	2.32	1.35	0.798
10.0	4.02	0.030	0.050	3.16	0.86	0.596
10.0	4.02	0.0100	0.050	2.64	1.38	0.590
10.0	4.02	0.0050	0.050	2.22	1.80	0.585

Laws governing exchange of sodium and calcium ions on ion exchange resins in concentrated solutions. Ion exchange over a wide range of ion concentrations conforms to Nikolsky's equation [4], which has the form:

$$\frac{m_1^{1/z_1}}{m_2^{1/z_2}} \cdot \frac{\overline{f}_1^{1/z_1}}{\overline{f}_2^{1/z_2}} = K^x \frac{c_1^{1/z_1}}{c_2^{1/z_2}} \frac{f_1^{1/z_1}}{f_2^{1/z_2}}, \qquad (3)$$

where f_1 and f_2 are the activity coefficients of the ions in solution and on the resin respectively.

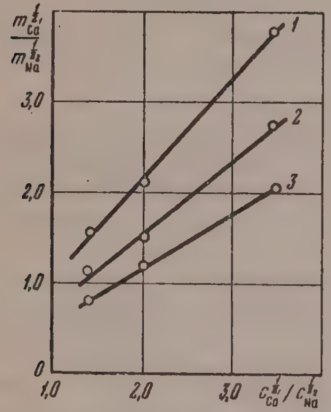

Fig. 2. Exchange of calcium ions with sodium ions on SNF sulfonated resins with different swelling coefficients: 1) 2.64; 2) 4.44; 3) 10.0.

For exchange of ions of different valencies, Equation (3) should include all the variables, and the ratio of the activity coefficients of the ions in solution, $f_1^{1/z_1} / f_2^{1/z_2}$, should vary considerably with changes in the ionic strength of the solution. Nevertheless, as can be seen in Fig. 3, in the exchange of sodium and calcium ions on KFU carboxylic resins the exchange constant K, calculated without activity coefficients taken into account, retains a constant value over a very wide range of concentrations of the ions in solution.

The data given in the beginning of this paper, showing that the ion exchange law is obeyed for the same system of ions on sulfonated resins, are related to low ion concentrations. In such conditions the exchange constant K was independent of the ion concentrations. The exchange constant for Ca^{2+} and Na^+ ions was then determined for solutions of higher ionic strengths.

It is seen in Fig. 3 that in this case the ion exchange constant increases considerably. These results can be interpreted as follows.

The following conditions should be satisfied in the exchange of calcium and sodium ions on carboxylic resins:

$$\frac{\bar{f}_1^{1/z_1}}{\bar{f}_2^{1/z_2}} = \frac{f_1^{1/z_1}}{f_2^{1/z_2}}. \tag{4}$$

This condition is not satisfied in the exchange of the same ions on sulfonic resins. It is possible that Equation (4) is valid if the resin swells strongly. In that case the ions present in the resin are surrounded by a solution which exerts the same electrostatic action on the ions as is exerted by the solution outside the resin on the ions present in the solution.

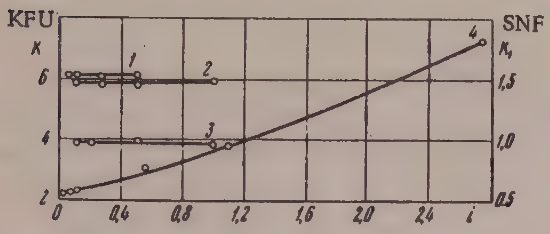

Fig. 3. Variation of the exchange constants for calcium and sodium ions on carboxylic and sulfonic resins with ionic strength of the solution: 1) KFU, $K_s = 2.0$; 2) KFU, $K_s = 3.3$; 3) KFU, $K_s = 11.0$; 4) SNF, $K_s = 10.0$.

It is probable that a significant role is also played by the weakness of the interaction of the ions with the carboxylic resin polymer, so that the solvate shell surrounding the ion is not changed substantially. The validity of Equation (4) depends on the presence of two factors – swelling of the resin and weak interaction between the ions and the resin. In such cases ion exchange conforms to the following equation over a wide range of concentrations:

$$\frac{m_1^{1/z_1}}{m_2^{1/z_2}} = K\,\frac{c_1^{1/z_1}}{c_2^{1/z_2}}.$$

SUMMARY

1. The exchange of sodium and calcium ions on KFU carboxylic resins and SNF sulfonic resins of various degrees of swelling has been studied. The selectivity of ion sorption diminishes with increasing degree of swelling.

2. The sorption of calcium ions by KFU resins increases with increasing dilution of solutions containing calcium and sodium ions.

3. The exchange of sodium and calcium ions on carboxylic resins obeys the ion exchange equation in which the activity coefficients of the ions are not taken into account, over a wide concentration range. Exchange of these ions on the sulfonic resins does not conform to this equation at high ionic strengths of the solution.

Institute of High Molecular Compounds
Leningrad

Received November 19, 1956.

LITERATURE CITED

[1] G. V. Samsonov, Colloid J. 18, 592 (1956).*

[2] A. A. Vansheidt, A. A. Vasilyev, and O. I. Okhrimenko, Theory and Practice of Ion Exchange Materials, Collected Papers (Izd. AN SSSR, Moscow, 1955) p. 110.

[3] K. K. Gedroits, The Sorption Capacity of Soils (1933); E. N. Gapon and A. O. Pryanishnikov, Colloid J. 3, 347 (1937); E.N. Gapon and A. I. Ivanov, Colloid J. 3, 443 (1937); E. N. Gapon and N. I. Gorbunova, Colloid J. 3, 447 (1937); K. M. Saldadze and E. D. Bozhevolnov, Colloid J. 16, 387 (1954);* G. V. Samsonov and S. E. Bresler, Colloid J. 18, 88 (1956);* G. V. Samsonov and S. E. Bresler, Colloid J. 18, 337 (1956).*

[4] B. P. Nikolsky and V. I. Paramonova, Progr. Chem. 8, 1539 (1939).

---

* [See C. B. translation].

HYDRATES OF THE CALCIUM SALTS OF CERTAIN FATTY ACIDS

V. I. Solnyshkin

The formation of hydrates of saturated and unsaturated salts of fatty acids (soaps) plays an important role in the production of lubricant greases and in flotation processes of ore beneficiation, in which soaps are used as collecting agents, and especially in the use of these substances as stabilizing and peptizing agents in disperse (colloidal) systems.

Earlier investigations [1, 2] show that soaps can be obtained in hydrated form under certain conditions, while determinations of the heats of wetting of the water-insoluble calcium salts of stearic, oleic, and ricinoleic acids may give an indication of the amounts of water coordinated by the polar groups.

The calcium salts of stearic and oleic acids were prepared by two methods: by Trapeznikov's method [3], based on direct reaction of the fatty acid with Ca^{2+} ions, which ensures that the final product is free from univalent metals which may enter it in exchange reactions with sodium salts. The product was then treated, in powder form, with 96% ethyl alcohol and then dried in ampoules under vacuum. Calcium oleate and ricinoleate were also prepared by neutralization of alcoholic solutions of the fatty acids with calcium oxide.

The following method was used for neutralization of fatty acids in alcoholic solution: a weighed sample of oleic acid was dissolved in 3-4 times its own volume of alcohol and heated to boiling in a flask under reflux. Finely divided chemically pure calcium oxide, previously heated at 800°, was then added in 0.5-0.6 g portions to the solution in the flask. When all the calculated amount of calcium oxide had been added, the calcium soap, which is insoluble in the alcohol–water mixture, settled on the bottom of the flask. The neutral soap was boiled for 12-20 hours in the aqueous alcohol mixture until the calcium oleate melt changed from a turbid white into a pale yellow clear layer. The aqueous alcohol solution was decanted hot from the flask, as at temperatures below 40° the formation of an acid soap in the surface layer is possible [4].

The preparation of calcium ricinoleate is made difficult by its good solubility in alcohol. Therefore the neutralization must be carried out in absolute alcohol. The solubility of calcium ricinoleate in alcohol is probably due to the presence of a hydroxyl group in its molecule, situated at the 12th carbon atom from the acid group. The method of preparation was as before, but instead of 96% ethyl alcohol anhydrous rectified spirit prepared by boiling with CaO was used. The end of the reaction was indicated by the appearance of a pale pink color with phenolphthalein. A few drops of ricinoleic acid were added to take the pH of the solution to 7. At the end of the reaction the aqueous alcohol was distilled off; the temperature was then raised sharply to 120° and the residual alcohol was distilled off under vacuum. Slow heating of the calcium ricinoleate mass leads to formation of a plastic modification of the soap [5].

The products were ground, sifted through a sieve of 0.1 mm^2 mesh, and packed into ampoules.

The temperature of the vacuum drying in ampoules depended on the melting points of the fatty acid salts. Fusion of calcium oleate and ricinoleate began at 69.2 and 64.6° respectively. The drying temperature used was therefore 55°. The calcium stearate powder was heated under vacuum at 110° under a residual pressure of 10^{-2} mm.

The heats of wetting of the calcium soaps by water were determined in an adiabatic calorimeter, which is more correctly described as a calorimeter with equivalent heat transfer, as in this case heat transfer between the calorimetric beaker and the water is not zero. This heat transfer must be taken into account, as the calorimeter contains constant heat transferrers: the stirrer and the basket (if the temperature of the surrounding medium is higher than the temperature of the experiment). Therefore the water jacket of the calorimeter is maintained at a higher temperature when the temperature of the surrounding air is below the temperature of the experiment, and at a lower temperature when the air temperature is higher than the experimental temperature. If the water jacket and beaker temperatures are equal, the initial period may take a positive or a negative course, depending on the temperature of the surrounding medium, as the projecting portions – the stirrer, crusher, and thermometer – absorb or give up a definite quantity of heat. The main difficulty therefore lies in strict maintenance of constant heat transfer between the calorimetric beaker and the water jacket; this is controlled by means of the external Beckmann thermometer.

The average results of the determinations are given in the Table.

TABLE

Heats of Wetting of Soaps and Numbers of Coordinated Molecules of Water

Fatty acid salt	Method of preparation	q_c in cal./g	n			Hydrate forms
			Calorimetric	Solution of hydrate in oil	Saturation in aqueous xylene	
Calcium stearate	A. A. Trapeznikov's	—	—	—	1.81	$CaSt_2 \cdot 2H_2O$
Ditto	Ditto	8.4	3.6	3.84	—	$CaSt_2 \cdot 4H_2O$
Calcium oleate	Ditto	13.8	5.8	—	—	$CaOl_2 \cdot 6H_2O$
Ditto	Neutralization of fatty acid by CaO in ethyl alcohol	13.9	5.8	—	—	$CaOl_2 \cdot 6H_2O$
Calcium ricinoleate	Ditto	17.9	7.9	—	—	$CaRz_2 \cdot 8H_2O$
Calcium stearate	Neutralization of fatty acid by 50% aqueous solution of NaOH in alcohol	4.3	0.92	0.96	—	$NaSt \cdot H_2O$

The number of coordinated water molecules was calculated by means of the equation [1]

$$n = \frac{q_c M_s}{K_W M_W}, \tag{1}$$

where q_c is the heat of wetting in cal./g; n is the number of water molecules coordinated by one soap molecule; K_W is a quantity of the order of 80 cal / g; M_s and M_W are the molecular weights of the soap and water.

The data on calcium stearate were verified by other methods: by saturation of weighed samples with different amounts of water followed by wetting in the calorimeter. The heat effect in the wetting of calcium stearate containing water in 1:4 molar ratio is within the limits of experimental error. The saturation curve is given in Fig. 1. It must be noted that the measurements of the heats of wetting and the saturation of the calcium stearate samples were carried out immediately after drying. If the samples are kept in the anhydrous state the heat effects decrease, probably owing to intracrystalline transformations of the hydrophilic surface.

The amounts of water coordinated by the polar groups were also determined by solution of the soap hydrates in vaseline oil, as follows: a weighed sample of the dry soap, saturated with water vapor for 25-30 hours, was mixed with vaseline oil (10-12 times its own volume). The suspension of the hydrated calcium stearate in the oil was heated at 125-130° until the soap was completely dissolved and foaming ceased. In these experimental conditions water is removed, as the most rapid evaporation of vaseline oil (GOST 3164–46) commences at about 185° [6]. With the weights of the soap hydrate and vaseline oil known, the difference between the weights before and after heating is determined and the number of water molecules removed per one soap molecule is calculated from the equation

$$n = \frac{xM_S}{(g-x)\,M_W}, \tag{2}$$

where g is the weight of soap hydrate, in grams; x is the amount of water removed, in grams (the difference between the weights before and after heating).

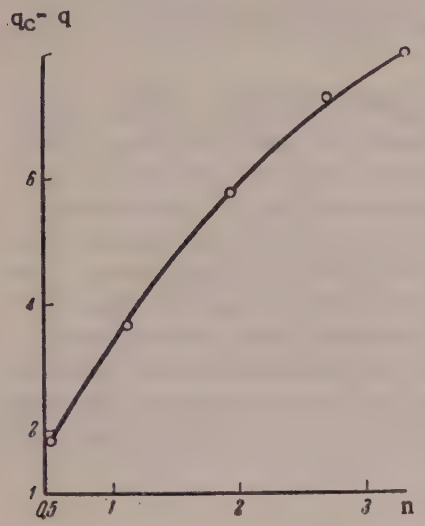

Fig. 1. Curve for saturation of calcium stearate with water (from heats of wetting).

This method was used to check the amount of water coordinated by the polar groups of sodium and calcium stearates. The amount of water coordinated by the polar groups of calcium stearate was also determined by saturation of a weighed sample in aqueous xylene [7]. The results are given in Table 1; the number n was calculated from the equation

$$n = \frac{x_1 M_S}{m M_W}, \tag{3}$$

where x_1 is the amount of water in cubic centimeters, distilled off in the Dean and Stark apparatus; m is the weight of dry soap in grams.

DISCUSSION OF RESULTS

The physicochemical concepts of the surface forces whereby water molecules are coordinated are based on the formation of two layers in dynamic equilibrium. A monomolecular water layer directly balances the greater part of these forces, being in a strictly oriented position. The diffuse layer balances the remainder and thus in the first case, when a free surface is present, water dipoles are adsorbed by two layers (Fig. 2, I).

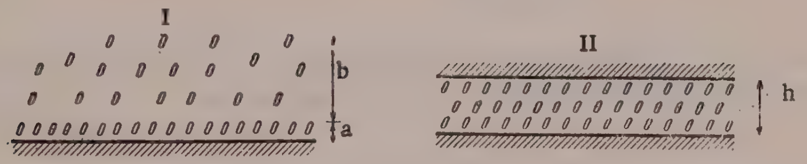

Fig. 2. Surface adsorption of water molecules (I); a) monomolecular layer; b) diffuse layer; formation of multimolecular layers (II).

The distribution of the forces is somewhat different from this if these surfaces approach each other to within a few angstroms. Then, on complete contact, a cleavage plane of a soap crystal is formed. However, mechanical, thermal, and chemical influences on the crystal split it along the planes and give rise to planar tunnels which adsorb polar substances. Planes in this position are shown in Fig. 2, II; different numbers of molecules of the polar substance will be adsorbed in the tunnel, according to the distance h.

An analogous situation is found when water is adsorbed by polar groups of soap molecules. The adsorbing planes are formed from rows of mutually oriented acid groups of the soap molecules [5].

It follows from the experimental data that the amounts of water adsorbed by the planar polar group tunnels vary. Calcium stearate forms the following hydrates [8]:

$CaSt_2 \cdot 4H_2O$, $CaSt_2 \cdot 2H_2O$ and $CaSt_2 \cdot H_2O$.

Sodium stearate forms the same number of hydrates:

$$8NaSt \cdot H_2O,\ 2NaSt \cdot H_2O,\ [9]$$

and also $NaSt \cdot H_2O$ [10].

Our own data and data from the literature suggest that for the formation of hydrated forms of soaps there are quite definite discrete values of $\underline{h}$ at which hydrate formation is possible; phase transitions in soaps depend on these as much as on the slope of the hydrocarbon chains relative to the basal planes. A similar conclusion follows from Hoppler's data [11]; he found that the hydrate form of calcium oleate is $CaOl_2 \cdot 2H_2O$; data on heats of wetting indicate that the hexahydrate, $CaOl_2 \cdot 6H_2O$ is formed.

The numbers of water molecules coordinated by calcium salts of stearic, oleic, and ricinoleic acids, in relation to the structure of the latter, confirm that the acid group coordinates four water molecules, and the double bond and the hydroxyl group, one each [2]. The formation of bimolecular layers in the planar tunnels formed by hydrophilic groups is most likely, but the possibility of coordination of water by calcium ions is not excluded. The removal of coordinated water from the planar tunnels involves a much greater expenditure of energy than removal of water from an open hydrophilic surface. Simple drying of the soap therefore does not give the desired result, and for this reason the method of dissolving the hydrates in vaseline oil was used. In such conditions the planar tunnels are destroyed, and the amount of coordinated water can therefore be determined much more completely. The conditions for preparation of the samples lead to another hypothesis which, in our opinion, characterizes the state of the hydrophilic surface. Preliminary treatment of the samples with alcohol not only clears the basal plane of the polar groups, but also increases the distance $\underline{h}$, while xylene treatment diminishes it.

SUMMARY

1. It is shown that the calcium salts of stearic, oleic, and ricinoleic acid may exist in the following hydrated forms after alcohol treatment followed by drying:

$$CaSt \cdot 4H_2O,\ CaOl_2 \cdot 6H_2O,\ CaRz_2 \cdot 8H_2O.$$

2. Saturation of dry calcium stearate in aqueous xylene resulted in formation of a soap dihydrate:

$$CaSt_2 \cdot 2H_2O.$$

3. The calcium salts of the series of saturated and unsaturated fatty acids with equal numbers of carbon atoms become increasingly hydrophilic with increasing number of polar groups:

$$CaSt_2 < CaOl_2 < CaRz_2.$$

An acid group can coordinate four molecules of water, and double bonds and hydroxyl groups one each.

4. It is suggested that the formation of several hydrate forms is possible owing to the existence of discrete distances between the basal planes of the acid groups in the soaps.

Institute of Mining, Academy of Sciences
USSR Moscow

Received October 5, 1956.

LITERATURE CITED

[1] V. I. Klassen and V. A. Mokrousov, Introduction to Flotation Theory (Metallurgy Press, 1953).*

[2] A. V. Dumansky, V. I. Solnyshkin and P. A. Demchenko, Ukrain. Chem. J. 20, 635 (1954).

[3] A. A. Trapeznikov and S. Kh. Zakieva, Colloid J. 8, 429 (1946).

[4] E. Lederer, Colloid Chemistry of Soaps (Moscow, 1934).*

---

* [In Russian].

[5] A. A. Trapeznikov and E. M. Shlosberg, Colloid J. 8, 421 (1946).

[6] R. G. Ivanov et al., Lubricating Oils and Greases (Standards State Press, Moscow, 1949).*

[7] R. V. Voitsekhovsky and P. A. Demchenko, Colloid J. 17, 261 (1955).**

[8] M. J. Vold, C. S. Hattiangdi and R. D. Vold, J. Colloid Sci. 4, 93 (1949).

[9] M. J. Buerger, Proc. Natl. Acad. Sci. 28, 526 (1942).

[10] P. A. Demchenko, Dissertation, Inst. General and Inorganic Chemistry Acad. Sci. Ukrainian SSR (Kiev, 1952).

[11] F. Hoppler, Fette und Seife 49, 700 (1942).

---

* [In Russian].

** Original Russian pagination. See C. B. translation.

THE SHRINKAGE OF COLLAGEN

N. N. Stefanovich and A. N. Mikhaĭlov

The alteration which collagen undergoes on heating, known as shrinkage, is usually compared with the fusion of crystalline substances [1-4], denaturation of proteins [5], or changes in the state of aggregation of high polymers under the influence of heat [6]. These three types of transitions have different mechanisms. Fusion is accompanied by considerable absorption of heat, whereas the two latter processes usually involve absorption of small amounts of heat.

Investigations of the heat of shrinkage of collagen have been carried out by Wöhlisch [2, 3] and by Küntzel [4]. However, there are objections to the methods used by them, as they are based on a wrong concept of the reversibility of the shrinkage process. Moreover, the results obtained by these two authors differ greatly. Determinations of the heat of shrinkage may assist in elucidation of the mechanism of the process, and we therefore determined the heats of shrinkage of collagen.

All the experiments were carried out with specimens from the same raw cowhide. The specimens were cut in the form of an asymmetric fringe from the middle layer (derma) of the saddle region of the hide. Specimens of the untreated raw material, limed material (after treatment with $Ca(OH)_2$), and leather tanned with quinone and phosphotungstic acid, were tested in the form of small pieces 2 x 2 mm in size. All the specimens were thoroughly washed after treatment, dialyzed against distilled water, and dehydrated with acetone. Half of the total number of each kind of specimens were treated in boiling water for 10 minutes.

The characteristics of the specimens are given in Table 1.

TABLE 1

Characteristics of the Specimens

Specimens	Moisture, %	Protein (derma substance) as % on absolutely dry weight	Shrinkage temperature, °C
Raw derma	15.1	98.6	66
Shrunken raw derma	12.8	97.9	–
Limed derma	18.5	98.9	66
Shrunken limed derma	14.3	97.2	–
Leather, phosphotungstate-tanned	12.4	70.2	63
Leather, quinone-tanned	–	–	90

The heat of shrinkage was determined by two methods — calorimetrically and thermographically. A variable-temperature calorimeter with an isometric jacket was used for the calorimetric analysis. The temperature in the calorimeter was kept constant with the aid of anultrathermostat, and was measured to an accurary of 0.003° with a Beckmann thermometer.

Prior to the determinations of the heats of shrinkage, the specific heats of the shrunken and raw derma were determined. For the specific heat determinations, previously soaked weighed samples of the derma were heated through 1.0-1.5°. The heating was carried out in water. To prevent strong evaporation, the water was covered with a layer of mineral oil. The usual heat balance equation was used for the calculations.

The results of the specific heat determinations are given in Table 2.

TABLE 2

Specific Heats of Shrunken and Raw Derma

Temperature, °C	Specific heat in cal / g. degree	
	Shrunken derma	Raw derma
20	0.33 ± 0.04	0.32 ± 0.04
30	0.38 ± 0.02	0.31 ± 0.02
40	0.42 ± 0.03	0.41 ± 0.04
50	0.42 ± 0.04	0.43 ± 0.02
60	0.44 ± 0.04	0.33 ± 0.02
70	0.48 ± 0.07	—

The specific heat – temperature relationship conforms to the equation $C_p = 2.2 \cdot 10^{-7} T^{2.5}$.

For determination of the heats of shrinkage, specimens of the shrunken and unshrunken material were introduced into the calorimeter at 74°. To eliminate the effect of wetting, the specimens were first moistened. Excess water was removed by means of filter paper before the experiments. The heat of shrinkage is the difference between the heat effects produced when unshrunken and shrunken material is introduced into the calorimeter; these heat effects were calculated by the heat balance equation. The calculated values for the heats of shrinkage are given in Table 3.

TABLE 3

Heats of Shrinkage of Various Collagen Specimens

Specimen	Heat effect in cal / g on introduction of		Heat of shrinkage in cal / g	
	Unshrunken material	Shrunken material	Absolutely dry material	Protein
Derma	10.3 ± 0.1	8.4 ± 0.2	1.9 ± 0.3	1.9 ± 0.3
Limed derma	12.8 ± 0.2	9.2 ± 0.2	3.6 ± 0.4	3.6 ± 0.4
Phosphotunstate-tanned leather	3.8 ± 0.3	0	3.8 ± 0.3	5.4 ± 0.3

According to the calorimetric data, the heat of shrinkage of collagen is small, of the order of 2.0-5.4 cal / g.

Specimens of unlimed derma were used for the thermographic investigations. The comparison standard was shrunken derma. Specimens of the unlimed and shrunken dermas were shredded and kept in water for 12-16 hours. Equal amounts of the unlimed and shrunken materials were then placed in crucibles. The specimens were heated in water. To prevent evaporation, the contents of the crucibles were covered with a few drops of mineral oil. The thermograms in Fig. 1 show an endothermic heat effect at 65-70°. Moreover, this effect is small, as the ordinary trace does not show a halt in the temperature rise, and the jump in the differential curve is small.

Cooling and repeated heating curves (Fig. 2) show that the shrinkage is irreversible, as these curves do not show the corresponding jumps.

These thermograms show that shrinkage is an endothermic irreversible process which takes place at a definite temperature with absorption of a small quantity of heat. An approximate quantitative estimate of the shrinkage heat effect was obtained by simultaneous heating of derma with substances of known heats of transition. The standard, as in the previous experiments, was shrunken derma.

The substances used for comparison were sodium sulfate decahydrate (mirabilite), $Na_2SO_4 \cdot 10H_2O$, which has

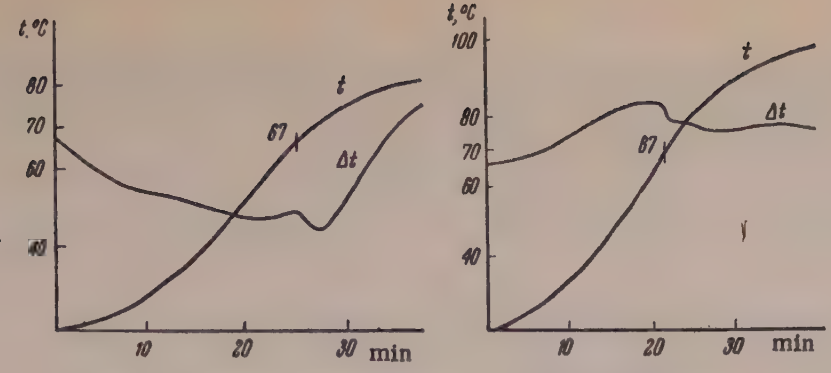

Fig. 1. Heating thermograms for two specimens of derma.

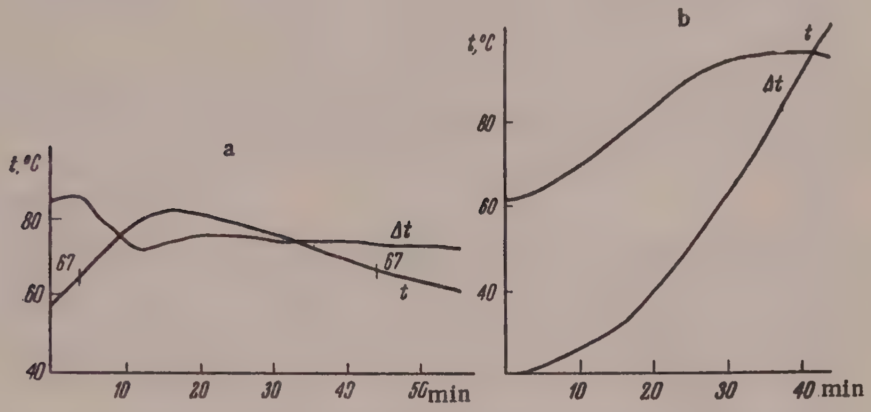

Fig. 2. Cooling (a) and repeated heating (b) thermograms for derma.

a transition at 32°, and potassium palmitate $C_{15}H_3CO_2K$, with a transition at 63°. The heat of transition of mirabilite is 57.36 cal / g, and of potassium palmitate, 5.46 cal / g.

TABLE 4

Thermographic Calculations

Specimens	Standard	m_2 in g	m_1 in g	l_1 in cal./g	S_1	S_2	$l_2 = \frac{S_2 m_1}{S_1 m_2} l_1$ in $\frac{\text{cal}}{\text{g}}$
Unshrunken derma in water	Potassium palmitate	0.14	0.69	5.46	15	3	5.4
Unshrunken derma and mirabilite	Shrunken derma	0.20	0.46	57.36	258	10.4	5.3
Unshrunken derma and mirabilite	Al_2O_3	0.26	0.22	57.36	254	3	0.5
Unshrunken derma in water	Shrunken derma and mirabilite	0.46	0.14	57.36	81.2	2.86	0.6

Note. m_1, l_1, and S_1 are the weight in g, the heat of transition in cal./g, and the area of the loop on the differential curve in arbitrary units due to the heat of transition of mirabilite or potassium palmitate. m_2, l_2, and S_2 are the weight in g (on the absolutely dry substance), the heat of shrinkage, and the area of the loop due to the heat of shrinkage.

The thermograms recorded for quantitative evaluation of the heat of shrinkage are given in Fig. 3. The loops formed by the differential curves are closed along the zero line. The required heat of shrinkage is calculated from the ratio of the areas of the loops and the known heat effects.

The results of the thermographic calculations are given in Table 4.

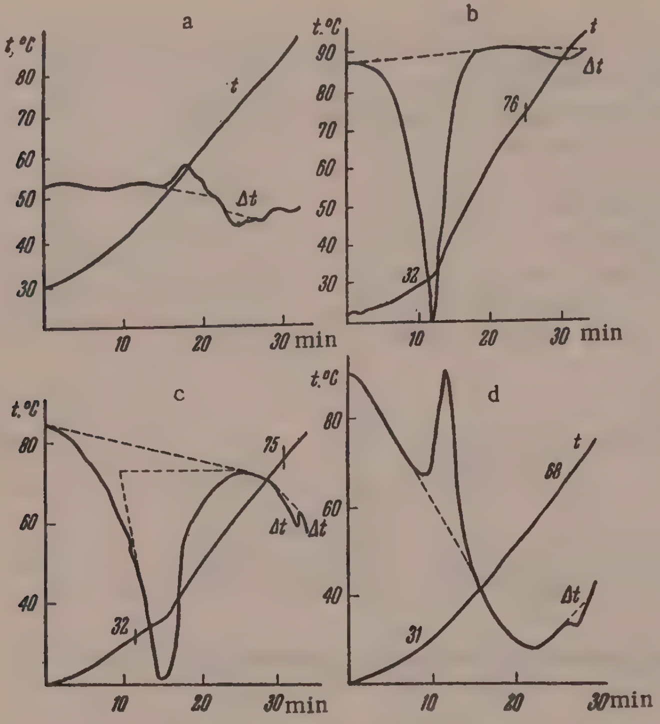

Fig. 3. Heating thermograms for derma; standards: K palmitate (a), shrunken derma (b), Al_2O_3 (c), shrunken derma and mirabilite (d).

In view of the fact that the heating was performed in water, the accuracy of the determinations was very low. However, the results of thermographic analysis do not contradict the calorimeteric data, and confirm that the heat of shrinkage is very small, between 0.5 and 5.4 cal. per g of derma.

DISCUSSION OF RESULTS

The absence of a difference between the specific heats of the shrunken and unshrunken material, the low value of the heat of shrinkage, and the irreversibility of the process suggest that it is necessary to revise the existing views of the shrinkage process. In our opinion, the interpretation of shrinkage as a phase transition of the fusion type must be abandoned. The analogy between shrinkage and the melting of crystals is largely based on the fact that Wöhlisch [2, 3] found a large heat effect on shrinkage, comparable with the heats of fusion of other organic compounds (16.8 cal per g of collagen). However, Wöhlisch wrongly assumed that the shrinkage is reversible, and took the sum of the heat of shrinkage and the heat of isothermal contraction to be the heat of shrinkage. Recalculation of Wöhlisch's data with the heat of isothermal contraction taken into account leads to a different result. This recalculation is given below. Wöhlisch found the following temperature changes during isothermal contraction and extension at 76° for three specimens of previously stretched tendons:

	t°C		
Isothermal contraction and heat shrinkage . . .	— 3.48	— 3.36	— 3.12
Isothermal extension.	+ 2.16	+ 1.75	+ 1.15
Temperature change due to absorption of heat during heat shrinkage (Δ T)*	— 1.32	— 1.61	— 1.97

---

* Calculated by us.

When the load is removed from stretched specimens, isothermal contraction and heat shrinkage occur: the temperature of the specimens falls as the result of these processes. On subsequent extension the temperature rises again, but does not reach the intial value. In our opinion, only this irreversible change must be taken into account in calculations of the heat of shrinkage.

As the specific heat of collagen is 0.4 cal / g· degree, and only one third of the weight of wet tendon is organic substance, the heat of shrinkage is:

$$1.32 \cdot 0.4 \cdot 3 = +1.58 \text{ cal / g}; \quad 1.6 \cdot 0.4 \cdot 3 = 1.93 \text{ cal / g}; \quad 1.97 \cdot 0.4 \cdot 3 = 2.36 \text{ cal / g}.$$

The values so obtained are of the same order as found in our experiments.

The criteria of fusion regarded as a phase transition are: 1) a difference between the specific heats of the substance before and after the transition; 2) a heat effect comparable in magnitude to heats of fusion of crystals; 3) change of specific volume during the transition.

It follows from the experimental data that the specific heats of shrunken and unshrunken derma differ very little. The difference lies within the limits of experimental error. The heat of shrinkage, determined by two methods, was found to be small, not comparable with the heats of fusion of crystalline substances. The volume change, according to literature data [2, 7, 8] is very small, not over 1%. Thus the above criteria of a phase transition are absent.

The analogy between heat shrinkage and fusion is confined to the factthat shrinkage and fusion both take place at definite temperatures. All this suggests that the nature of heat shrinkage differs from that of phase transition processes. There are also objections to an analogy between shrinkage of collagen and aggregative transitions of high polymers. The transitions of high polymers are reversible, and are accompanied by changes of specific volume, whereas the heat shrinkage of collagen is an irreversible process.

In our view there is a sounder basis for an analogy between heat shrinkage and denaturation of proteins. Most of the changes in proteins during heat shrinkage of collagen and in the heat denaturation of proteins occur in one direction. In both cases the water absorption of the protein decreases after heat treatment. The isoelectric point is shifted in the direction of higher pH values, the stability to enzymes decreases, and the reactivity increases [1]. The heat of shrinkage determined in the present investigation is close in value to the heats of denaturation of globular proteins.

The heat of shrinkage is 1-3 cal / g of protein; the heat of denaturation is ~ 1 cal / g of protein [9]. Protein denaturation and shrinkage of collagen both occur abruptly. However, in denaturation of globular proteins the asymmetry of the particles increases. The reverse is found in the heat shrinkage of collagen – the molecular chains become coiled. This difference in behavior can be ascribed to differences in the native structure of collagen and globular proteins. Both types of proteins approach the same equilibrium state on denaturation.

Moreover, the denaturation of globular proteins is in principle regarded as a reversible process. However, research on the regeneration of denatured proteins has shown that the native properties are not fully restored [10].

SUMMARY

1. The specific heat of shrunken and unshrunken collagen is ~ 0.4 cal / g in the 20-70° range. The heat of shrinkage has an average value of 2-5 cal / g of collagen.

2. Heat shrinkage differs substantially from phase transition of the fusion type and from aggregative transitions of high polymers. The heat shrinkage process must be regarded as denaturation of the fibrous protein.

The authors are deeply grateful to Professor A. V. Nikolaev and to Cand. Chem. Sci. I. S. Rassonskaya for interest in the work and for assistance in the thermographic analysis.

Central Scientific Research Institute for the
Leather and Footwear Industry, Moscow

Received October 7, 1956.

LITERATURE CITED

[1] A. N. Mikhailov, Physicochemical Principles of Leather Technology (State Light Industry Press, 1949).*

[2] E. Wöhlisch, René du Mesnil de Rochemont Z. für Biologie, 85, 406 (1927).

[3] E. Wöhlisch, Biochem. Z. 247, 329 (1932).

[4] A. Küntzel, Angew. Chem. 52, 175 (1939).

[5] A. G. Pasynsky, Proteins in Industry and Agriculture (Izd. AN SSSR, 1952)* p. 85.

[6] G. I. Kutyanin, Proc. Acad. Sci. USSR 82, 405 (1952),

[7] V. D. Chater, Heat Shrinkage of Tanned Leather (State Light Industry Press, 1932).*

[8] C. Weir, J. Soc. Leather Trades Chem. 36, 155 (1952).

[9] F. Haurowitz, Chemistry and Biology of Proteins (IL, 1953). [Russian translation].

[10] V. S. Tongur, Colloid J. 11, 274 (1949); Doctorate Dissertation, Institute of Nutrition (Moscow, 1951).

---

* [In Russian].

THE HYDROPHILIC PROPERTIES OF CLAYS OF THE KAOLINITE GROUP

E. T. Uskova

It is known that the hydrophilic nature of clays depends on their mineralogical composition, the degree of dispersion, and the composition of adsorbed cations [1]. The electrokinetic potentials of clays should also have a considerable influence on their hydrophilic properties [2]. However, very few experimental data are available on the relationship between the zeta potential and the hydrophilic character of clays [3].

In the present work the variations of the hydrophilic nature of a kaolinite clay with different proportions of bivalent and univalent ions, and with the zeta potential, were studied.

The material used for the study was Chasov Yar clay No. 5. The test samples were prepared as follows. The clay was covered with five times its own bulk of distilled water for 24 hours. The resultant suspension was rubbed through a sieve of 4900 mesh per cm^2. It was then allowed to settle for 24 hours, the water over the sediment was decanted off, and the sediment was treated with 1 N sodium chloride solution to a negative reaction for Ca^{2+}. Excess electrolyte was removed by washing with decantation. During washing of the sodium clay two clearly distinct layers were formed in the deposit: a lower pale, almost white layer of a coarse fraction, and an upper gray-pink layer of a fine fraction. These fractions were separated, and treated and studied separately. The washed sodium clay was dried at 105°, ground, and sifted without residue. Weighed samples of the Na clay were covered with solutions of calcium or magnesium chloride of various concentrations in 1:5 ratio, stirred, and left to stand for 24 hours. Complete saturation with Ca and Mg was effected by threefold treatment with 1 N solutions of the corresponding chlorides. The samples were washed free of electrolyte, until the suspensions had a conductivity of 10^{-4} ohm^{-1} cm^{-1}. After settling, the sediments in the suspensions were reduced to equal volumes by decantation of the liquid, and dried at 105°.

The amounts of adsorbed calcium and magnesium in the samples were determined by K. K. Gedroits' ammonium chloride method. The analytical results are given in the Table.

It follows from the tabulated data that the exchange capacity depends on the degree of dispersion of the clay particles and on the nature of the sorbed cation; it is almost twice as high for the fine as for the coarse fraction; magnesium is adsorbed more actively than calcium.

The hydrophily was characterized by the amount of water bound by the surface of 1 g of the clay sample [4]. The amount of bound water was determined by Dumansky's indicator method [5]. The calculations were based on the Dumansky– Voitsekhovsky equation with soluble substances taken into account [5]. The indicator used was sucrose of analytical purity grade. The solution concentration was of the order of 13-15%, at which the amount of bound water determined by the indicator method is approximately equal to the amount found by the heat of wetting method [6]. Changes of sucrose concentration were determined by means of a Zeiss interferometer for liquids, with a cell 20 mm long, calibrated against sucrose. For determination of the bound water, two weighed samples of the material, previously dried for 12 hours at 110°, were put into weighing bottles; one sample was covered with sucrose solution, and the other with distilled water. After thorough stirring with a rod, the suspensions were left in the stoppered bottles for 15 minutes to reach equilibrium. The samples were then centrifuged for 15 minutes in closed centrifuge tubes.

It was assumed in the investigations that the degree of dispersion of the clay samples within the experimental series remains unchanged (this applies to primary particles; the size of secondary formations should not have any significant effect on the amount of bound water). Formation of microaggregates occurs by contact

Adsorption of Ca^{2+} and Mg^{2+} by Chasov Yar Coarsely and Finely Disperse Clay in the Sodium Form as a Function of Electrolyte Concentration

Calcium chloride			Magnesium chloride		
Concentration in g-equiv./liter	Adsorption in micro-equiv./g	Substitution, %	Concentration in g-equiv./liter	Adsorption in micro-equiv./g	Substitution, %
Coarsely disperse clay					
0.005	20	19	0.002	19	16
0.01	33	31	0.005	36	31
0.02	50	47	0.01	60	52
0.05	75	71	0.02	84	75
0.1	84	80	0.1	95	83
0.5	95	90	0.5	105	92
1.0	105	100	1.0	111	100
Finely disperse clay					
0.005	48	25	0.002	23	11
0.01	62	32	0.005	65	32
0.02	126	65	0.01	103	51
0.1	158	82	0.02	139	69
0.5	170	88	0.1	168	83
1.0	193	100	0.5	181	89
			1.0	202	100

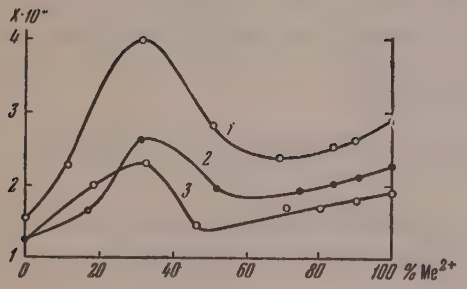

Fig. 1. Variation of the amount of bound water with the degree of substitution of sodium in a sample of Chasov Yar clay in sodium form; 1) fine fraction, substitution by magnesium; 2) coarse fraction, by magnesium; 3) coarse fraction, by calcium.

between the primary particles over small regions of their surface. Water molecules can easily penetrate into the micropores, and therefore the surface of the sample accessible to water does not change appreciably in the presence of aggregates.

The results of the determinations are given in Fig. 1; it is seen that introduction of bivalent ions into the exchange complex makes the clay more hydrophilic. However, this increase is not linear, or even continuous. With gradual increase of the content of bivalent ions in the exchange complex, the clays at first rapidly become more hydrophilic; a maximum is reached when the contents of adsorbed calcium or magnesium ions reach 30-35% of the capacity, and there is then a rapid decrease in the hydrophily. Despite this, samples containing between 50 and 80% of the maximum capacity values of adsorbed bivalent ions (the region in which they are least hydrophilic) are still more hydrophilic than the pure sodium clay. The minimum is followed by a new rise, smaller than that found on addition of small amounts of bivalent cations, in the hydrophilic properties.

The appearance of the hydrophily maximum cannot be attributed to a higher degree of hydration of the introduced bivalent ion than that of the sodium ion. The mineralogical composition and active surface of the particles remain unchanged. It is evident that some other factors influence the hydrophilic properties of the clays. Changes of the zeta potential may have an effect. To test this supposition, the zeta potentials of the clays were determined.

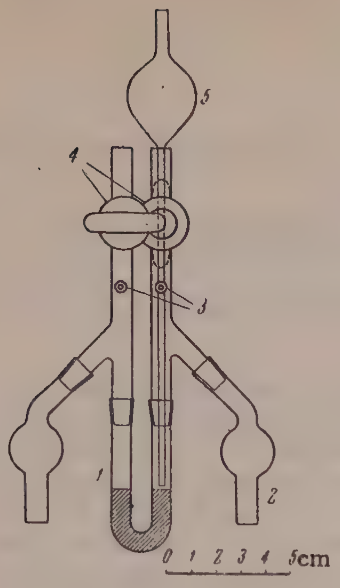

Fig. 2. Apparatus for determination of zeta potential by the electroosmotic method: 1) U-tube; 2) siphon filled with agar; 3) measuring capillaries; 4) stopcocks for meniscus regulation in the measuring capillaries; the right stopcock is open; 5) pipet.

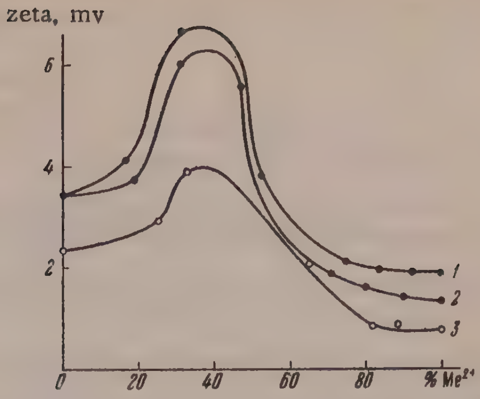

Fig. 3. Variations of zeta potential of Chasov Yar clay samples with different degrees of substitution of sodium in sodium clays: 1) coarse fraction, substitution by magnesium; 2) coarse fraction, by calcium; 3) fine fraction, by magnesium.

The zeta potential determinations were carried out by the electroosmotic method with the aid of apparatus based on Gortikov's design [7]. We met a number of inconveniences in work with Gortikov's apparatus, and therefore the latter was modified in some respects. The siphon tubes were placed at an acute angle, to prevent formation of air bubbles in them. Meniscus regulation in the measuring capillaries can be conveniently carried out with the aid of stopcocks with 1.5-2 mm openings, through which the apparatus is filled with the intermicellar liquid by means of a pipet with a drawn-out tip (Fig. 2). The U-tube of the instrument was kept at constant temperature by means of a circulating termostat. The thermostatic vessel with the U-tube was fixed in a special clamp with a device for tilting in two mutually perpendicular directions. The diaphragm was made by centrifugation of the suspension in the U-tube; the centrifugate served as the intermicellar liquid.

The electrokinetic potential was calculated by the Helmholtz-Smoluchowski equation.

Figure 3 gives the variations of zeta potential of sodium Chasov Yar clay samples with the degree of substitution of sodium by calcium or magnesium.

Introduction of calcium or magnesium ions into the exchange complex of Chasov Yar sodium clay does not produce a steady decrease of zeta potential. There is a considerable increase of zeta potential in samples with low contents (up to 30%) of Ca^{2+} or Mg^{2+}. The maximum is followed by a decrease of zeta potential, but the value of the latter when the content of adsorbed bivalent cations is in the region of 30-50% remains higher than for the sodium clay. At higher contents (70%) of Ca^{2+} or Mg^{2+} the zeta potential becomes less than for the sodium clay.

A comparison of the curves for variations of the hydrophily and zeta potential with the composition of the exchange cations shows that maxima in the region of 30-35% substitution by bivalent cations coincide in the two types of curves. This confirms our supposition that the hydrophily maximum has its origin in the value of the zeta potential. The sharp increase of zeta potential produced by the introduction of the first portions of bivalent ions increases the hydrophily. It is evident that increased diffuseness of the electric double layer leads to thickening of the hydrate shells of the particles.

The zeta potential of samples with high contents of bivalent ions is low, and therefore its relative influence on the binding of water is less. The influence of the higher hydration of the bivalent ions becomes predominant in this case. However, the absolute value of the increase of hydrophily caused by the adsorbed cations is less than in samples with the maximum value of the zeta potential. Thus, the zeta potential is a powerful factor in the binding of water by clay particles.

SUMMARY

1. The effect of the ratio between ions of different valencies in the exchange complex on the hydrophilic properties of kaolinite clay has been studied.

2. The amount of bound water increases to a maximum from sodium clays to clays containing increasing amounts of adsorbed bivalent ions; this is followed by a minimum and then again by a rise.

3. The effect of the ratio between ions of different valencies in the exchange complex on the zeta potential of kaolinite clay has been studied.

4. The maxima on the hydrophily curves coincide with the maxima on the zeta potential curves.

5. The value of the zeta potential is an important factor in the binding of water by clay particles.

In conclusion, the author expresses her deep gratitude to A. V. Dumansky for valuable advice and guidance.

The Ukrainian Academy of Agricultural
Sciences Kiev

Received September 2, 1956.

LITERATURE CITED

[1] L. G. Kapp, Soil Sci. 29 (1930); A. A. Rode, Soil Moisture (Izd. AN SSSR, 1952); E. M. Sergeev, General Soil Sciences (Izd. MGU, 1952); P. F. Melnikov, Sci. Mem. MGU 133, 1, 39 (1949); V. S. Sharov, Colloid J. 5, 521 (1939); K. K. Gedroits, Communications of the Bureau of Agriculture and Soil Science 15, 36 (1914).

[2] E. M. Sergeev, General Soil Science (1952); V. A. Priklonsky, Soil Science, pt. 1 (State Geol.-Tech. Press, 1955); I. V. Popov, Principles of Engineering and Geological Soil Science (Moscow–Leningrad, 1941); L. G. Melnichenko, Refractories 2, 81 (1951); N. Ya. Denisov, Colloid J. 6, 835 (1940); S. S. Filatov, Bentonites of the Georgian SSR (Izd. AN SSSR, 1943).

[3] F. I. Arkhipov, Colloid J. 6, 241 (1940).

[4] A. V. Dumansky, Lyophily of Disperse Systems (Voronezh University Press, 1940).

[5] A. V. Dumansky, Koll.-Z. 65, 178 (1933); A. V. Dumansky and O. V. Neiman, Colloid J. 2, 625 (1936); A. V. Dumansky and R. V. Voitsekhovsky, Colloid J. 10, 413 (1948).

[6] A. V. Dumansky and M. V. Chapek, Colloid J. 2, 95 (1936); F. D. Ovcharenko, Ukrain. Chem. J. 19, 139 (1953).

[7] V. N. Gortikov, Colloid J. 1, 233 (1935).

DISCUSSION

MORE ON THE SUBJECT OF THERMOMECHANICAL CURVES

E. I. Regirer and M. S. Kalantarova

Kargin and Malinsky [1], in their discussion of our paper [2], consider that this paper "in addition to views and generalizations which are worthy of attention, contains certain incorrect deductions based on an erroneous concept of the nature of the measurements made for the plotting of thermomechanical curves". Unfortunately, in challenging us to a discussion, the authors did not state with which views and generalizations they agree; this makes the formulation of our reply difficult.

We shall confine ourselves to the three aspects of thermomechanical curves (TM curves) touched upon by our critics.

The nature of the measurements carried out for the plotting of thermomechanical curves. It is clear from our paper that in our view the plotting of TM curves is not an isolated technique, but is one of the methods of physicochemical analysis. Since it is not clear whether our critics accept this, we shall attempt to answer possible objections.

It might be objected that Kurnakov [3] regarded physicochemical analysis as a science of phases, not applicable to amorphous polymers.

However, modern views on different states of aggregation do not discard the concept of phases, but extend it, as within the limits of the same (liquid) phase three states of aggregation are postulated – glassy, high-elastic, and viscofluid.

A further possible objection is that the fundamental method of physicochemical analysis is the measurement (over a wide temperature range) of heat effects; this is not applicable to studies of transitions from one state of aggregation into another. However, in addition to heat effects, physicochemical analysis involves the study of such properties as fusibility, relaxation time, the coefficient of thermal expansion, and also properties characterized by susceptibility to external forces – hardness, efflux pressure, viscosity, elasticity moduli, etc. [4]. It is therefore quite reasonable to include the curves plotted for vitrified rosin by Tamman, a disciple of physicochemical analysis, in the category of TM curves.

Finally, another possible objection is that, in contrast to TM curves, the diagrams obtained as the result of physicochemical analysis are usually plotted in "composition–property" coordinates. However, are the final diagrams obtained as the result of TM measurements not plotted in these usual physicochemical coordinates? As an example, we may cite Fig. 2 in the article [5], obtained by TM measurements, which is a typical physicochemical analysis diagram.

On the above considerations we believe that it would be correct to define TM curves as those special cases of primary physicochemical analysis curves (of the property–temperature type) in which the given substances in different states of aggregation are characterized by the influence of temperature on susceptibility to changes of form (in other words, on mechanical properties).

The definition given by our critics: "A thermomechanical curve should be understood to mean a curve which expresses the variation of deformation with temperature over a fairly wide temperature range, when the deformation is produced by an external force" appears to us inappropriate in the following respects:

1. There are no grounds for restricting the evaluation of the effects of temperature on mechanical

properties to deformation only (several physicochemical characteristics of susceptibility are given above). To emphasize more clearly that this restriction is not essential, we may note that, with some modification of the method, a TM curve may be plotted as a curve for the varying force required to produce a constant deformation over a wide temperature range – the experimental technique would be different, but essentially the method would be the same.

2. Under practical conditions it is difficult to eliminate completely the influence of internal factors on deformation, and therefore in practice a pure picture of the action of external forces only is not usually obtained. Apart from the external forces, the deformation of a specimen is also determined by "internal factors", such as chemical processes within it. Our critics state that dimensional changes of the specimen caused by internal factors "must not be regarded in this case as deformation"; nevertheless, it is difficult in practice to separate the two kinds of deformation, since internal changes may take place even during the relatively short time (of the order of two hours) required for plotting a TM curve (this is sometimes seen in differences between TM curves plotted for the same specimen). The desire to distinguish between these two forms of deformation is understandable, but it is necessary to make the definition more precise so that it cannot be taken as meaning that the field of application of TM curves excludes the investigation of internal factors, as this exclusion would impoverish the TM method of investigation. We therefore drew attention in our paper to the possibility of using TM curves for studying "thermoreactive" changes in polymers, i.e., chemical processes of oxidation, condensation, and so forth, in them which are not induced by external mechanical forces. As was made known later, Kargin and Shteding [6] made effective use of TM curves for the same purpose. It would therefore be erroneous to suppose that TM investigations should be restricted to studies of the action of external forces only. On the contrary, it must be emphasized that the action of an external force is merely a method of detecting internal changes.

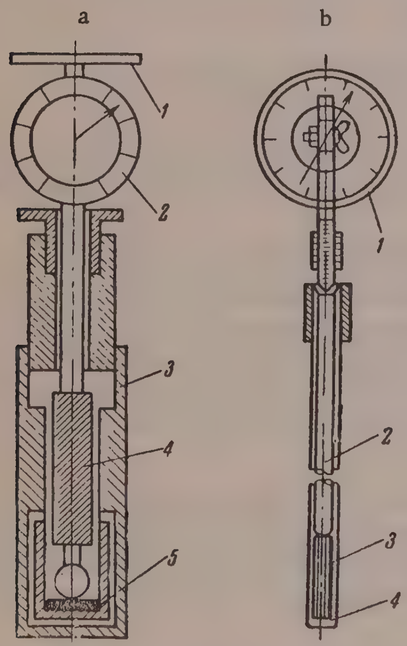

a) Zhurkov's apparatus: 1) platform for a constant load; 2) scale for measurement of deformation; 3) outer case; 4) insulating ebonite cylinder; 5) specimen. b) Quartz dilatometer; 1) graduated dial; 2) insulating quartz tube; 3) specimen; 4) outer case.

Our critics saw fit to put forward yet another consideration, also in the form of a definition of TM curves: "the term 'thermomechanical curves' should be applied only to curves for the dependence of the difference between the deformations of the specimen under two loads on the temperature, with the smaller load so chosen that the specimen undergoes practically no deformation". This, an even narrower definition, is also difficult to accept:

1. It is possible to use only one (working) load, if: 1) this load is not too large, so that the specimen should retain a reserve amount of height over which its deformability could be manifested further, in measurements over the entire temperature range; 2) the temperature is raised rapidly provided that a homogeneous temperature field is maintained through the whole volume of the specimen. If one of these conditions is satisfied, it is possible to eliminate entirely the use of small (preliminary) loads, which serve as "pauses" to protect the specimen from the action of large loads between readings. Although there are practical difficulties in satisfying these requirements, that is not a reason for considering the use of two loads necessary in principle and for raising this requirement to the rank of a definition by which curves plotted without the use of small loads are not to be termed TM curves, but are to be given some other name, although they are similar in appearance and reveal the same characteristics, corresponding to transitions from one state of aggregation into another.

2. The selection of the smaller (preliminary) load which produces practically no deformation in the specimen is difficult to achieve if it is considered that the determinations are carried out over a wide temperature range and that a small load, which does not deform the specimen at low temperatures, may produce appreciable deformations at high temperatures. However, the deformation of the specimen under the small load, although it is technically inconvenient, is not decisive, since differences of deformation are measured.

Explanation for the S-shaped course of certain curves. As has already been stated, internal factors the influence of which increases with the temperature are added to various extents to the external forces. Therefore the resultant curve may represent the aggregate course of these superposed effects. We observed one instance in which such superposition caused the curve to be S-shaped (this was because the specimens were molded at an insufficiently high temperature). As such an instance is possible, if an S-shaped curve is obtained it is necessary to prove that it is not the consequence of such an extraneous factor. Otherwise, the S-shape may be attributed to the presence of a plasticizer; this is evidently not applicable for interpretation of results obtained with unplasticized polymers. The curves taken from the paper [5]* include an example of an S-shaped curve, which the authors attribute to separation of the polymer molecules at high plasticizer contents. As our observations showed that S-shaped curves may also be the consequence of test conditions which do not exclude undesirable "extraneous" deformations, we put forward views which explained why this effect may be particularly prominent in highly plasticized specimens. We are not able to verify the effect of molding conditions in the case of tributyrin, but we do not believe that the cause of the S-shape observed for polyvinyl chloride and Vinylite cannot be impossible in principle for tributyrin. We did not assert, of course, that the cause of the S-shape found by us is the only one possible, and we think that such assertions should not be made with regard to any other cause of the S-shape.

Relationship between methods for plotting TM curves and methods for the contact measurement of linear thermal expansion. As our critics did not agree with our view that these methods are identical, but did not put forward any special considerations on the subject, we wish to explain our assertions by comparing concrete examples of both methods.

The Fig. (1,a) shows Zhurkov's apparatus [7], which has proved fully suitable for the plotting of TM curves, while Fig. (1,b) shows the "quartz dilatometer" [8], used in the United States as a standard instrument for determination of the coefficients of linear expansion of plastics. These two instruments are quite different in name and purpose. Nevertheless, the acting factor in both instruments is temperature, measured by its function, dimensional change. It is readily seen that even the design details of the two instruments are similar (in both instruments a cylindrical specimen is gradually heated and changes in its height are measured). Therefore the assumption that we are dealing here not with one but two characteristics of the material would imply that a specimen, placed under similar conditions and unaware of the operator's intentions is able to exhibit different properties in the two cases. It is surely more correct to say that the same is done in both cases, namely, a TM curve is plotted, showing variations of the linear dimensions of the specimen, found by contact measurement (i.e. with application of an external load), in the direction of the applied mechanical force. We therefore consider that the contact method for measurement of coefficients of linear thermal expansion is, in implicit form, a method for the plotting of TM curves; for example, there is nothing to prevent us "switching these instruments over" – by using Zhurkov's apparatus for carrying out tests by the American standard method for determination of the "coefficient of thermal expansion of plastics", and using the quartz dilatometer for the plotting of TM curves; if the tests are carried out in the same temperature region on the same specimens, similar TM curves will be obtained in both cases. This surely shows that the two are identical. Therefore there is nothing strange in the fact that determinations of uniaxial deformation (in the direction of the load) by means of the contact dilatometer can yield typical TM curves, as the measuring pressure can serve as the load. Hence follows our suggestion that the coefficients of linear thermal expansion of polymers should not be determined by contact methods.

We offered our paper on the methods of plotting and interpreting TM curves in the belief that discussion of a number of methodological questions would assist the wide adoption of the method. We became convinced that a paper on this subject is of topical interest when, after our paper had already been accepted by "Colloid

---

* By an error, the number of the next literature citation was given in the caption to Fig. 4 in the paper [2], which gave the critics cause to state that we attribute this figure to Kobeko, although in the text (p. 442) the number of the citation is given correctly.

Journal", an interesting article [9] of similar nature was published; unfortunately, the question of instruments used for TM determinations was not discussed in this paper. Yet there are still instances of not fully realized use of different instruments for the plotting of TM curves (for example, TM curves can be plotted with the aid of the Höppler consistometer [10] with a flat tip, this version being very similar to Zhurkov's apparatus).

If too narrow a definition of TM curves is adopted, there would be a tendency to regard any such instrumental modification as a new method, and not as a special case of the general TM method. This may even lead to TM curves being "discovered" again, and studied independently of V. A. Kargin's fundamental investigations. An example is provided by a paper [11] (based on differences of apparatus and method), which gives TM curves, not only not described as such, but not subjected to any deep analysis of their nature.

We therefore felt obliged to enter into the proposed discussion and to defend the wider definition of TM curves.

Received March 27, 1957.

LITERATURE CITED

[1] V. A. Kargin and Yu. M. Malinsky, Colloid J. 18, 372 (1956).*

[2] E. I. Regirer and M. S. Kalantarova, Colloid J. 17, 439 (1955).*

[3] N. S. Kurnakov, Introduction to Physicochemical Analysis, 3rd Ed. (ONTI, Leningrad, 1935) p. 91.

[4] Ibid, p. 92.

[5] V. A. Kargin and Yu. M. Malinsky, Collected Papers "Chemistry and Physical Chemistry of High Polymers" (Izd. AN SSSR, Moscow, 1952) p. 256.

[6] V. A. Kargin and M. N. Shteding, Chemical Industry 3, 137 (1955).

[7] S. N. Zhurkov, Trans. 1st and 2nd Conf. on High. Mol. Compds. (Izd. AN SSSR, 1945) p. 68.

[8] "Coefficient of Linear Thermal Expansion of Plastics", Appendix to ASTM D 696-44.

[9] V. A. Kargin and M. N. Shteding, Chemical Industry 2, 74 (1955).

[10] F. Höppler, Forschungsberichte des Prüfgerätewerkes Madingen (1940) N. 5.

[11] W. H. Willert, Ind. Rubber World 124, 324 (1951).

---

* [Original Russian pagination. See C. B. translation].

LETTERS TO THE EDITOR

KINETICS OF THE SPRAYING OF WATER DROPS IN AN ELECTRIC FIELD

V. I. Arabadzhi

The question of the spraying of water drops in an electric field is of considerable importance for understanding processes occurring in thunderstorms. Some authors even consider that the spraying of drops in an electric field is a necessary condition for further intensification of the field and development of electric discharge. To investigate the influence of a vertical electric field on water drops, we took motion pictures of the emergence of water drops from a capillary of 1 mm internal diameter. Photograph 1,a shows the emergence of drops 2.7-3 mm in radius without the influence of an electric field, and Photograph 1,b shows the influence of a vertical electric field of 2.5 kv/cm on the process. The field was created by an electrostatic machine, one electrode of which was introduced into the upper part of the capillary and the other was connected to the water surface under the capillary, onto which the drops fell. The emergence of the drops from the capillary, with and without the field, was photographed at 200 frames per second. Apart from the field, all the experimental conditions were the same in both cases. It is seen from the photographs that under the action of the field a stream of water with a sharp tip was drawn out of the capillary; this stream then began to break up in the middle. This resulted in the formation of much smaller drops than those obtained in absence of a field. Photograph 1,c shows the deformation of a drop passing through a vertical electric field of 3.5 kv/cm, photographed at 1500 frames per second. In more powerful fields, according to Mecky [1], the drops should become drawn out into thin threads and, starting from the tail, should disintegrate into numerous small droplets.

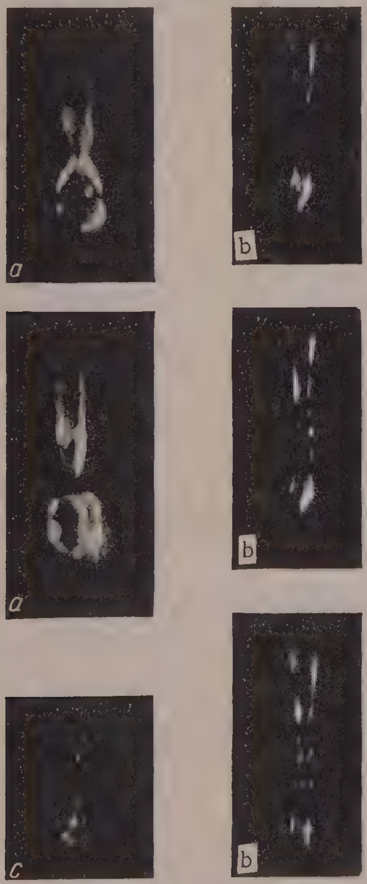

Deformation of drops in an electric field: a) emergence of a drop from a capillary without the action of a field; b) the same, in a field of 2.5 kv/cm; c) deformation of a drop in a field of 3.5 kv/cm.

In our view, drops play the following role in the development of discharge: as is known from electrostatics, the field strength at the opposite ends of a drop reaches a value three times that of the external polarizing field strength; this greatly favors the development of discharge.

SUMMARY

1. Under the action of a 2.5 kv/cm electric field, a stream of water with a sharp tip emerges, instead of a drop, from a capillary of 1 mm internal diameter; this stream begins to break up in its middle portion.

2. When a field of 3.5 kv/cm acts on a falling drop, the drop becomes thickened at the base; a

tail is formed at the upper end and becomes thinner during flight of the drop.

Received October 24, 1956.

LITERATURE CITED

[1] Mecky, Proc. Roy. Soc. 133, 565 (1931).

THE DEVELOPMENT OF A KINETIC THEORY OF GELATION

I. F. Efremov and S. V. Nerpin

The publication of the letter by Hamilton and Hamm [1] concerning the distant-packing mechanism of colloid particles and the formation of a quasicrystalline lattice has prompted us to publish this communication. The letter cited above contains certain elements of our kinetic theory of gelation, based on a series of papers published by one of us [2], the general principles of which are presented below.

1. The existence, under certain conditions, of a resemblance between the potential curve of molecular interaction and the potential curve of colloid particle interaction makes it possible to draw an analogy between the transition of substances with a molecular structure from the liquid into the solid state, and some instances of transition of a colloid system from a sol into a gel. In the latter case, instead of attraction and repulsion forces between individual molecules, forces of molecular attraction and ionic electrostatic repulsion between the colloid particles come into play. In this case the fixation of particles is determined by the presence of potential pits, the depth of which should be found with the collective interaction of the particles taken into account. Numerical calculations may be based on previous publications [3, 4].*

2. The occurrence of shearing elasticity G in a system of fixed particles, which is a characteristic sign of gel formation, is determined by the expression:

$$G = \frac{d^2F}{d\varphi^2}, \tag{1}$$

where F is the free energy of the system and φ is the angle of shear. The system will then act as a gel provided that the relaxation time of the colloid particles, both in cohesion processes and in transitions into vacant spaces of the quasicrystalline lattice, considerably exceeds the time of action of external influences. If these conditions are not satisfied, either the system will age rapidly or its elastic properties will be masked by fluidity.

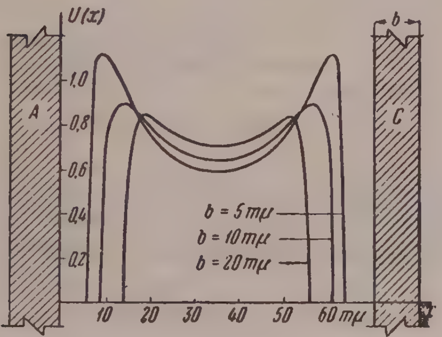

Total potential curves of interaction of a "test" particle with particles A and C (of different thicknesses b).

3. The conditions of fixation of the particles are considerably influenced by their shape and dimensions. For example, the interaction energy of two plates can be represented by the following approximate expression:

$$U = \frac{\pi}{2} D \left(\frac{kT}{ze}\right)^2 \cdot 1/H - \frac{\zeta\delta^2\sigma}{H^2}\left[1 - \frac{2}{(1 + b/H)^2} - \frac{1}{(1 + 2b/H)^2}\right], \tag{2}$$

---

* Hamilton and Hamm wrongly consider that the theory of Levine and Dube, which was shown by Deryagin [4, 5] to be erroneous, is applicable, and do not mention publications [4-6] in which the theory of the ionic electrostatic interaction of colloid particles was first developed.

where D is the dielectric constant of the medium; z is the electrovalency of the gegenion; e is the electron charge; ζ is a constant near to unity; b is the thickness of the plate; δ is the size of the molecules in the plate; σ is the surface tension at the plate–solution interface; H is the distance between the plates; kT has the usual meaning.

Equation (2) can be easily used to find the value of the potential energy of interaction between a "test" particle and its neighboring particles A and C. The diagram shows U(x) curves for different thicknesses of the interacting particles; it is seen that as the particle thickness is decreased from 20 to 5 mμ the depth of the potential pit is approximately trebled; therefore fixation of thin particles will be more rigid and the system will age more slowly than if particles of greater thickness are present.

4. The above considerations, which relate to the nature of gelation processes, may be extended in their entirety to such systems as highly concentrated emulsions and foams. In the latter case the equilibrium state of the layer separating the gas bubbles is determined by the algebraic sum of the molecular component of the disjoining pressure, which is in this case negative (corresponding to a tendency of the bubbles or droplets to come closer together), and the ionic electrostatic component of this pressure, which is positive in sign.

A distinguishing feature of foamlike systems is that shear in these systems is accompanied not only by deformation of the layers separating the particles, but also by changes in the specific surface of the latter. In the simplest case, when the potential energy of interaction between the molecules within the layer separating the bubbles remains unchanged during shearing of the system, we may write the following expressions for the shearing force and the shear modulus G:

$$\tau = \frac{2\varphi}{d}\left(\sigma + \frac{d\sigma}{d\omega}\,\omega\right), \tag{3}$$

$$G = \frac{d\tau}{d\varphi} = \frac{2}{d}\left(\sigma + \omega\,\frac{d\sigma}{d\omega}\right), \tag{4}$$

where d is the size of a bubble; ω is the specific surface, and σ is the surface tension.

The Lensoviet Technological Institute Leningrad Received July 4, 1956.

LITERATURE CITED

[1] J. E. Hamilton and F. A. Hamm, J. Appl. Phys. 27, 190 (1956).

[2] I. F. Efremov, Trans. Leningrad Inst. of Soviet Trade (Leningrad, 1950); Colloid J. 10, 337 (1948); 15, 429 (1953);* 16, 4, 264 (1954);* 18, 3 (1956).*

[3] S. V. Nerpin, Dissertation** (Leningrad, 1956).

[4] B. Deryagin and L. Landau, J. Exp. Theoret. Phys. 11, 802 (1941) (reprinted 15, 662 (1945)); Acta Phys. Chim. 14, 633, 1941.

[5] B. Deryagin, Trans. Faraday Soc. 36, 203, 1940; 36, 730 1940; Colloid J. 6, 291 (1940); 7, 285 (1941).

[6] B. V. Deryagin, Bull. Acad. Sci. USSR, Chem. Ser. 5, 1153 (1937); Acta Phys. Chim. 10, 333 (1939); E. J. W. Verwey and J. Th. C. Overbeek, Koll.-Z. 141, 44, (1955); Coll. Sci. 10, 224 (1955).

---

* [Original Russian pagination. See C. B. translation].

** [In Russian].

THE NATURE OF THE CHROMATOGRAPHIC METHOD

S. G. Mokrushin

The principles of chromatography have been considered in a number of publications. In particular, Rachinsky [1] states the "fundamental law of chromatography" as follows: "Any liquid or gaseous mixture is separated when passing through a layer of sorbent if there are differences in the sorptional interaction between the components of the mixture and the sorbent". If follows from this definition that the sorbent (solid phase) is the stationary portion of a chromatographic system, while the liquid or gaseous mixture is the motile phase. This definition of the nature of chromatography fully conforms to Tswett's classical chromatographic method [2].

It is the present author's view that Tswett's method should be given a wider intepretation, namely: it should not be confined to the motion of a liquid or gaseous phase through a solid sorbent, but the concept of relative motion should be accepted; i.e., the motion of a disperse sorbent through a stationary liquid or gaseous phase should be included in the concept. This second case may be regarded as an inversion of Tswett's classical method.

If the condition of relative directed motion is accepted, the above formulation of the fundamental law of chromatography is extended to the following form: "Any liquid or gaseous mixture is separated when it moves through a layer of sorbent or, conversely, in the directed movement of a disperse sorbent through a layer of the liquid or gaseous mixture, if there are differences in the sorptional interaction between the components of the mixture and the sorbent".

If follows from this that the Tswett method should include three other forms in addition to the generally accepted forms, namely: suspension, emulsion and foam chromatography.

Suspension chromatography takes place when particles of a finely divided solid sorbent are in directed motion (by sedimentation) through a stationary layer of liquid (or gas). As the result of selective sorption, the components will be consecutively sorbed from the liquid as the solid settles and new portions of it are added. Ultimately a chromatogram will be formed, i.e., the lowest layer of the settled sorbent will contain the most sorbable, and the topmost layer will contain the least sorbable component.

At the author's suggestion, Shveikina carried out experiments on the separation of ferric chloride (2%) and nitrates of copper (3%) and cobalt (2%) dissolved in water. Into a tube (31 cm high, 1.5 cm in diameter) containing 15 ml of the solution, 33 g of aluminum oxide was added. After 1 hour 15 minutes the salts had been completely sorbed from solution, and the sediment consisted of three distinct layers: a bottom brown layer (ferric chloride), a middle blue layer (copper nitrate), and a top pink layer (cobalt nitrate). The cobalt, copper, and iron salts were succesively isolated from the sediment by elution with water.

This experiment shows that the method of suspension chromatography is analogous to Tswett's classical method, being an inversion of the latter with respect to the relative and directed phase motion. The suspension method was used by Aleskovsky [3] for low concentrations. It must be noted that suspension chromatography is considerably more rapid than Tswett's classical method.

In emulsion chromatography the sorbent consists of liquid droplets ascending through the layer of liquid to be separated. As Shedlovsky [4] points out, this method has been developed very little as yet.

In foam chromatography small air bubbles ascend through the liquid layer. The term "foam chromatography" was used by Ermolenko [5]. The isolation of surface-active substances from solutions with the aid of foam was suggested by Dumansky [6], Ostwald and Siehr [7], and Schutz [8], while Mokrushin [9] proposed the use of the method for separation of colloids.

On the basis of the foregoing, all chromatographic methods may be divided into two groups: 1) the classical method of Tswett, in which a liquid or gas flows through a porous sorbent, and 2) inversion of the classical Tswett method, or sedimentation (or ascent) of solid, liquid, or gaseous sorbent particles through a stationary layer of a solution of the components to be separated.

The S. M. Kirov Polytechnic Institute of the
Urals, Sverdlovsk

Received July 25, 1955.

LITERATURE CITED

[1] V. V. Rachinsky, Trans. Commission on Analytical Chem. 6 (9), 21 (1955).

[2] M. S. Tswett, Selected Works (Izd. AN SSSR, 1946) p. 141.

[3] V. B. Aleskovsky, Summaries of Papers at the Scientific-Technical Conference of the Lensoviet Technological Institute, Leningrad (Goskhimizdat, Leningrad, 1955) p. 27.

[4] L. Shedlovsky, Chromatography, Coll. edited by Academician M. M. Dubinin (Moscow, 1949) pp. 178, 186.

[5] A. F. Ermolenko, Chromatographic Adsorption Analysis and its Development (Acad. Sci. Belorussian SSR Press, Moscow, 1956) p. 81.

[6] A. V. Dumansky, J. Sugar Ind. 4, 427, 440 (1930).

[7] Wo. Ostwald and A. Siehr, Koll.-Z. 76, 33 (1936).

[8] F. Schutz, Trans. Faraday Soc. 42, 437 (1946).

[9] S. G. Mokrushin, Summaries of Papers at the Conference on the Use of M. S. Tswett's Chromatographic Method in Chemical Analysis (Izd. AN SSSR, 1953) p. 14.

THE ROLE OF FILLER GRAIN STRUCTURE IN THE FORMATION OF STRUCTURES IN BITUMEN SUSPENSIONS

L. S. Terletskaya

Addition of fillers to bitumen leads, at definite concentrations, to formation of a structural network and its reinforcement. The strength of the structure formed is determined to a considerable extent by the properties of the filler [1]. Our investigations have shown that, in addition to the magnitude and nature of the surface and the mineralogical composition, special importance attaches to the porous structure of the filler grains, characteristic of both natural and artifical finely divided materials used as fillers. When such fillers are introduced into bitumen, the structure of the filler grains may change significantly the properties of the whole system and of the structure formed in it [3].

In the present investigation, a study was made of the pore structure of mineral grain fillers, and its effects on bitumen–filler interaction and on the mechanical properties of the system formed. Two types of mineral fillers, differing in chemical composition, were chosen for the study:

1. Carbonate rocks – calcite, marble, limestones of different structures, and chalk.
2. Rocks consisting mainly of silica – quartzite, tripoli, opoka, and quartz sand.

Investigations of the structure of these fillers by means of electron microscopy in conjunction with dye adsorption showed that they have different internal structures – compact, finely porous, porous, and coarsely porous. Filler– bitumen interaction was studied by adsorption and luminescence methods. The physicochemical characteristics of the fillers are given briefly in the Table.

Luminescence analysis showed that the bitumen components are zonally distributed over the cross sections of grains of the finely porous fillers (tripoli, opoka, limestone I) extracted from mixtures with bitumen. Oils, followed by tars, are ranged from the grain center to the periphery. Asphaltenes do not penetrate into the grains at all, and gradually merge with the free bitumen. The same is found in porous fillers (limestone II, marble, chalk) but the luminescence is less intense, and the above-named bitumen components penetrate deeper into the grains. Coarsely porous specimens do not show the characteristic luminescence, as the bitumen penetrates completely into the pores, without fractionation. In compact fillers bitumen does not penetrate through the whole bulk of the grain, but only along the microcrevices and faulty cleavage planes of the crystals. Thus, the structure of the filler grains participates in different ways in filler–bitumen interaction processes.

A finely porous grain structure causes fractionation of the bitumen as the result of selective capillary suction of the least viscous components of the dispersion medium of the bitumen. In consequence the bitumen becomes richer in structure-forming components, so that its interlayers acquire higher mechanical strength, viscosity, and shear modulus.

Moreover, selective removal (mainly of surface-inactive oils) by capillary suction may raise the concentration of high-molecular and colloidally dispersed surface-active components in the layers between the external surfaces of the particles, aiding adsorptive saturation and hence oleophilization of the external surfaces of the filler grains, and so causing greater adhesion of bitumen to these surfaces.

The mechanical strength of the bitumen interlayers is the principal factor in the mechanical strength of the system as a whole. Structurized bitumen–filler systems are densely packed plastic systems in which the solid phase particles are separated by thin layers of bitumen. It has been shown by Rebinder and his

Some Physicochemical Properties of the Fillers

Filler	Chemical composition, %					Loss on ignition	Specific surface in cm²/g		Adsorption in mg/g	Type of structure
	SiO_2	Al_2O_3	Fe_2O_3	CaO	MgO		total	internal		
Tripoli	83.08	7.61	0.19	1.18	0,87	4.0	287500	285300	10.0	Finely porous
Opoka	85.86	4.13	1.07	1.35	0.96	6.63	145000	142580	9.5	Ditto
Quartz sand	99.38	0.39	0.04	0,06	0,05	0.28	8300	4070	0.65	Compact
Quartzite	—	—	—	—	—	—	6400	3010	0.40	Compact
Limestone I	1.02	0.07	0.39	55.22	0.36	43 28	21400	18210	5.0	Porous
Limestone II	0.79	0.64	0.84	55.92	0.55	43.09	15500	12290	3.70	Porous
Chalk	0,48	0.08	0.1	55.63		43.71	17800	15690	—	Ditto
Marble	0.16	0.03	0.09	55,59	0.38	44.05	16700	13080	5.90	"
Calcite	0.43	0.05	0.5	55.8		43.42	10500	6720	2.80	Compact

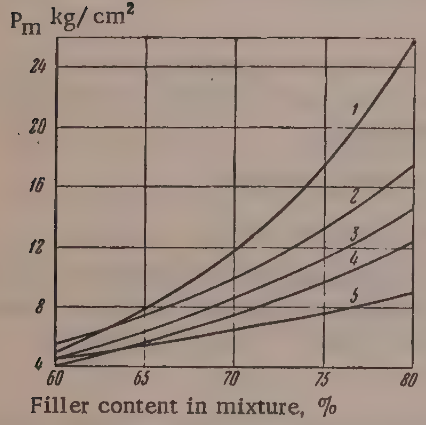

Variations of plastic strength of filler—bitumen mixtures with filler concentration: 1) tripoli; 2) limestone; 3) marble; 4) chalk; 5) quartz sand.

associates [2] that the susceptibility of such systems to plastic deformation is caused by the fact that the particles are not connected directly, but are joined through thin solvate layers of the medium, which allow free relative slippage of the particles. The mechanical strength of such systems depends on the properties of the layers separating the particles.

Structure formation in thin adsorbed solvate layers of bitumen, caused by removal of oils by capillary suction, leads to their reinforcement and an increase of the mechanical strength of the whole system. To verify the above views, the structural and mechanical properties of mixtures of bitumen containing from 60 to 80% of the fillers were studied. As a measure of the mechanical strength, the limiting shear stress (plastic strength P_m) was determined by the cone plastometer method [2, 3]. As the filler content approaches the concentration at which a structure is formed, differences between the properties of the fillers become prominent (see Fig.). Mineral fillers with a finely porous structure, which give rise to strong bitumen films, form mixtures of high mechanical strength. On the other hand, compact and coarsely porous fillers give mixtures of low plastic strength.

Thus an important property of mineral filler grains, in addition to their molecular nature and the total specific surface, is the nature of the pore structure.

The Kharkov Automobile Road Institute
Department of Chemistry

Received February 1, 1957.

LITERATURE CITED

[1] P. A. Rebinder, G. A. Ab, and S. Ya. Veiler, Proc. Acad. Sci. USSR 31, No. 5, 444 (1941); Ya. T. Aron and P. A. Rebinder, Proc. Acad. Sci. USSR 52, 235 (1946).

[2] E. E. Segalova and P. A. Rebinder, Colloid J. 10, 223 (1948).

[3] P. A. Rebinder and N. A. Semenenko, Proc. Acad. Sci. USSR 64, 835 (1949).

COLLOID JOURNAL OF THE U.S.S.R. IN ENGLISH TRANSLATION

November-December, 1957

TABLE OF CONTENTS

	Page	Russ. Page
1. The Coagulation Mechanism of Butadiene–Styrene Latex. S. A. Glikman and E. P. Korchagina	657	657
2. Analysis of the Forms of Moisture Bonding in Porous Adsorbents With the Aid of Drying Thermograms. M. F. Kazansky	661	662
3. Study of Gelation Processes in Fruit Candy Masses by Means of the Cone Plastometer. L. S. Kuznetsova and A. L. Sokolovsky	667	668
4. The Adsorptive Activity of Cadmium Hydroxide in Relation to the Conditions of its Formation. S. A. Levina and N. F. Ermolenko	671	673
5. A Study of Changes in the Structural and Mechanical Properties of Photographic Emulsions During Drying. L. A. Lepilkina	677	678
6. The Swelling of Ion Exchange Resins and the Nature of Their Selectivity. V. P. Meleshko and O. N. Myagkoi	683	684
7. The Solution State of Direct Dyes and Their Diffusion in a Cellophane Film. B. N. Melnikov and P. V. Moryganov	687	689
8. Electron Microscope Study of the Structure of Aluminosilicate Hydrogels by the Replica Method. Ya. V. Mirsky	695	696
9. General Principles of Formation of Metal Alloy Organosols at the Cathode in a Two-Layer Bath. E. M. Natanson and N. N. Kozachek	697	698
10. Influence of the Reaction of the Precipitation Medium and of the pH of the Wash Water on the Structure of Chalky Silica Gels. I. E. Neimark and I. B. Slinyakova	705	706
11. Gelatin–Glycerol Gels as Materials For Studying Stresses by the Optical Polarization Method. D. N. Osokina	713	713
12. The Selection of Plasticizers For High Polymers. S. P. Papkov	721	722
13. Exchange of Sodium and Calcium Ions on Swelling Sulfonic and Carboxylic Resins. G. V. Samsonov, A. A. Vasilyev and V. A. Orestova	729	730
14. Hydrates of the Calcium Salts of Certain Fatty Acids. V. I. Solnyshkin	735	736
15. The Shrinkage of Collagen. N. N. Stefanovich and A. N. Mikhailov	741	741
16. The Hydrophilic Properties of Clays of the Kaolinite Group. E. T. Uskova	747	747

Discussion

	Page	Russ. Page
17. More on the Subject of Thermomechanical Curves. E. I. Regirer and M. S. Kalantarova	751	752

Letters To The Editor

	Page	Russ. Page
18. Kinetics of the Spraying of Water Drops in an Electric Field. V. I. Arabadzhi	755	756
19. The Development of a Kinetic Theory of Gelation. I. F. Efremov and S. V. Nerpin	756	757
20. The Nature of the Chromatographic Method. S. G. Mokrushin	758	759
21. The Role of Filler Grain Structure in the Formation of Structures in Bitumen Suspensions. L. S. Terletskaya	760	760

RUSSIAN PHARMACEUTICAL RESEARCH
IN COMPLETE ENGLISH TRANSLATION

SOVIET PHARMACEUTICAL RESEARCH
Chemistry Collection No. 4 — Just published

Covers all aspects of Soviet pharmaceutical research; papers selected by one of the top pharmaceutical research chemists, of one of the major drug companies, from all Russian chemistry journals translated by Consultants Bureau, **1949–1955.** Sections may be purchased as follows:

I. PHARMACEUTICAL CHEMISTRY. Sections: Solubility; Stability: Ion Exchange; Emulsions, Suspensions, Gels; Miscellaneous. 74 papers, 447 pages, **$95.00**

II. PHARMACOGNOSY. Sections: Alkaloids; Oils; Glycosides; Miscellaneous. 87 papers, 399 pages, **$90.00**

III. MEDICINAL CHEMISTRY. Sections: Structure-Activity Relationships; General. 91 papers, 556 pages, **$100.00**

THE COMPLETE COLLECTION, 252 papers, 1,402 pages, **only $200.00**
*Single articles available — Table of Contents sent on request

All Consultants Bureau's translations by bilingual scientists, equally familiar with Russian and the technical terminology. All diagrammatic and tabular material integral with the text is included; text is clearly reproduced by multilith process from IBM cold type; books are staple bound in durable paper covers. Complete catalogs of Consultants Bureau translations available

CONSULTANTS BUREAU, INC.
227 WEST 17th STREET, NEW YORK 11, N. Y. — U.S.A.
Telephone: ALgonquin 5-0713 • Cable Address: CONBUREAU, NEW YORK

– CONSULTANTS BUREAU, INC. –

RUSSIAN-ENGLISH TRANSLATION – PUBLISHING

Cover-to-cover Translations by Bilingual Scientists

Bulletin of Experimental Biology and Medicine

Covers physiology, pathology, immunology, biophysics, pharmacology, oncology, morphology. Translation began with the 1956 volume, and is by special arrangement with the National Institutes of Health. Annual subscription, English translation, 12 issues, approximately 1000 pages –240 articles. Only $20.00

Pharmacology and Toxicology

By special arrangement with the American pharmaceutical industry; translation began with the 1957 volume. Annual subscription, English translation, 6 issues, approximately 600 pages – 150 articles. Only $25.00

Biochemistry Section, Proceedings, Academy of Sciences, USSR, (Doklady)

Doklady contains concise reports by leading Soviet scientists; represents a comprehensive survey of the most advanced Soviet research. Translation began with the 1957 volume. Annual subscription, English translation, 6 issues (Doklady is originally published in 36), approximately 400 pages – 115 articles. Only $65.00

Biochemistry

Most comprehensive Soviet biochemical journal; covers plant and animal biochemistry. Translation began with the 1956 volume, and is by special arrangement with the National Institutes of Health. Annual subscription, English translation, 6 issues, approximately 600 pages – 120 papers. Only $20.00

Soviet Journal of Atomic Energy

"Atomnaya Energiya" in complete English translation. Covers latest advances in peaceful uses, including biological-medical work with radioactive isotopes. Translation began with 1956 (first) volume. Annual subscription, 12 issues, approximately 1200 pages – 240 papers. Only $75.00

Soviet Pharmaceutical Research

Chemistry Collection No. 4 – Covers all aspects of Soviet pharmaceutical research; papers expertly selected from the following Russian chemical journals translated by Consultants Bureau, 1949-1955: Journal of General Chemistry; Journal of Applied Chemistry; Bulletin of the Academy of Sciences, USSR, Division of Chemical Sciences; Journal of Analytical Chemistry; Colloid Journal. Sections–may be purchased separately:

I. Pharmaceutical Chemistry: Solubility; stability; ion exchange; emulsions, suspensions, gels; miscellaneous.
74 papers, 447 pages, $95.00

II. Pharmacognosy: Alkaloids; oils; glycosides; miscellaneous. 87 papers, 399 pages, $90.00

III. Medicinal Chemistry: Structure-activity relationships; General.
91 papers, 556 pages, $100.00

Complete: 252 papers, 1402 pages $200.00
Single papers, $7.50–free table of contents on request.

German-English Neurophysiology Glossary

Compiled, with a preface, by Roger M. Morell, M.D. Covers neuroanatomy, biochemistry, physiology, neurology, electrical engineering, electronics, idioms, selected general vocabulary.
9000 terms, 181 pages, $7.50

RADIOBIOLOGY SYMPOSIUM–Seven reports by four famous Soviet biologists on X-ray irradiation of mice. English translation. 134 pages, $50.00

REMOTE CONSEQUENCES OF INJURIES CAUSED BY IONIZING RADIATION – Summaries of 22 papers; effects on dogs, rabbits, mice.
74 pages, $10.00

Text clearly reproduced by multilith process from IBM "cold type"–includes all diagrammatic and tabular material; books and journals staple bound in durable paper covers. Sample journal Tables of Contents on request.

CONSULTANTS BUREAU, INC.
227 W. 17th St., New York 11, N. Y.